A UNIFIED SLOPE DESIGN FRAMEWORK FOR DIFFERENT ROCK SLOPE FAILURE MECHANISMS

A THESIS SUBMITTED TO
THE GRADUATE SCHOOL OF NATURAL AND APPLIED SCIENCES
OF
MIDDLE EAST TECHNICAL UNIVERSITY

BY

MUSTAFA SERHAN KAHVECİ

IN PARTIAL FULFILLMENT OF THE REQUIREMENTS
FOR
THE DEGREE OF MASTER OF SCIENCE
IN
MINING ENGINEERING

JANUARY 2024

Approval of the thesis:

A UNIFIED SLOPE DESIGN FRAMEWORK FOR DIFFERENT ROCK SLOPE FAILURE MECHANISMS

submitted by **MUSTAFA SERHAN KAHVECİ** in partial fulfillment of the requirements for the degree of **Master of Science** i**n Mining Engineering, Middle East Technical University** by,

Prof. Dr. Halil Kalıpçılar
Dean, Graduate School of **Natural and Applied Sciences** _____

Prof. Dr. N. Emre Altun
Head of the Department, **Mining Engineering** _____

Asst. Prof. Dr. Ahmet Güneş Yardımcı
Supervisor, **Mining Engineering, METU** _____

Examining Committee Members:

Assoc. Prof. Dr. Mehmet Ali Hindistan
Mining Engineering, Hacettepe University _____

Asst. Prof. Dr. Ahmet Güneş Yardımcı
Mining Eng, METU _____

Assoc. Prof. Dr. Onur Gölbaşı
Mining Eng, METU _____

Date: 25.01.2024

I hereby declare that all information in this document has been obtained and presented in accordance with academic rules and ethical conduct. I also declare that, as required by these rules and conduct, I have fully cited and referenced all material and results that are not original to this work.

Name Last name : Mustafa Serhan Kahveci

Signature :

ABSTRACT

A UNIFIED SLOPE DESIGN FRAMEWORK FOR DIFFERENT ROCK SLOPE FAILURE MECHANISMS

Kahveci, Mustafa Serhan
Master of Science, Mining Engineering
Supervisor: Asst. Prof. Dr. Ahmet Güneş YARDIMCI

January 2024, 122 pages

Slope stability analysis requires an extensive knowledge on geomechanics and computational simulations. This research develops a practical approach in the preliminary analysis of slope failure modes for rock slopes with different specifications in terms of rock mass quality, slope height, overall slope angle, upper face inclination and discontinuity orientations. Parametric analyses were conducted on computational models using Finite Element Method and Limit Equilibrium Method. In total, 10041 different conditions were simulated to generate a reliable database for the construction of a new slope design framework. Slope performance was evaluated in terms of the mechanical indicators such as the total displacement, max shear strain and factor of safety. The model outputs were used to train an Artificial Neural Network (ANN) model to overcome the difficulties in interpretation of conventional tables and plots. The ANN model was tested using benchmark cases. The results provided a high correlation implying the proposed

method is successful in predicting the failure mode in rock slopes. The study outcomes have potential to provide a reliable tool for slope stability that may be useful for inexperienced technical staff.

Keywords: Rock Slope Stability, Finite Element Method, Limit Equilibrium Method, Slope Failure Mode, Machine Learning

ÖZ

FARKLI KAYA ŞEVİ YENİLME MEKANİZMALARI İÇİN BİRLEŞTİRİLMİŞ BİR ŞEV TASARIM SİSTEMİ

Kahveci, Mustafa Serhan
Yüksek Lisans, Maden Mühendisliği
Tez Yöneticisi: Dr. Öğr. Üyesi Ahmet Güneş YARDIMCI

Ocak 2024, 122 sayfa

Şev duraylılık araştırması jeomekanik ve hesaplamalı benzetimler konusunda geniş bir bilgi birikimi gerektirmektedir. Bu araştırma, kaya kütle kalitesi, şev yüksekliği, genel şev açısı, üst basamak eğimi ve süreksizlik yönleri gibi farklı koşullar altında şev yenilme modunun belirlenmesinde kullanılabilecek pratik bir öncül çözümleme yöntemi geliştirmektedir. Hesaplamalı modeller üzerinde sonlu elemanlar yöntemi ve denge eşitlik yöntemi kullanılarak parametrik çözümlemeler yürütülmüştür. Yeni geliştirilen şev tasarım yönteminde kullanılacak güvenilir bir veri tabanı oluşturmak üzere toplam 10041 farklı senaryo üretilmiştir. Şev performansı; toplam yer değiştirme ve en yüksek kesme gerinimi gibi mekanik faktörler ve güvenlik faktörü cinsinden değerlendirilmiştir. Konvansiyonel tablo ve grafiklerin değerlendirilmesinde oluşan zorlukları gidermek amacıyla model çıktılarıyla bir yapay sinir ağları (YSA) modeli eğitilmiştir. YSA modeli referans modellerle karşılaştırılarak test edilmiştir. Sonuçlar, önerilen yöntem ile kaya şevlerinde yenilme modunun başarıyla tahmin edilebileceğini gösteren yüksek korelasyon

değerleri sağlamıştır. Çalışma çıktıları şev duraylılık değerlendirmelerinde tecrübesiz teknik personel için faydalı olabilecek güvenilir bir araç sağlama potansiyeline sahiptir.

Anahtar Kelimeler: Kaya Şev Duraylılığı, Sonlu Elemanlar Yöntemi, Denge Eşitlik Yöntemi, Şev Yenilme Modu, Makine Öğrenmesi

To my beloved family

ACKNOWLEDGMENTS

For his valuable contribution and guidance in determining the thesis topic, elaborating its scope, interpreting the results, and full support throughout this study, I would like to express my endless thanks to my thesis advisor, Assist. Prof. Dr. Ahmet Güneş Yardımcı.

I extend my gratitude to my thesis defense committee members, Assoc. Prof. Dr. Mehmet Ali Hindistan and Assoc. Prof. Dr. Onur Gölbaşı, for making my defense a remarkable experience, and for their valuable feedback and recommendations.

Lastly, I would like to express my heartfelt gratitude to my family and friends for their unwavering support and guidance throughout my journey. Their contributions have been instrumental in my success at every stage.

TABLE OF CONTENTS

LIST OF TABLES

TABLES

LIST OF FIGURES

FIGURES

LIST OF ABBREVIATIONS

ABBREVIATIONS

ANN	Artificial neural network
AI	Artificial intelligence
BEM	Boundary element method
BRNN	Bayesian regularization
c	Cohesion
DBSCAN	Density-Based Spatial Clustering of Applications with Noise
DEM	Distinct element method
DENN	Differential evolution algorithm
DT	Decision tree
E	Modulus of elasticity
EPR	Evolutionary polynomial regression
FA	Firefly algorithm
FDM	Finite difference method
FEM	Finite element method
FoS	Factor of safety
FPA	Failure plane angle
FPD	Failure plane dip
FPDD	Failure plane dip direction
GAN	Generative adversarial network
GBM	Gradient boosting machine
GSI	Geological Strength Index
H	Height of slope
JMP	Joint material property
JRC	Joint roughness coefficient
LEM	Limit equilibrium method

LMNN	Levenberg-Marquardt
LR	Logistic regression
MP	Material property
MSS	Maximum shear strain
MSSR	Modified stress-strain reinforcement
MTD	Maximum total displacement
OBI	Overall base inclination
OSA	Overall slope angle
PFC	Particle flow code
PSO	Particle swarm optimization
RF	Random forest
RMR	Rock Mass Rating
RMSE	Root mean square error
RQD	Rock quality designation
SSR	Shear strength reduction
SVM	Support vector machines
T	Tensile strength
TJD	Toppling joints dip
TJS	Toppling joints spacing
UCS	Uniaxial compressive strength
UFI	Upper face inclination
W	Weight

CHAPTER 1

INTRODUCTION

Slope stability is a concern of mining, geology, and civil engineering disciplines due to elevating mining operations, urbanization, and infrastructure constructions. Regarding soil and rock bears different geomechanical characteristics and slope mass may involve both, slope stability can be considered a multidisciplinary act to protect safety. Empirical tools are the common language to handle communication between technical staff with different backgrounds. Slope mass classification systems and slope performance charts have been widely used as a preliminary stage of stability assessment. However, these methods may also be misleading as they are either valid under restricted conditions or lacks of mechanical or kinematical considerations. Computational simulations of slope stability provide more comprehensive information about the slope performance by investigation of stress and deformation fields, before, during and after the excavation. However, they require skilled operators with a solid background in geomechanics, mathematics and computer programming. Even for the numerical simulations, a preliminary design tool would be considered useful as the computational expense would be reduced by determining a brief scope for modeling. Parametric studies have potential to provide the overall slope behavior under various circumstances. However, as the slope performance longs to a crowded parameter set with extensive ranges, interpretation of the simulation outputs poses difficulties. Conventional two-dimensional data plots would involve multiple data series and still all of the variables cannot be represented in a single graph. Therefore, alternative methods would be considered to provide a user-friendly interface for the interpretation of parametric studies.

This study investigates the slope performance with mechanical simulations for various conditions and suggests an auxiliary tool for the preliminary slope stability analysis. The current literature on the empirical and numerical slope evaluation proposes solutions for rock masses of particular quality, slope geometries, structural conditions, and depths. The purpose of this study is to cover a wider range of geometric, geomechanical and structural conditions with a reliable database comprised of mechanical assessments. The proposed method makes use of the current empirical methods and expert view to assign the elastic and plastic behavior of the rock mass. Initially, the parametric study outputs were presented using traditional charts and tables to compare similar conditions and assess suitable slope design. Later, a machine learning-based model was developed to provide a user-friendly tool for interpreting the numerical simulations. The study aims to make geomechanical data accessible to inexperienced users by reducing modeling and computational difficulties and avoiding potential modeling errors.

1.1 Problem Statement

The main focus of this research is the mitigation of accidents caused by slope failures. Slope failures can have significant and dire consequences, including damage to critical infrastructure, loss of life, disruption of ecosystems, and economic hardship. It is crucial to address and mitigate the risks associated with slope instability to ensure the safety and well-being of individuals, communities and sustainable production in mines.

Traditional slope design methods are often limited in their applicability and can be costly and difficult to update due to their reliance on case histories. As a more effective alternative, numerical models are used to simulate slope behavior under various conditions. However, these models can be complex and require advanced knowledge of geomechanics to prepare, run, and interpret. Additionally, solving

complex problems using numerical models can be computationally intensive and time-consuming, making them impractical for quick analyses.

Furthermore, interpreting model results often requires specialized expertise. This study introduces an improved methodology that enables users with basic skills to effectively utilize numerical model results.

1.2 Objectives and Scope of the Study

The objective of this study is to provide a simple and reliable tool for assessing slope stability. This will be achieved by computational simulations to monitor the effects of different factors such as slope height, overall slope angle, material properties, upper face inclinations, and failure plane properties on the slope performance. Instead of relying on traditional tables and 2D plots to interpret model outputs, advanced statistical models will be used. To summarize, the study aims to achieve the following objectives:

I. To create a user-friendly slope design tool for non-experts in geomechanical simulations.
II. To assess the efficiency of different slope designs featuring diverse geomechanical characteristics.
III. To create a reliable database of mechanical indicators for slope performance through numerical simulations with parametric analyses.
IV. To compare conventional tables and 2D plots with a machine learning-driven model.

1.3 Research Methodology

The research methodology is illustrated in the Figure 1.1, depicting the stages involved in designing and implementing the study. The following steps were taken to achieve the research objectives:

I. Outlining the modeling scenarios.
II. Determining geomechanical and geometrical properties for the rock mass and structural discontinuities.
III. Determining the numerical simulation method conforming to the simulated case.
IV. Tracking the mechanical slope performance indicators from the numerical simulations.
V. Examining the relationship between the parameters by interpreting numerical modeling data using conventional tables and 2D plots.
VI. Determining the limitations of the conventional data presentation methods and their inability to clearly present numerical model results.
VII. Using artificial neural networks to train a statistical model from numerical data

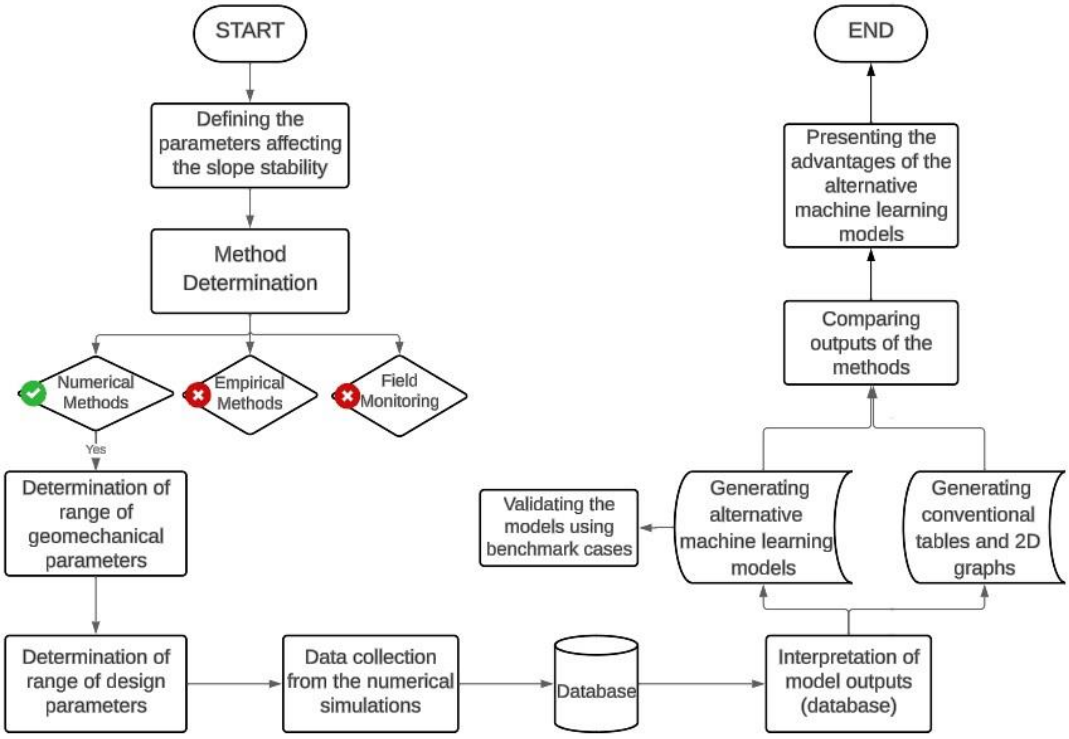

Figure 1.1 The flowchart of the methodology

1.4 Expected Contributions to Literature

The proposed method is expected to provide a reliable alternative for the preliminary design of rock slopes. Based on the comprehensive mechanical background, it is expected to be a complementary solution to the kinematic analysis and slope performance charts. Also, the numerical workload can potentially be reduced with the quick assessment of slopes. It is expected to induce a new understanding in developing slope stability methods by numerical simulations instead of the empirical tools based on field observations.

1.5 Organization of the Thesis

This dissertation presents a new approach to the assessment of rock slope stability. It places special emphasis on the continuum and discontinuum material behavior. In Chapter 1, the research's context, importance, and goals are discussed, along with the thesis structure and research questions.

In Chapter 2, the current state of knowledge on slope stability analysis, machine learning applications, and geomechanical parameters is thoroughly examined from the literature. The chapter offers a comprehensive review, detailing the key concepts and theories within the field, and provides a strong foundation for subsequent chapters to build upon.

In Chapter 3, the approach and procedures utilized to determine the geomechanical parameters are covered. It discusses the techniques and data collection methods employed in this crucial aspect of the research. The following part of the chapter describes the numerical analysis techniques used to evaluate slope performance, including the models and simulations applied. The chapter delves into a detailed discussion of the specific models and simulations used, providing an in-depth analysis of their applications.

Chapter 4 presents a novel and advanced method for analyzing slope stability in various scenarios. The method involves utilizing a comprehensive database of mechanical indicators that are obtained from numerical investigations. To provide a more convenient way of obtaining accurate simulation results, artificial neural network (ANN) models are utilized. The ANN models' performance is validated by comparing them to various cases simulated in previous chapters. This chapter also provides a detailed comparison and discussion of the recommendations and performance of hypothetical cases based on traditional empirical methods, numerical analysis, and the ANN models.

In Chapter 5, a comprehensive analysis of the research outcomes is presented. The exploration of geomechanical parameter determination, numerical analysis, and machine learning interpretation is conducted with a detailed discussion of the findings. The results obtained from each of these methods are thoroughly examined and compared to provide a comprehensive understanding of the research topic. This chapter's aim is to offer an in-depth insight into the research outcomes and provide a clear understanding of the research's implications.

The concluding chapter serves as a comprehensive summary of the most significant findings of the study and their potential implications. Additionally, the chapter offers valuable recommendations for future research directions and practical applications that can be derived from the study's outcome.

CHAPTER 2

LITERATURE REVIEW

This section presents a comprehensive review of the literature to point out the research gap. The scope is the slope design practice, rock slope failure modes, and stability assessments. Previous studies were investigated to outline the current research. Historical evolution of computational methods was used as a guide in planning the structure of the proposed method. The following sections cover the applied and theoretical basis of rock slope stability research.

2.1 Slope Failure Mechanisms

According to Morgenstern & Tchalenko (1967), 'failure' in the context of a landslide refers to the movement that significantly deforms the slope geometry. Experience, knowledge, and careful observation can provide valuable insights into the possible failure mechanisms of slopes that have already failed or those that are yet to be excavated. Identifying the potential failure mechanism is an important step in conducting an accurate slope stability analysis, as it enables the use of the most effective methods and techniques to address the issue (Öge, 2008).

Because slope stability depends on a number of factors and they are difficult to determine, it is a challenge to accurately estimate the stability of a rock or soil slope (Sakellariou & Ferentinou, 2005).

Ensuring the stability of a slope involves analyzing the driving and resisting forces and their interaction. While some factors contribute to the driving forces, others

contribute to the resisting forces. Therefore, it is crucial to consider these factors when performing a stability assessment for rock slopes (Raghuvanshi, 2019b).

The stability of slopes is commonly evaluated using the Factor of Safety (FOS), which is computed by dividing the resisting forces by the driving forces acting on the slope. If the resisting forces are greater than the driving forces, the FOS is greater than one, indicating that the slope is theoretically stable. On the other hand, if the driving forces exceed the resisting forces, the FOS is less than one, indicating that the slope is theoretically unstable (Amirkiyaei & Ghasemi, 2022).

Slope failure mechanisms can be categorized into two primary types as mass-failure and discontinuity driven failure. Mass failure occurs when a large amount of soil or rock slides down the slope on a circular surface, while failures driven by discontinuities happen when the slope mass is disturbed by geological features such as faults, fractures or joints. Understanding these mechanisms is crucial for evaluating the stability of slopes and preventing potential hazards.

2.1.1 Slope Mass-Failure

Slope stability can be affected by a variety of surface and body forces as well as the dynamic loadings. However, gravity has the most significant influence that may dominate the failure. The gravitational force acting on a slope is directly proportional to its inclination (Raghuvanshi, 2019b). In other words, the steeper the slope, the stronger the gravitational force that triggers a soil or rock mass slide, leading to a global slope failure. Therefore, understanding the interaction between gravity and slope inclination is crucial for predicting and mitigating the risks associated with slope instability.

There are two modes of rock mass failure; circular and non-circular. Circular failure occurs when material moves in a circular pattern, while non-circular failure has a

pattern that is composed of conjunction of linear sections with various inclination. The Figure 2.1 represents a sample circular failure surface (Amirkiyaei & Ghasemi, 2022).

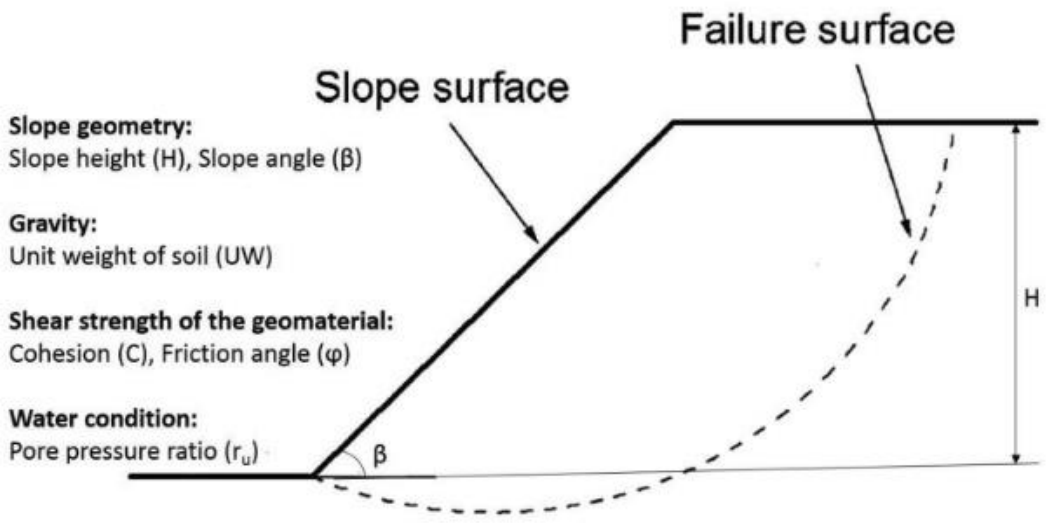

Figure 2.1 A sample circular failure surface (Amirkiyaei & Ghasemi, 2022)

Circular failure is not the only possible mode of slope failure for weak or structurally disturbed rocks. Structural geology may dominate the shape of the slip surface, resulting in a noncircular configuration (Duncan, 1996). A sample for a typical non-circular failure surface is shown in Figure 2.2.

Over the years, numerous studies have tackled the noncircular critical slip surface search in computational solutions. These studies have aimed to transform the search process into an optimization problem (Mafi et al., 2021).

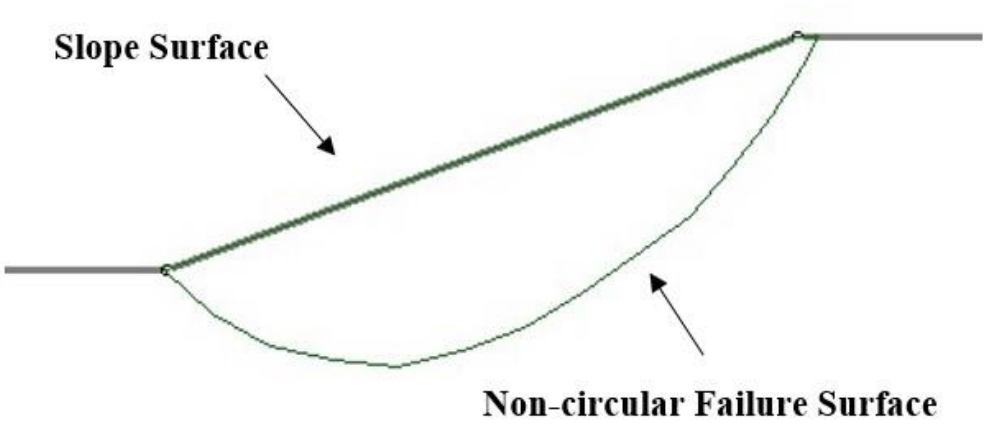

Figure 2.2 A sample non-circular failure surface

2.1.2 Discontinuity Driven Slope Failure

Discontinuities are another reason for rock slope failure. Sliding potential is largely influenced by the shear strength of the contact surfaces. The failure path can be traced along a single discontinuity, across two or more discontinuities, or along a combination of intersecting discontinuities (Sjöberg, 1996).

Slope mass involving structural discontinuities may experience a range of failure modes. These are the planar failure, where a flat sliding surface forms along a joint plane; wedge failure, where a wedge-shaped block detaches from the main rock mass; and toppling failure, where an overhanging block rotates and falls away from the slope (Mantrala et al., 2021). Those are the common modes of failure in rock slopes (Lee & Wang, 2011).

A plane failure typically occurs in rock slopes that are excavated in stratified sedimentary and meta-sedimentary formations. The rock block intersected by a plane can mobilize when a structural plane dips or daylights towards the free surface at an angle that is smaller than the slope face angle, but greater than the angle of friction of the discontinuity surface (Sharma et al., 1995). In other words, it happens when a

weakness plane in the rock is oriented in such a way that it dips towards the free face with an angle that can no longer support the weight of the rock above it (Tang et al., 2017).

The plane failure potential depends on various factors including the inclination of the slope, the inclination of the upper slope surface, the height of the slope, the dip of the potential failure plane, the presence of tension cracks, as well as the shear strength parameters (such as cohesion and angle of friction) of the potential failure surface. Additionally, the height of water in tension cracks and horizontal earthquake acceleration are also important factors (Raghuvanshi et al., 2015) (Raghuvanshi et al., 2014) (Turrini & Visintainer, 1998). The rock block is held in place mainly by the shear strength and the weight of the sliding mass that works against it. These two forces are the primary factors that resist and prevent the failure of the plane (Raghuvanshi, 2019a). A sample view of the plane failure is shown in the Figure 2.3 (Hoek & Bray, 1981).

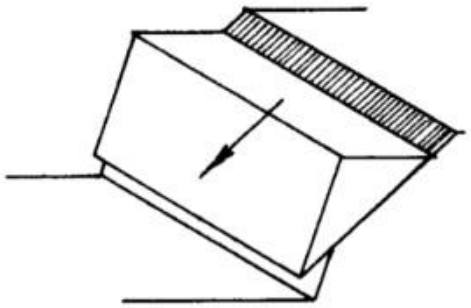

Figure 2.3 A typical plane failure (Hoek & Bray, 1981)

Plane failure occurs rarely and can be considered as a special type of wedge failure. There are various geological and geometric conditions that may lead to a wedge failure. Therefore, the stability of wedge blocks plays a crucial role in rock slope engineering (Wyllie & Mah, 2004).

Wedge failure occurs due to intersection of two or more discontinuity planes and the sliding block may lead to disastrous consequences if not addressed promptly (Bowa, 2020). The stability of a wedge block is influenced by the joint strike and the slope face strike. Therefore, identification of the structural orientations is crucial for evaluating and managing theslope stability (Mantrala et al., 2022). A sample wedge failure is illustrated in Figure 2.4 (Hoek & Bray, 1981).

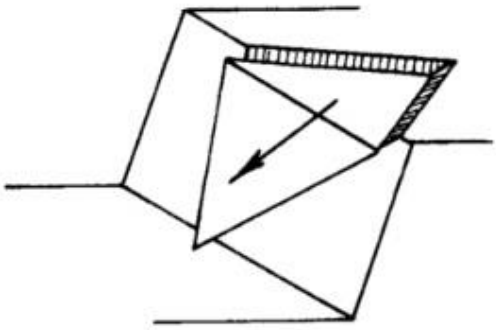

Figure 2.4 A sample wedge failure (Hoek & Bray, 1981)

Toppling is another discontinuity driven failure mechanism, which was first introduced by Ashby (1971) for a single rock block. In rock slopes where steeply dipping structural planes exhibit with a similar strike as the slope, the rock pillar may bend and lead to the toppling failure (Tao et al., 2019). Toppling is commonly observed in natural and man-made rock slopes. They have complex mechanisms and the main modes are flexural, blocky, and block-flexure, where the weight of the rock columns typically causes them to overturn. Flexural failure occurs when a rock mass has only one major discontinuity set, which is steeply dipping into the slope face. In this case, the rock columns may bend. Blocky failure occurs when the rock mass has an additional discontinuity set, perpendicular to the main set, dividing the rock columns into several sub-blocks. The movement of these blocks, whether it is sliding or overturning, can lead to a failure mode characterized by the formation of blocky

failure. Sometimes, block-flexure failure mode is also observed, which is a combination of these two failure modes (Ardestani et al., 2021). A typical presentation of the toppling failure is shown in Figure 2.5 (Hoek & Bray, 1981).

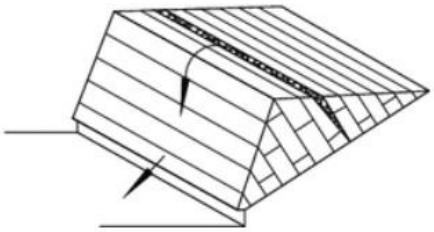

Figure 2.5 A sample view of toppling failure (Hoek & Bray, 1981)

2.2 Slope Stability Assessment

Rock slope stability deals with the influence of forces on the rock mass. Mainly three methods exist for analyzing the stability of rock slopes: conventional methods, computational methods, and physical models. Each method has advantages and limitations due to slope conditions, application, and expert capabilities (Raghuvanshi, 2019b).

Conventional methods involve the kinematic analysis, limit equilibrium analysis, probability analysis and empirical systems. These methods make use of observations or assumptions to assess the stability for simple slope geometry. Numerical simulation methods, on the other hand, use computational models to simulate the behavior of rock slopes under different conditions. These methods can be further divided into continuum modeling with finite-element and finite-difference analysis, and discontinuum modeling with distinct-element and discrete-element analysis. Hybrid modeling techniques may also be used to combine the advantages of both continuum and discontinuum models (Tang et al., 2017).

In situ measurements and physical model tests involve the measurement and analysis of the deformation and stress in the rock mass. These tests provide valuable information about the behavior of rock slopes and can help to validate the numerical models.

2.2.1 Empirical Methods

Empirical techniques are widely used for the preliminary slope stability analysis. They are based on experience and observation, enabling quick and efficient decision-making with a thorough understanding of the slope mass condition (Singh & Goel, 2011; Azarafza et al., 2020; Azarafza et al., 2022).

Mainly for rock mass, various classifications have been developed to quantify the slope mass condition, and to recommend measures for reducing the risk of instability. Empirical classification systems for geo-materials were first developed by Ritter (1879) and Terzaghi (1946).

In 1946, Terzaghi introduced a quantitative classification system for tunnels supported with steel sets in various host rock types. This system provided a more comprehensive understanding of the behavior of tunnels under different geologies. The system was mostly relying on the expert opinion.

Based on Terzaghi's method, Lauffer (1958) developed a classification system to determine the amount of time a tunnel or underground cavern can remain stable without supporting.

Deere, Hendron, and Patton (1966) and Deere (1970) proposed a new method for assessing the quality of a rock mass called the Rock Quality Designation (RQD) index which was modified later by Deere & Deere (1988) . The RQD index provides a quantitative measure of the degree of fragmentation of a rock mass and it is based on the percentage of rock core recovered in lengths greater than 10 cm. The RQD

index is used to evaluate the quality and suitability of a rock mass for engineering purposes, such as tunneling, slope stability, and foundation design. The higher the RQD value, the better the quality of the rock mass and the more suitable it is for construction. It defines the rock mass quality in a range of 0 to 100 and the score is classified under five quality classes; excellent, good, fair, poor, very poor (Sánchez et al., 2021).

The Q-system for rock mass classification was first introduced by Barton et al. (1974). It is widely used for assessing the quality of rock masses. It is based on a comprehensive evaluation of geological parameters such as rock strength, joint conditions, and groundwater conditions. The system assigns a numerical value, known as the Q-index, to the rock mass. This value is then used to provide design recommendations and support guidelines. In 2014, modifications were made to update the rating system (Barton & Grimstad, 2014).

After that, Cecil (1975) made modifications to Terzaghi's approach and used it to estimate properties of rock masses. In 1976, Bieniawski introduced the Rock Mass Rating (RMR) system, a quantitative method for assessing the quality of rock masses. The RMR system is based on five basic parameters that are used to evaluate the strength, deformability, and other engineering properties of the rock mass. These parameters are uniaxial compressive strength of intact rock, rock quality designation, spacing of discontinuities, condition of discontinuities and groundwater conditions.

The RMR system was later updated in 1989 (Bieniawski, 1989) (Figure 2.6), and the revised version included additional parameters, such as in situ rock stress, seismicity, and the presence of soft or weathered zones. The updated system also provided new guidelines for the classification of rock masses into different categories based on their RMR values.

A. CLASSIFICATION PARAMETERS AND THEIR RATINGS

	Parameter		Range of values						
1	Strength of intact rock material	Point-load strength index	>10 MPa	4 - 10 MPa	2 - 4 MPa	1 - 2 MPa	For this low range - uniaxial compressive test is preferred		
		Uniaxial comp. strength	>250 MPa	100 - 250 MPa	50 - 100 MPa	25 - 50 MPa	5 - 25 MPa	1 - 5 MPa	< 1 MPa
	Rating		15	12	7	4	2	1	0
2	Drill core Quality *RQD*		90% - 100%	75% - 90%	50% - 75%	2% - 50%	< 25%		
	Rating		20	17	13	8	3		
3	Spacing of		> 2 m	0.6 - 2 . m	200 - 600 mm	60 - 200 mm	< 60 mm		
	Rating		20	15	10	8	5		
4	Condition of discontinuities (See E)		Very rough surfaces Not continuous No separation Unweathered wall rock	Slightly rough surfaces Separation < 1 mm Slightly weathered walls	Slightly rough surfaces Separation < 1 mm Highly weathered walls	Slickensidd surfaces or Gouge 5 mm thick or Separaton 1 -5 mm Continuou	Soft gouge >5 mm thick or Separation > 5 mm Continuous		
	Rating		30	25	20	10	0		
5	Groundwater	Inflow per 10 m tunnel length (l/m)	None	< 10	10 - 25	25 - 125	> 125		
		(Joint water press)/ (Major principal σ)	0	< 0.1	0.1, - 0.2	0.2 - 0.5	> 0.5		
		General conditions	Completely dry	Damp	Wet	Dripping	Flowing		
	Rating		15	10	7	4	0		

B. RATING ADJUSTMENT FOR DISCONTINUITY ORIENTATIONS (See F)

Strike and dip orientations		Very favourable	Favourable	Fair	Unfavourable	Very Unfavourable
Ratings	Tunnels & mines	0	-2	-5	-10	-12
	Foundations	0	-2	-7	-15	-25
	Slopes	0	-5	-25	-50	

C. ROCK MASS CLASSES DETERMINED FROM TOTAL RATINGS

Rating	100 ← 81	80 ← 61	60 ← 41	40 ← 21	< 21
Class number	I	II	III	IV	V
Description	Very good rock	Good rock	Fair rock	Poor rock	Very poor rock

D. MEANING OF ROCK CLASSES

Class number	I	II	III	IV	V
Average stand-up time	20 yrs for 15 m span	1 year for 10 m span	1 week for 5 m span	10 hrs for 2.5 m span	30 min for 1 m span
Cohesion of rock mass (kPa)	> 400	300 - 400	200 - 300	100 - 200	< 100
Friction angle of rock mass (deg)	> 45	35 - 45	25 - 35	15 - 25	< 15

E. GUIDELINES FOR CLASSIFICATION OF DISCONTINUITY conditions

Discontinuity length (persistence) Rating	< 1 m 6	1 - 3 m 4	3 - 10 m 2	10 - 20 m 1	> 20 m 0
Separation (aperture) Rating	None 6	< 0.1 mm 5	0.1 - 1.0 mm 4	1 - 5 mm 1	> 5 mm 0
Roughness Rating	Very rough 6	Rough 5	Slightly rough 3	Smooth 1	Slickensided 0
Infilling (gouge) Rating	None 6	Hard filling < 5 mm 4	Hard filling > 5 mm 2	Soft filling < 5 mm 2	Soft filling > 5 mm 0
Weathering Ratings	Unweathered 6	Slightly weathered 5	Moderately weathered 3	Highly weathered 1	Decomposed 0

F. EFFECT OF DISCONTINUITY STRIKE AND DIP ORIENTATION IN TUNNELLING**

Strike perpendicular to tunnel axis		Strike parallel to tunnel axis	
Drive with dip - Dip 45 - 90°	Drive with dip - Dip 20 - 45°	Dip 45 - 90°	Dip 20 - 45°
Very favourable	Favourable	Very unfavourable	Fair
Drive against dip - Dip 45-90°	Drive against dip - Dip 20-45°	Dip 0-20 - Irrespective of strike°	
Fair	Unfavourable	Fair	

Figure 2.6 The updated RMR system (Bieniawski, 1989)

Over the years, many researchers such as Selby (1980), Chen (1995), Singh & Goel (1999), Hack et al. (2003), Romana et al. (2003), and Marinos et al. (2005) have proposed different quantification systems for civil and mining engineering purposes.

Marinos and his colleagues, in their 2005 publication, proposed modifications to the Geological Strength Index (GSI) classification system, which was introduced by Hoek & Brown in 1997. The revised classification system takes into account additional factors that were not included in the original classification, such as rock mass disturbance, alteration, and weathering.

The majority of these classification systems focus on intact material strength (e.g. uniaxial compressive strength) and geometrical features of slope mass (Nickmann et al., 2006). The stability of a slope is directly influenced by geological conditions, which can lead to weathering and reduced durability. However, some classifications do not properly consider these factors (Miščević & Vlastelica, 2014).

The geomechanical classification system was initially created with the aim of mainly providing a standardized approach to assess and classify rock masses in underground spaces. Over time, the RMR and Q-systems gained prominence and became widely accepted as they constitute a foundation for developing specialized classification systems for various rock slope engineering purposes (Azarafza et al., 2020) such as Slope Rock Mass Rating (Robertson, 1988), which is used to evaluate the stability of rock slopes; the Chinese Slope Mass Rating (Chen, 1995), which is a rock slope stability classification system that considers the geological and geotechnical characteristics of the slope; Slope Mass Rating (Romana et al., 2003), which is a modification of the Rock Mass Rating system that uses a weighted average of the Geological Strength Index (GSI) and the Rock Quality Designation (RQD) to evaluate the stability of rock slopes; Slope Stability Probability Classification (Hack et al., 2003), which is a probabilistic method that uses the factor of safety and the probability of failure to evaluate slope stability.

Other methods include Continuous Slope Mass Rating (Tomás et al., 2007), which is a modification of the Slope Mass Rating system that considers the continuous variation of the geological and geotechnical properties of the slope; Fuzzy Slope Mass Rating (Daftaribesheli et al., 2011), which is a fuzzy logic-based system that considers the uncertainty and vagueness in the geological and geotechnical data; Graphical Slope Mass Rating (Tomás et al., 2012), which is a graphical method that uses a chart to evaluate the stability of slopes; Slope Stability Rating (Taheri, 2013), which is a classification system that uses slope geometry and soil properties to evaluate slope stability; Global Slope Performance Index (Sullivan, 2013), which is a comprehensive approach that considers various factors such as geological, hydrological, and geotechnical properties of the slope to evaluate its stability; and Q-slope (Bar & Barton, 2017).

Some of these systems were specifically developed for open pit mine rock slopes. However, these systems are not always effective for weak rocks, which are typically composed of clay or other fine-grained materials.

This is due to the fact that weak rocks often exhibit complex behavior that is not adequately captured by existing classification schemes. As a result, these systems may not provide an accurate description of the properties and behavior of weak rocks (Azarafza, Hajialilue Bonab, et al., 2022).

2.2.2 Kinematic Analysis

Kinematics is a branch of physics and it is about the movement of solids. In slope engineering, kinematics is concerned with describing the motion of rock blocks without considering the forces. Kinematics is sometimes referred as the "geometry of motion" because it deals with the spatial relationships between moving objects.

In the context of geotechnical engineering and slope stability kinematics refers to the examination of potential failure modes and mechanisms based on the geometry of slopes. It focuses on understanding the motion of various failure surfaces within a slope. Displacement of rock blocks, as well as the potential failure mechanism, is governed by the slope kinematics (Donati et al., 2023). A common method for analyzing planar intersections is by utilizing the Stereographic projection of discontinuities (Kheok & Leung, 1986). This technique involves projecting the discontinuities onto a 2D plane to visualize their orientation and interrelationship. In particular, planar sliding, toppling, and wedge mechanisms are the three types of failures that has potential to occur in slopes (Read & Stacey, 2019). Although there are numerous studies on landslides, there is not much research done on rock slope kinematics (Kusumayudha et al., 2023).

Kinematic analysis is a valuable tool for preliminary slope stability assessments and it is often used to guide more detailed and comprehensive analyses. It helps engineers and geologists understand the geometry of potential failure surfaces and informs the design of appropriate stabilization measures. However, kinematic analysis does not consider the mechanical properties of the rock mass. Therefore, kinematic analysis is often used in conjunction with other methods, such as limit equilibrium analysis.

2.2.3 Physical Models

Physical modeling is one of the techniques used to assess the stability of slopes and is based on the creation of a scaled physical replica of a rock structure (Khorasani et al., 2019). Physical modeling experiments are typically conducted in a laboratory setting, where researchers can control and manipulate various parameters to simulate the real-world conditions. The intricacy of natural field locations, the challenge of gathering data in the field, and the absence of control over boundary conditions have all contributed to the growth of laboratory physical modeling techniques. By

analyzing the results of physical modeling experiments, geotechnical engineers can obtain valuable data about the behavior of slopes under different conditions. Physical modelling strategies offer better control over boundary conditions and material properties, as well as providing a means for detailed monitoring. Field data collection can be difficult due to the complexity of natural environments, making laboratory modelling a valuable tool in research (Harris et al., 2008).

Physical models are often used to study the effects of gravity on the smaller scale. Base friction or centrifuge model testing are two methods used to achieve this. By replicating the effects of gravity on the model, engineers can investigate and validate various numerical approaches related to slope stability analysis. Physical models are also useful in identifying any potential issues with the design of the structure and can help to optimize the stability of the slope. Overall, physical models play a crucial role in ensuring the safety and reliability of structures (Chen, 1995). Physical models also can be used to study the failure (Huang et al., 2021).

However, when analyzing the behavior of physical models, it is important to consider the effects of scale.Iif the model consists of blocks with perfectly flat contacts, exact geometries, and frictional strength, the scale effects may not be noticeable. In such cases, the behavior of the model remains largely consistent regardless of the scale at which it is observed. This is due to the fact that the interaction between the blocks, which is primarily influenced by the frictional forces and the geometry of the contacts, remains unchanged regardless of the size (Alejano et al., 2011). Moreover, creating physical models requires a considerable amount of effort and resources, including materials, equipment, and skilled labor. This process can be time-consuming, as it involves multiple stages of design, prototyping, and testing. Additionally, the cost of producing physical models can be high, as it requires the use of expensive machinery and materials. Furthermore, any errors or design changes during the production cycle can result in additional costs and delays.

2.2.4 Numerical Methods

Slope stability has been a research focus since the 1920s, and numerous methods have been proposed for analyzing and predicting it (Arya Babu & Chandrakaran, 2022). One of them is numerical methods, which are critical in assessing slope stability, providing insight into failure mechanisms and complex interactions. Various numerical techniques are commonly utilized in geotechnical engineering for slope stability analysis. These are mainly Finite Element Method (FEM), Finite Difference Method (FDM), Distinct Element Method (DEM), Boundary Element Method (BEM) and Limit Equilibrium Method (LEM).

FEM is a numerical technique that is commonly used for modeling complex geometries and material behaviors. It works by dividing the object or structure being analyzed into small elements, which makes it possible to analyze local stress and strain conditions. By utilizing interpolation functions, the FEM assumes that accurate displacements at any point within the element can be obtained from the displacements at the nodes (Bobet et al., 2009). FEM is particularly well-suited for analyzing materials that are heterogeneous or anisotropic and for taking into account nonlinear soil behavior and various boundary conditions. This method is highly versatile and can be employed in a variety of scenarios involving complex geometries, diverse materials, seepage, consolidation, and other coupled hydrological and mechanical phenomena (Arya Babu & Chandrakaran, 2022). Its flexibility makes it a valuable tool for tackling complex hydro-mechanical problems that may arise in various fields of engineering and science.

FDM is a numerical technique that involves dividing the slope into a grid and approximating the differential equations with finite differences. This method is particularly useful in modeling dynamic processes that change over time. FDM is commonly employed for analyzing slope stability and can accurately simulate variations in slope conditions over time.

DEM is a technique that involves modeling the movements and interactions of individual particles or blocks within a slope. It is highly effective in analyzing materials that are considered discontinuous, such as rock masses and soils containing cracks, fractures, or voids (Lin et al., 2022). By simulating the behavior of jointed rock masses, DEM modeling can provide valuable insights into the stability of slopes and the potential impact of discontinuities on their stability.

BEM is a numerical technique that divides the domain of a slope into two parts: the interior and the exterior, along the boundary. It is an effective approach for solving problems with well-defined boundaries and complex geometries, such as excavations and foundations. By separating the interior and exterior, BEM simplifies the analysis of the slope's behavior and allows for precise calculations of stresses and displacements.

LEM is a widely-used technique for assessing the stability of a slope. It works by analyzing potential failure surfaces and evaluating the equilibrium conditions of the slope. This approach simplifies complex problems into a set of equilibrium equations, making it a popular method for routine stability analyses. Its simplicity and ease of use make it a reliable tool for engineers and geologists.

PFC is a computer modeling software that is based on the principles of DEM. It is designed to simulate the movement and interactions of individual particles within a slope. PFC is predominantly used to study the behavior of granular materials, such as soil and rock, and help understand the underlying micro mechanics that govern their behavior (Cundall & Strack, 1979). In other words, it provides an in-depth analysis of how individual particles interact with each other and how these interactions can affect the overall behavior of a slope.

Additionally, there are hybrid approaches like discrete and finite element modeling (Havaej et al., 2014). However, the most common slope stability analysis methods are FEM and LEM (Griffiths et al., 2004). It is important to note that the

Limit Equilibrium Method (LEM) does not account for the stress-strain relationship and simplifying assumptions affects their accuracy (Feng et al., 2018). Despite this limitation, LEM is still the most widely used approach in geotechnical engineering due to its simplicity and capacity of evaluating the overall stability and finding the most critical failure surface (Mafi et al., 2021). FEM holds a significant edge over LEM due to its advanced capability of calculating the stress state before mining starts. This feature enables FEM to predict the behavior of rocks at much greater details than LEM. As a result, FEM provides a more comprehensive analysis of the rock's behavior and is highly preferred in geological engineering (Read & Stacey, 2019).

2.2.5 Novel Methods

Geomechanics problems often involve complex and dynamic systems, and traditional methods may not always provide reliable solutions. In recent years, machine learning algorithms have emerged as a powerful tool to address these challenges. By analyzing large amounts of data, machine learning can identify patterns and relationships that traditional methods might miss.

There are several categories of machine learning, each with its own unique approach. The four main categories are supervised, unsupervised, semi-supervised, and reinforcement learning (Tehrani et al., 2022). Out of these, supervised and unsupervised learning methods are the most widely used (Alamri, 2022). The learning type and algorithms are shown in the Figure 2.7.

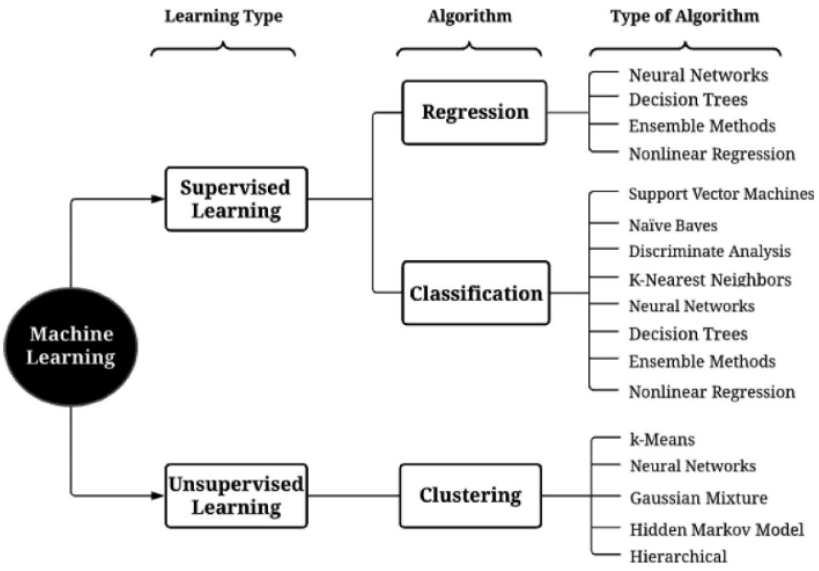

Figure 2.7 Types of machine learning (Alamri, 2022)

Supervised learning algorithms are an essential subset of machine learning, which involve analyzing and predicting labeled datasets. They are used to train machines to learn from input and target variables so that they can map inputs to corresponding outputs. These algorithms are designed to continue learning until they achieve the desired level of accuracy on the training data. The model's validity is then assessed through testing on unseen data (Tehrani et al., 2022). In other words, supervised learning involves the use of raw data to design a function that can make predictions or decisions based on new input data (Wojtecki et al., 2022). There are various supervised learning algorithms, including Decision Trees, Tree ensembles, such as Random Forest and Gradient Boosting algorithms like AdaBoost, XGBoost, and others, support vector machines, and artificial neural networks including multi-layer perceptron neural nets and supervised deep learning algorithms.

Unsupervised learning is a type of machine learning where the objective is to analyze and derive insights from data without the need for a target or label variable. The focus is on understanding the inherent structure of the data and identifying patterns, relationships, and similarities that may not be immediately apparent. One common

application of unsupervised learning is clustering, which involves grouping populations of data into distinct categories, subgroups, or clusters. This can be useful for identifying specific interventions or for making predictions about future data. Hierarchical clustering, K-means, and Density-Based Spatial Clustering of Applications with Noise (DBSCAN) are examples of unsupervised learning algorithms that can be used for clustering. Deep learning algorithms can also be applied to unsupervised learning tasks. Generative deep learning algorithms such as autoencoders and generative adversarial networks (GANs) can be used to learn representations of data without explicit supervision (Tehrani et al., 2022).

The application of Artificial Intelligence (AI) techniques in predicting slope stability also has gained widespread recognition and acceptance due to their numerous benefits. Soft computing methods, including Artificial Neural Networks (ANNs), Support Vector Machines (SVMs), Evolutionary Polynomial Regression (EPR), and Fuzzy Logic Systems, are used to obtain accurate predictions. ANNs, for instance, are capable of learning from past data and can model complex non-linear relationships, while SVMs are known for their ability to handle high-dimensional data and classify data points into different categories. EPR is a type of regression analysis that combines polynomial equations and genetic algorithms, while Fuzzy Logic Systems utilize fuzzy sets to represent uncertain and imprecise information. One of the primary advantages of these AI techniques is that they do not require any prior knowledge of specific model forms, making them flexible and adaptable to different scenarios. They are also capable of modeling non-linear relationships and can outperform traditional methods in terms of accuracy and efficiency (Arya Babu & Chandrakaran, 2022).

There are lots of research about using ANN in slope modelling. As an example, in 2003, Lu & Rosenbaum conducted a study on slope stability using artificial neural networks (ANN) to estimate the factor of safety (FoS) and shear strength against two failure mechanisms: circular and wedge. They relied on historical data collected by

Sah et al. in 1994 to train and test the ANN models. The study found that the ANN models were able to accurately predict the FOS and SS of slopes against these failure mechanisms.

Das et al. conducted a study in 2011, where they aimed to develop models that can accurately predict the factor of safety (FoS) and state of slopes that are at risk of circular failure. To achieve this, they created several artificial neural network (ANN) models and trained them using three distinct methods: Bayesian regularization (BRNN), differential evolution algorithm (DENN), and Levenberg-Marquardt (LMNN). These methods had different approaches towards training the ANN models. Bayesian regularization aimed to reduce overfitting by incorporating prior knowledge, while the differential evolution algorithm sought to optimize the model's parameters. The Levenberg-Marquardt algorithm is a widely used method that attempts to minimize the difference between the predicted and actual output values.

Rukhaiyar et al. (2018) aimed to predict the factor of safety (FoS) of slopes using a hybrid model that combined artificial neural networks (ANN) and particle swarm optimization (PSO). To achieve this, they compiled a database of 83 natural slopes from various studies and used them to train the model. Another study by Qi & Tang (2018) was focused on predicting slope stability using six different machine learning algorithms, namely logistic regression (LR), decision tree (DT), random forest (RF), gradient boosting machine (GBM), support vector machine (SVM), and artificial neural network (ANN). They also applied firefly algorithm (FA) for hyper-parameter tuning. The study database consisted of 148 slope cases collected from five published research works. By comparing these six integrated artificial intelligence approaches based on metaheuristic and machine learning algorithms, Qi and Tang aimed to identify the most effective method for predicting SS and its influencing variables.

With its ability to analyze vast amounts of data and identify complex relationships, machine learning has the potential to be useful in geomechanics and provide more accurate and reliable solutions to complex problems.

2.3 Previous studies

Slope stability analysis is a challenging and complex process that involves evaluating the soil and rock properties, analyzing the slope geometry, and identifying potential failure mechanisms. Furthermore, the academic importance of slope studies lies in advancing our understanding of geological processes and phenomena, which can lead to the development of new theories and models for predicting slope behavior. As such, slope studies continue to be an essential and evolving field of research that contributes to the safety and sustainability. In this manner, some of the studies from literature about slope stability are presented in this section.

Sonmez et al. (1998) addressed the difficulty of determining shear strength parameters in closely jointed rock masses, proposing a practical back-analysis method with a computer solution for failed slopes. It acknowledges the limitations of conventional approaches in such rock formations, introducing adjustments for discontinuity orientation. Three practical examples demonstrate the method's application, showing consistency between back-calculated and predetermined values of Rock Mass Rating (RMR) with constants. The study concludes that the proposed method serves as a practical tool for back-analyzing slopes in jointed rock masses, verifying rock mass ratings obtained from field and laboratory data. It suggests potential modifications in describing rock mass parameters for slopes. While expressing confidence in the Hoek-Brown failure criterion, the authors anticipate that applying the proposed method to additional case histories will enhance its accuracy and contribute to refining the understanding of jointed rock mass behavior.

Sonmez & Ulusay (1999) focus on improving the Geological Strength Index (GSI) classification scheme, especially for poor-quality rock masses in their study. It introduces quantitative terms like 'structure rating' and 'surface condition rating' to enhance GSI's precision, incorporating easily measurable parameters. The modified GSI chart is applied to five slope instability cases, confirming its effectiveness in geotechnical engineering. The study suggests that spoil pile materials can be classified as disintegrated rock masses in the GSI system, and the modified Hoek-Brown equations allow for estimating shear strength parameters for such materials. The authors acknowledge differing preferences among geologists and engineers regarding the GSI system's descriptive nature. Emphasizing the need for a better understanding of jointed rock mass behavior, the authors confidently endorse the Hoek-Brown failure criterion. They hope that applying the suggested modifications to various case histories will refine guidelines and validate the equations used by the non-linear failure criterion.

Hack (2002) highlighted in his article that some inherited properties and parameters from older systems may better suit for underground excavations than for surface applications like slopes. Additionally, the repeatability and reliability of classifications can be challenging due to difficulties in determining certain parameters. The article suggests that the question of the "best" system is subjective, with each developer advocating for their own. However, it encourages a more modest perspective, acknowledging that newer systems are generally an improvement based on experiences with older ones.

In his study, Cheng (2003) presented a new way of analyzing slope stability. The technique involves using simulated annealing to locate critical failure surfaces, both circular and non-circular, under general conditions. This method proves to be efficient and effective in handling even complex cases. The way to distinguish between circular and non-circular modes is by the number of control variables and criteria on kinematically acceptable mechanisms. The users can specify the precision

of the global minimum, which is not found in other methods. Furthermore, the author proposes a new method for determining the factor of safety without requiring an initial trial factor. Although this method requires more computations than classical iterative analysis, it avoids convergence issues, especially for complex problems like deep-seated non-circular failure surfaces. When combined, these techniques offer a simple and automated solution to slope stability problems. This makes it useful for both research and practical engineering scenarios.

Hammah et al. (2004) conducted a study to determine the factor of safety of slopes using the "shear strength reduction" method through finite element analysis. The method involves reducing the shear strength parameters in a step-wise manner until the slope becomes unstable. The results obtained were compared with those obtained using the limit equilibrium method. The comparison showed that FEM outputs were consistent with the LEM analyses.

Cala et al. (2004) conducted a study to see the difference between the Modified Stress-Strain Reinforcement (MSSR) method and Limit Equilibrium Method (LEM) for slope stability analysis. Unlike LEM, MSSR does not require assumptions about the shape and location of the slip surface, allowing it to consider multiple possible failure surfaces. However, the conclusion acknowledges that MSSR comes with certain limitations, including the need for a correct interpretation of multiple slip surfaces, requiring a thorough understanding of the failure mechanism.

Sakellariou & Ferentinou (2005) focused on dynamic slope stability assessment, aiming to understand the significance of various parameters and estimate the safety factor (FS) against circular and wedge failure mechanisms. Artificial Neural Networks (ANNs) were employed to predict the safety factor and stability for each failure mechanism. These networks, trained on diverse datasets, demonstrated success in capturing the relationships between input and output parameters. The use of ANN was highlighted for its advantage in handling multivariate problems, as they

do not require prior knowledge of the relationships and can accurately assess non-linear connections between parameters.

Baker (2006) studied the relation between safety factor, height and strength of slopes. In the study, it is mentioned that safety factors with respect to shear strength are acknowledged as useful but only hold clear physical significance at failure when they are equal to 1. The study establishes a simple analytical relation between safety factors with respect to strength and height through variational analysis. These alternative safety factors provide measures for slope stability, with the safety factor with respect to height offering clearer physical interpretation compared to shear strength-based factors.

Stead et al. (2006) emphasize the diverse range of tools available for analyzing rock slopes, particularly highlighting the significance of advanced numerical codes for simulating a realistic rock slope failure. They underscore the importance of considering brittle behavior and internal deformation in deforming rock slopes, influenced by a combination of yield and fracturing. The paper discusses the potential of discrete-element and hybrid finite/discrete-element codes in analyzing total slope failure, from initiation to deposition. To advance the application of these techniques, the authors suggest the need for improved rock slope characterization, encompassing both input properties and deformation instrumentation. They identify key issues for further research, including time-dependent or progressive rock slope failure, the role of cumulative internal damage, the influence of groundwater pore pressures on deformation, and scale effects related to rock mass strength and groundwater. While advanced numerical models have gained wider acceptance, the authors stress the importance of balancing their development with an increase in the quantity and quality of engineering geological field data. Good geological and geotechnical data are deemed essential for most numerical analyses, and the collaboration between engineers and geologists is crucial to maximize the use of current rock slope numerical models.

Cheng & Lau (2014) examined the results for SRM and LEM and it was found that the FOS and critical failure surfaces determined by both methods are quite similar for different combinations of soil parameters in most cases, except when friction angle is equal to 0. When the friction angle is greater than 0, the majority of FOS values calculated by SRM differs by less than 7.4% compared to the LEM results.

Liu et al. (2015) compared the Factor of Safety (FOS) and critical slip surfaces obtained from the Limit Equilibrium Method (LEM) and two finite element methods (ELSM and SRM) in the analysis of representative two-dimensional slope examples. Assuming the associated flow rule, the critical slip surfaces from the finite element methods and LEM generally align well, with the FOS from LEM slightly lower than the finite element methods. Notably, the SRM is identified as the most time-consuming solution, requiring multiple separate finite element analyses.

Neves et al. (2016) mention that the comparison of FEM and LEM has revealed significant differences in the o Factor of Safety values for purely granular materials. The LEM methods overestimate the slope's FoS by up to approximately 40%. However, in cohesive materials, the differences are mainly between 5% and 10%. Among the LEM methods, Janbu's simplified method produced the majority of MoS with the best correlation with the FEM results, specifically for cohesive soils. The differences between the MoS obtained from Janbu's method and the FEM results were mainly below 5%. Moreover, the correlation between this LEM method and the FEM results improved with a greater applied surcharge and a slacker slope.

In 2019, Raghuvanshi conducted a study on the various factors that affect the stability of slopes. The study analyzed 17 slope sections across different geological and geographical environments to identify the factors that influence rock slopes. To assess the relative importance of eight governing factors on the factor of safety (FoS), the study conducted statistical analyses, including sensitivity analysis and ANOVA. The eight factors that were studied include: slope inclination, upper slope surface

inclination, dip of potential plane failure, tension crack, slope height, cohesion, angle of friction, and height of water in tension crack. The results of the study indicate that all eight factors significantly affect the factor of safety, with variations in their relative importance observed among different slope types. The most statistically significant factors that emerged were dip of potential failure plane, water in tension crack, slope inclination, and slope height. Tension crack, angle of friction, upper slope surface inclination, and cohesion also played significant roles but were relatively lower in importance.

Gao et al. (2020) developed a hybrid model using artificial neural network and imperialist competition algorithm to predict the stability of slopes. The results showed that the hybrid model had a high-performance level, with R^2 and RMSE values of (0.9998 and 0.0017) and (0.9998 and 0.0017), respectively, for the training datasets, and (0.9988 and 0.0018) and (0.9987 and 0.0019) for the testing datasets.

Azarafza et al. (2021) presented a comprehensive systematic review of kinematical and limit equilibrium-based methods (LEMs) used in the analysis of stability in discontinuous rock and heavy jointed rock or soil-like lithologies. They indicated that LEMs, known for their flexibility, can be integrated with newer procedures like numerical and hybrid methods for efficient and rapid slope stability assessments. Looking ahead, Block theory, especially with Goodman's theorem, is identified as a robust approach for quantifying discontinuous rock slopes and evaluating stability conditions.

Ardestani et al. (2021) developed a computer program called TOPPLE2 that analyzes complex toppling slope failures which is mentioned in their article. It takes into account external loads such as groundwater and seismic forces to assess the stability of slopes. The program uses limit equilibrium equations to identify the possible toppling failure mechanisms in a defined slope and examine its stability. The accuracy and performance of TOPPLE2 were tested using case studies, which

showed good agreement between analytical and numerical solutions and the results obtained in TOPPLE2.

Marrapu et al. (2021) utilized an artificial neural network (ANN) to forecast slope stability. The findings make it evident that the ANN can accurately predict slope stability only when it is trained with high-quality and sufficient training data. Arya Babu and Chandrakaran (2022) compared the novel artificial neural network (ANN) approach with the conventional slope stability analysis techniques, which are limit equilibrium and the finite element method. 192 different slopes with six input parameters (unit weight of soil, cohesion, angle of internal friction, angle of slope, height of slope and pore water ratio) were used. The study found that all three methods provide factor of safety values that are very close to the actual FoS. On the other hand, FEM tends to give a slightly higher FoS value compared to LEM. Additionally, a slope stability prediction which was carried out using the ANN model, yielded an R2 value of 0.99473 and 0.99801 for the training and testing sets, respectively.

Azarafza et al. (2022) have developed a Limit Equilibrium Method (LEM)-based approach to assess the stability of slopes, specifically those comprised of weak materials like marls. The method, established through field surveys, geomechanical recording, and experiments, considers geotechnical and geological characteristics to accurately estimate instability conditions. The study focused on forty slopes in the South Pars special zone in southwestern Iran, resulting in the creation of stability charts. These charts, based on weathering conditions, provide insights into slope stability, angle of response, and shear strength of marls. The LEM methodology is applied to estimate the Factor of Safety in these charts, facilitating quick decisions in early-stage stability assessments based on slope angle, height, weathering degree, and geo-material type.

Idris (2022) evaluated the stability of abandoned laterite borrow pits in southwest Nigerian residential areas. Using a probabilistic method, the intrinsic variability of laterite soil was taken into consideration. Based on input parameters, the FLAC/Slope numerical analysis code computed factor of safety and simulated slope stability. An artificial neural network (ANN) was developed to link FoS with input parameters. A performance function that enables the prediction of the probability of slope failure using Monte Carlo simulations was constructed by integrating the ANN model with a critical FoS.

Jaiswal et al. (2023) studied slope stability through rock mass classification and kinematic analysis of some major slopes in Himalayas. The study evaluated the stability of 14 major slopes along NH 1-A in the Ramban district in the North Western Himalayas, an area prone to sliding. Rock mass classification systems and kinematic analyses were employed to identify stable zones and their susceptibility to sliding. The analysis revealed that seven slopes exhibit planar failure, one has toppling failure, and six have wedge failure. Toppling and wedge failures are predominant in granitic gneiss, while planar failure occurs in slate, phyllite, and schist rock types. The stability of slopes is mainly influenced by one or two discontinuity planes, with RMR values ranging from 37 to 74, indicating varying rock mass qualities from poor to good. Field investigations incorporated modification values of the Geological Strength Index (GSI) to assess slopes' conditions, resulting in SMR and CoSMR values indicating unstable to partially stable conditions, and SSR values calculated under dynamic and static conditions. The Q-slope approach categorized eight slopes as stable, four as uncertain, and two as unstable. An empirical equation establishing a correlation between RMR and SSR with a high coefficient of determination (R^2 value of 0.815) was developed. The overall findings suggest that most slopes in the study area are unstable and highly susceptible to failure, providing a foundation for further numerical analysis to identify critical slopes.

The studies conducted in the past have not comprehensively examined all the possible failure mechanisms simultaneously that can lead to slope failure. Moreover, most of the studies neglected upper slope inclination. Furthermore, these studies have also failed to offer any safety factor values and the failure type at the same time for any given slope, which is crucial for ensuring the safety of slopes.

CHAPTER 3

NUMERICAL ANALYSIS OF SLOPE PERFORMANCE

Rock slope stability has been investigated in various scales with monitoring instrumentations and computational methods. In-situ measurements on field scale trial excavations can shed light on similar cases with the utmost accuracy in terms of slope performance. However, investigation of different geomechanical and structural conditions can be costly and time-consuming. Alternatively, laboratory scale physical models sacrifice the material similarity but provide an overall insight about the slope mass behavior. Under these circumstances, computational simulations are favorable as they can be easily adopted to obtain detailed performance indicators for various scenarios involving complex geology and excavation sequences. Parametric studies provide the necessary background for developing a methodology for stable slope design.

This section presents the design and implementation of numerical simulations that investigate the slope performance with various specifications.In the pre-processing stage, the model layouts and the geomechanical parameters for continuous deformable bodies and discontinuity surfaces were determined. Commonly accepted rock mass quality classes were considered to be representative for intermediate conditions. Potential slope failures were evaluated by finite element and limit equilibrium methods. Characteristics of the mass and discontinuity driven failures were taken into account for selection of the suitable analysis technique. In this aspect, limit equilibrium method (LEM) and finite element method (FEM) were used for continuum models of mass failure. Discontiniuty-driven failures were only investigated by LEM. The following sections describes the determination of the

settings for computational model like the material models, geomechanical properties, model geometry and boundary conditions.

3.1 Determination of Geomechanical Parameters

Mechanical inputs control the material behavior under load in computational models. A realistic simulation requires a representative and reliable input data set for the geological materials. Despite in-situ experiments provide the best results they are both costly and labor-intensive. Hence, empirical approaches are commonly employed to determine the elastic and plastic properties for the rock mass. This study preliminarily focuses on representing various geomechanical properties to provide a basis for a unified slope stability analysis method. Continuum and discontinuum material models were characterized for hypothetical rock mass and structural surfaces to cover a wide range of problem domains in mass and discontinuity-driven slope failures.

3.1.1 Model Input Parameters for Continuous Slope Material

In a parametric study, the range and increment of input variables should be constrained regarding the computational limitations. In this study, five rock mass classes were identified with different geomechanical characteristics and named as MP_1, MP_2, MP_3, MP_4, and MP_5 where 'MP' stands for the 'Material Property'. Rock mass quality was indicated in terms of the RMR system developed by Bieniawski (1989) (Figure 2.6). Better rock mass quality conditions were associated with higher strength and stiffness properties. The highest quality class was labeled as MP_1 and the following classes indicate the rock mass with degrading mechanical properties. Table 3.1 presents the rock mass geomechanical parameters for the five distinct classes used in the current study.

Table 3.1 Rock mass properties for the mass failure numerical models

Parameters		**Rock Mass Quality Classes**				
		MP_1	**MP_2**	**MP_3**	**MP_4**	**MP_5**
Geological Strength Index (GSI)		90	70	50	30	20
Rock Mass Quality Description		**Very Good**	**Good**	**Fair**	**Poor**	**Very Poor**
Unit Weight, γ (MN/m^3)		0.026	0.026	0.026	0.026	0.026
Modulus of Elasticity, E (MPa) [(a)]		9200	3855	3536	2500	670
Poisson's Ratio, ν		0.25	0.25	0.25	0.25	0.25
Uniaxial Compressive Strength UCS (MPa) [(b)]		55.0	10.4	3.8	2.5	0.8
Peak	Cohesion, c (MPa)	11.4	2.7	1.1	0.8	0.3
	Internal Friction Angle, φ (°) [(c)]	45	35	30	25	15
	Tensile Strength, T (MPa) [(d)]	5.5	1.0	0.4	0.3	0.1
Residual	Cohesion, c (MPa) [(e)]	7.6	1.8	0.7	0.5	0.2
	Internal Friction Angle, φ (°) [(f)]	30	23	20	17	10
	Tensile Strength, T (MPa) [(g)]	3.7	0.7	0.3	0.2	0.1
Dilation Angle (°) [(h)]		5	4	3	3	2

Geological Strength Index (GSI) (Hoek & Brown, 1997) system was employed to associate the mass quality with the modeling parameters. Literature involves various correlations of rock mass quality and intact rock properties with the modulus of elasticity, uniaxial compressive strength, tensile strength, cohesion and internal friction angle. However, each approach has certain limitations regarding the conditions they cover. Considering the drawbacks of each method this study makes

adjustments and assumptions on the input parameter set based on expert view. Elastic and plastic parameters are mainly calculated according to the Hoek & Diederichs (2006) and the Hoek and Brown criterion (Hoek & Brown, 2019). The following section highlights the major steps of calculation for the parameters listed in Table 3.1.

First, the RMR scores were determined for each material class and the representative GSI scores were calculated according to equation (1).

$$GSI = RMR - 5 \quad \textit{(for RMR>25)} \tag{1}$$

Based on the RMR System table intact rock strength was determined (Bieniawski, 1989). Next, the modulus of elasticity for the intact rock was calculated from the modulus ratio, which depends on laboratory tests that propose a certain relationship between the UCS and E_i. Later on, the rock mass modulus of elasticity (a) was calculated with the Generalised Hoek & Diedrichs method (2006) (equation 2) for the very good and good rock classes. For the other rock classes, Hoek, Carranza-Torres and Corkum's method was used (Corkum et al., 2002) (equation 3) where; E_{rm}= Elastic modulus of rock mass, E_i= Elastic modulus of intact rock, D= Disturbance factor.

$$E_{rm}\ (MPa) = E_i\ (0.02+\frac{1-\mathrm{D}/2}{1+e^{(\frac{60+15D-GSI}{11})}}) \tag{2}$$

$$E_{rm}(GPa) = \left(1-\frac{D}{2}\right) \times \sqrt{\frac{\sigma_{ci}}{100}}\, 10^{((GSI-10)/40)} \quad \textit{(for } \sigma_{ci}\textit{<100 MPa)} \tag{3}$$

Uniaxial compressive strength of the rock mass (b) was calculated from the equation 4, where φ is internal friction angle and c is cohesion.

$$UCS = 2ctan\left(45 + \frac{90 - 2\phi}{2}\right) \quad (4)$$

Rock mass internal friction angles (ϕ) were adjusted regarding the recommendations in RMR table (Bieniawski, 1989). Rock mass tensile strengths (d) were calculated according to Sheorey (1997) who claims that the UCS is typically up to 10 times greater for many rock types. For the post failure stage, a softening model was assumed for all the material classes. The residual values denoted by (e), (f) and (g) were assumed to be equivalent to two-thirds of the corresponding peak values and dilation angles were taken as one-tenth of the respective internal friction angles.

3.1.2 Model Input Parameters for Structural Discontinuities

Mechanical characteristics of discontinuities were identified in terms of three joint classes named as JMP_1, JMP_2, JMP_3 where "JMP" stands for the "Joint Material Properties". JMP_1 represents the joint properties for almost smooth or slickensided surfaces with a high tendency to slide. Slightly rough and very rough surfaces were included in JMP_2 and JMP_3 classes. The joint material parameters are given in Table 3.2.

Table 3.2 The joint material properties used in the LEM models

Joint Material Properties	Cohesion (MPa)	Friction Angle (°)	Joint Roughness Coefficient (JRC)
JMP_1	0.2	35	4
JMP_2	0.5	38	9
JMP_3	0.8	54	19

The cohesion and friction angle of JMP_1 (Agharazi et al., 2012), JMP_2 (Agharazi et al., 2012) and JMP_3 (İşleyen, 2017) were defined regarding the literature that establish a correlation between the joint roughness coefficient (JRC) and the mechanical properties. JRC has a range of 1 to 20 (Barton & Choubey, 1977);

however, this study associated only three of these values to the determined joint classes (4 for $JMP_{1,}$ 9 for JMP_2 and 19 for JMP_3). Each class represents a unique shear strength and provides a basis for the computation of slope safety factor in plane, wedge, and toppling mechanisms. Finally, expert view was considered to adjust the joint sliding models and the outputs were used in the analysis of discontinuity-driven failures.

3.2 The Model Geometry and Boundary Conditions

Computational models were prepared regarding a parameter set that constitute the representative slope geometry and structural conditions conforming to the failure mode. For an open pit excavation, the geometrical inputs include the slope height (Figure 3.1), overall slope angle, upper face inclination and pit bottom width. Besides, the model extents were designed based on the specifications of the computational methods. Geological complexities were aimed to be ignored in this study. Therefore, a homogeneous, isotropic and continuous material was implemented in the slope mass and host rock. Geomechanical configurations were arranged to represent only some significant conditions. Structural discontinuities were also designed only for some significant orientations. The following section covers the model geometry for mass-driven and discontinuity-driven failures.

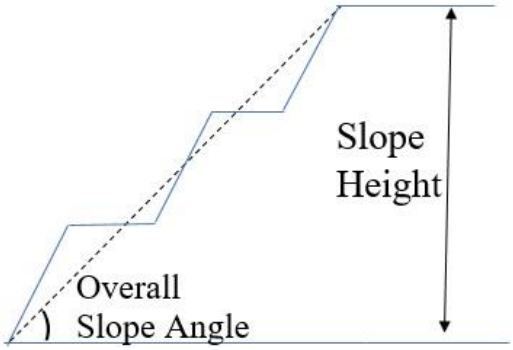

Figure 3.1 An example representation of slope height and overall slope angle

3.2.1 FEM Models for Mass Failure Analysis

A 2D plane strain code was employed for the FEM models. The external dimensions were determined regarding the excavation induced stress gradient. Considering the variation in slope height and large number of models in the parametric study, the model height was set to be 5 times the pit depth and the model width was arranged to be 10 times the ultimate pit extent. The pit bottom was fixed to 50 m in all models. A sample model view is given in Figure 3.2.

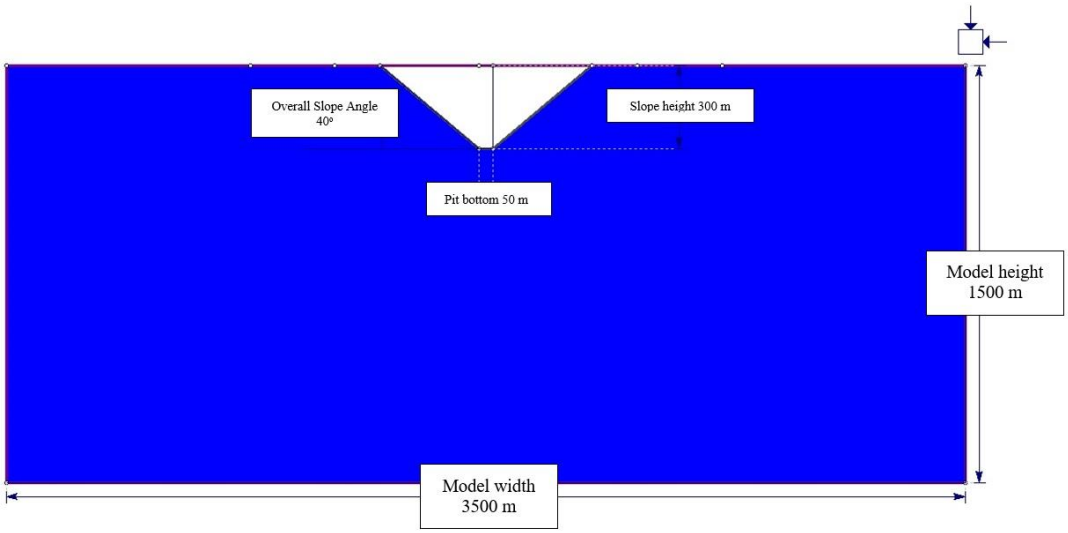

Figure 3.2 A sample FEM model

For the boundary conditions, the left and right bottom corners were fixed in both x and y directions to stop the body motion. The side walls were restrained only in x direction and the bottom was fixed only in y direction. The model top representing the topographical surface was set free in any direction.

The slope models were implemented in Rocscience RS2 software. Considering its improved performance, the model body was meshed with six noded triangles and a fine mesh density was allocated around the slope mass. A sample discretized and meshed model for slope design can be seen in Figure 3.3.

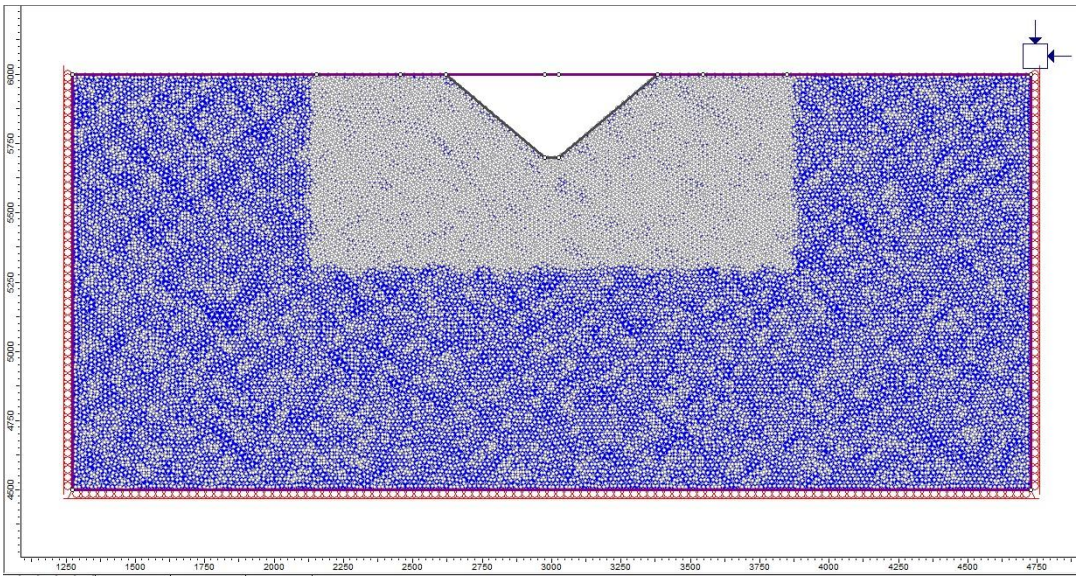

Figure 3.3 A sample model with FEM mesh and boundary conditions

FEM models were computed using the 'shear strength reduction (SSR)' method that provides a slope safety factor based on the degradation ratio of the strength and stiffness parameters.

In addition, stress and deformation can be observed to comment on the potential failure mechanism. The FEM models aim to examine the impact of geometrical and geomechanical variations on the slope stability. The model outputs with mechanical indicators were used to create a methodology to assess the slope stability under different conditions.

A total of 630 models were used to generate a comprehensive dataset of 3150 mechanical outputs, including critical factor of safety, maximum total displacement, and maximum shear strain. Data gathering steps are explained thoroughly in the following section.

The models were designed to include all meaningful combinations of input parameters. The slope height ranged from 50 to 300 meters, and the overall slope angle was studied between 10° to 80° with a 10° increment.

Additionally, three upper face inclination angles (0°, 10°, and 20°) and five different material properties were investigated. The range of model input parameters are shown in Table 3.3.

Table 3.3 Finite element model input parameters

Model Input Parameters	**Range**							
Slope Height, (m)	50	100	150	200	250	300		
Overall Slope Angle, (°)	10	20	30	40	50	60	70	80
Upper Face Inclination, (°)	0	10	20					
Material Property	MP_1	MP_2	MP_3	MP_4	MP_5			

Three mechanical readings were recorded from each model. The maximum total displacements (Figure 3.4) and the maximum shear strains (Figure 3.5) were traced around the slope mass.

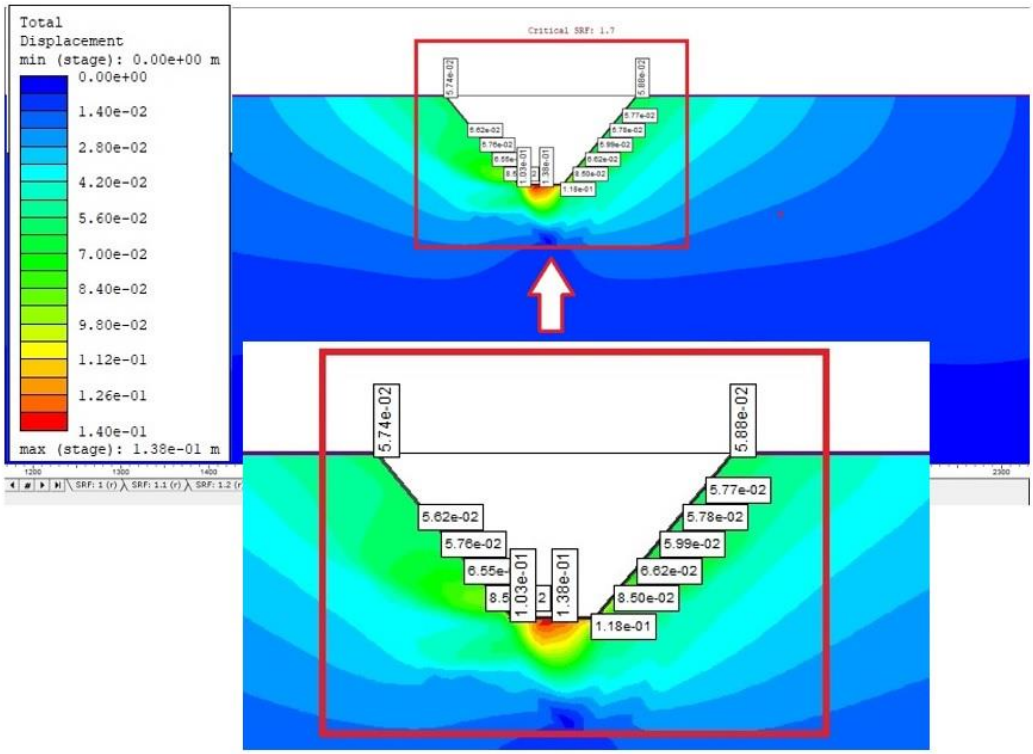

Figure 3.4 A sample maximum total displacement reading view from model

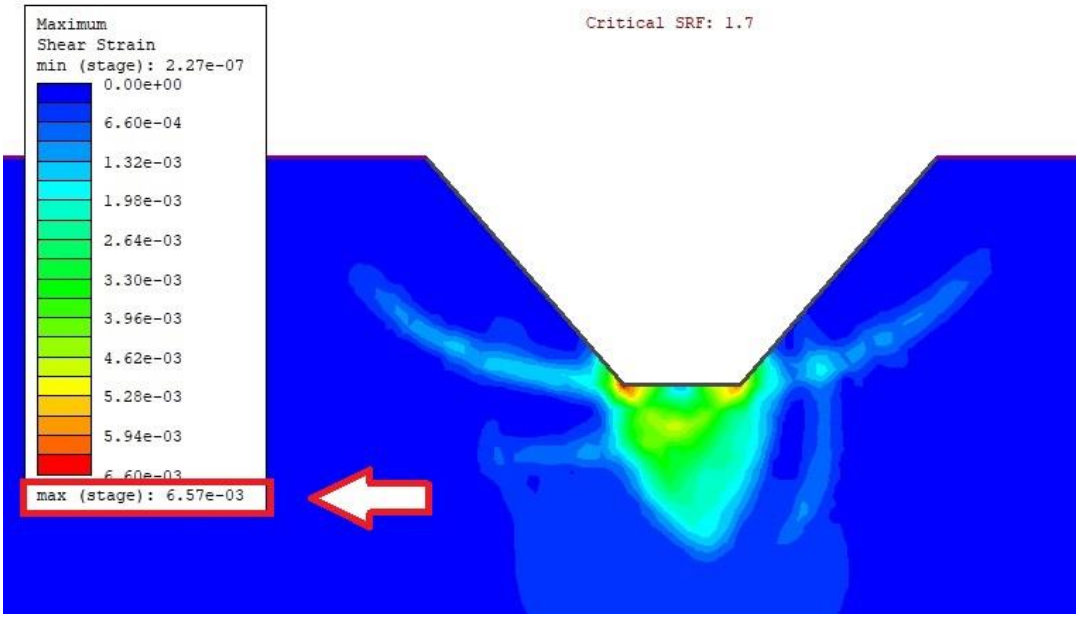

Figure 3.5 A sample maximum shear strain reading view from model

Critical factor of safety was manually determined by investigating the model interpretations and considering the critical strain for the related material classes. All the simulations were assumed to be in dry conditions.

3.2.2 LEM Models for Mass Failure Analysis

Another step of slope mass failure investigation was LEM modeling to determine the factor of safety. This method relies on force and moment equilibrium of the slices constituting the slope mass. The slices are assumed to be rigid and the output is a slope factor of safety. Compared to the FEM-SSR simulations, this method lacks in computation of stress and deformations. The FEM model geometry was used in LEM models to investigate only circular and non-circular failure modes. Multiple stochastic failure surfaces were generated using search algorithms and the factor of safety was calculated for each of them. The failure surface with the least safety factor was considered in each case. To generate random failure surfaces, slope search

algorithm was used for circular failure, and path search algorithm was opted for the non-circular failure analysis. The computational models were implemented in Rocscience Slide2. Figure 3.6 shows a sample view of the LEM models.

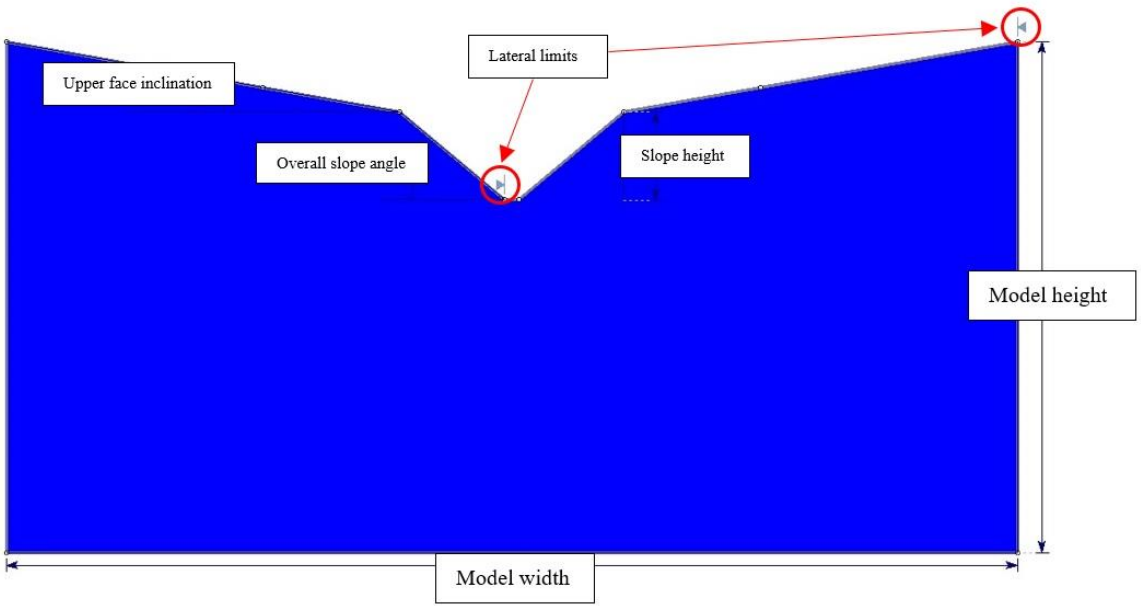

Figure 3.6 A sample LEM model

A dataset involving the slope safety factor for circular and non-circular failure modes were generated from 1260 models. The model settings and material properties were the ones shown in Table 3.3 that were also used in the FEM models.

Commonly two techniques are used in evaluating the slope safety factor for cohesive soils: the Bishop method, and the Janbu method. The Bishop method takes into account the interactions between adjacent slices and is capable of analyzing failures in cohesive soils. The Simplified Bishop method assumes that the forces between the slices are horizontal, but it has the drawback of being an iterative process and is less accurate in stratified soils. The Janbu method disregards the vertical and tangential components of the slices. However, it is particularly suitable for analyzing non-circular slip surfaces (Pereira et al., 2016). In this study, safety factors were

calculated by the Bishop Simplified Method (Bishop & Morgenstern, 1960) for circular failure and Janbu Simplified Method (Janbu, 1973) for non-circular failure analysis.

3.2.3 LEM Models for Plane Failure Analysis

Planar slide of discontinuity surfaces was analyzed using LEM based computational simulations in Rocscience RocPlane software. A sample model view is presented in Figure 3.7.

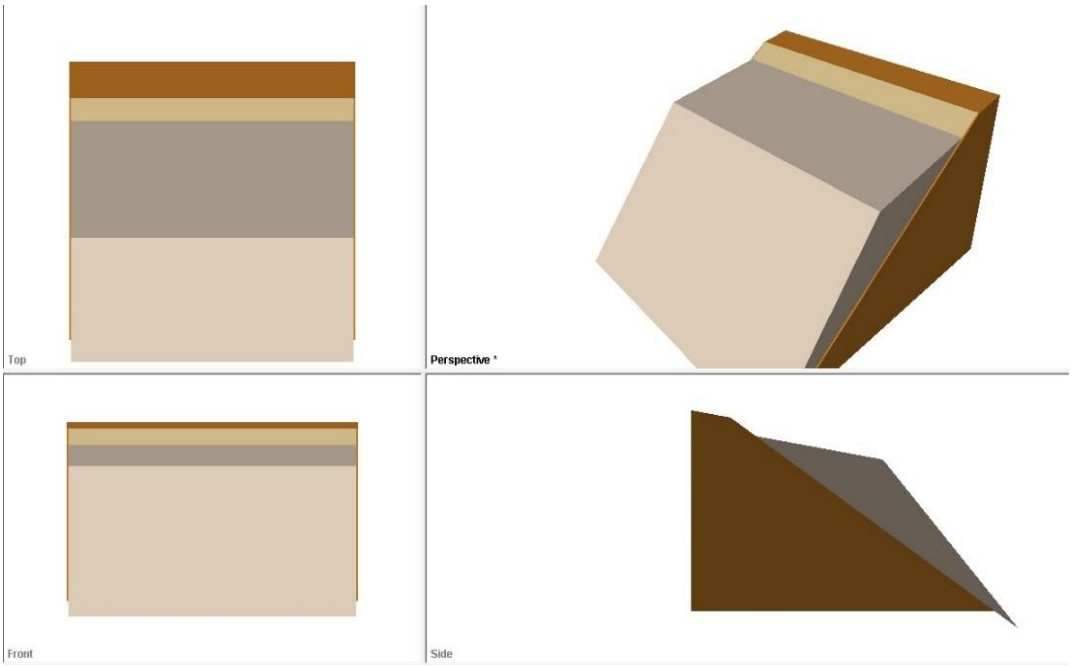

Figure 3.7 A sample view of planar slide analysis

Slope safety factors were calculated for a total of 342 models. Similar to the continuum models parametric studies were covered for various input parameters such as the slope height ranging from 50 to 300 meters, and seven different overall slope angle (OSA) between 20° to 80°. Additionally, simulations were conducted with five different discontinuity plane angles between 15° to 75° and three different

joint strength properties. The intervals of the model input parameters are shown in Table 3.4.

Table 3.4 Input parameters for plane failure models

Model Input Parameters	**Range**						
Slope Height, (m)	50	100	150	200	250	300	
Overall Slope Angle, (°)	20	30	40	50	60	70	80
Failure Plane Angles, (°)	15	30	45	60	75		
Joint Material Property	JMP_1	JMP_2	JMP_3				

Model design limitations are decided regarding the characteristics of plane failure and listed as follows;

- Failure plane angle must be less than overall slope angle
- Failure plane angle must be higher than upper face inclination.

The overall slope angle range started from 20° since the minimum failure plane angle was set to 15°. The upper face inclinations besides the horizontal surface were also modelled, but the findings point out that it is not significantly controlling the slope safety factor.

3.2.4 LEM Models for Wedge Failure Analysis

Wedge failure mode in rock slopes was analyzed using LEM based computational simulations in Rocscience RocSwedge software. A sample wedge failure model is given in Figure 3.8.

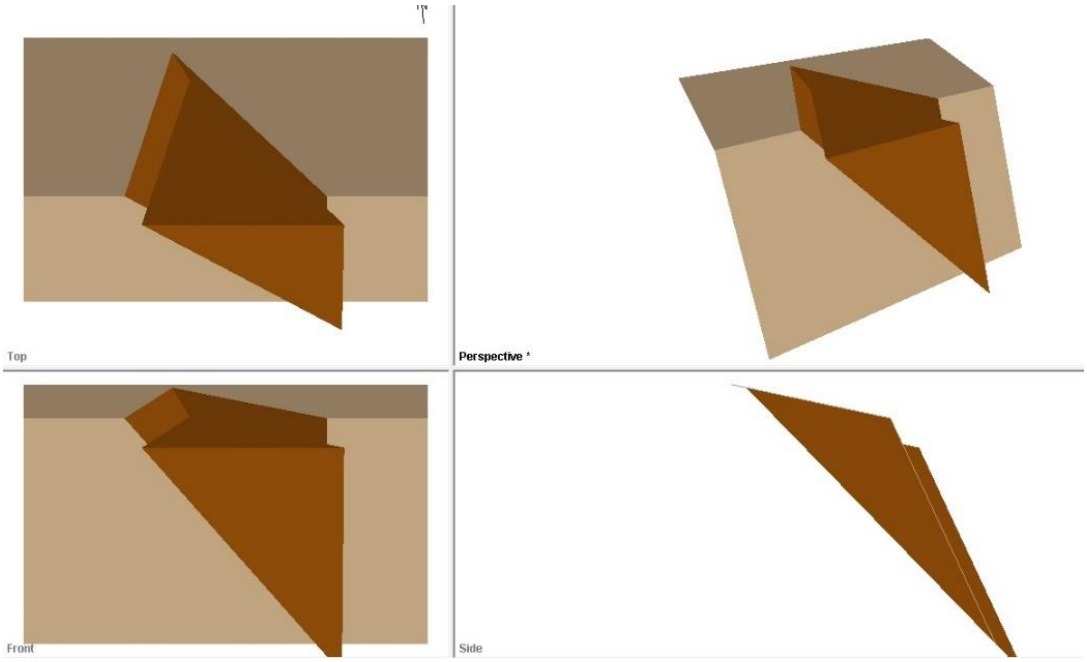

Figure 3.8 A sample wedge failure model

The parametric study explores 3547 models for the slope safety factors under different discontinuity orientations and shear strength characteristics.

Design parameters include the slope height, slope dip, discontinuity dip, the difference between slope dip direction and the dip direction of the first discontinuity plane, the difference between slope dip direction and the dip direction of the second discontinuity plane, and joint shear strength. The range of input parameters are shown in Table 3.5.

Table 3.5 Input parameters for wedge failure models

Model Input Parameters	**Range**							
Slope Height, (m)	50	100	150	200	250	300		
Slope Dip, (°)	10	20	30	40	50	60	70	80
Dip of the First Discontinuity, (°)	15	30	45	60	75			
Dip of the Second Discontinuity, (°)	15	30	45	60	75			

Table 3.5 (continued)

The Difference of Slope Dip Direction and the First Discontinuity Plane, (°)	30	60	90	120	150	180	210	240	270	300	330
The Difference of Slope Dip Direction and the Second Discontinuity Plane, (°)	30	60	90	120	150	180	210	240	270	300	330
Joint Shear Strength Class	JMP_1	JMP_2	JMP_3								

3.2.5 LEM Models for Toppling Failure Analysis

Finally, toppling failure was also included in the parametric study and implemented Rocscience RocTopple software using LEM. Two different toppling modes were investigated, which were block toppling (Figure 3.9) and flexural toppling (Figure 3.10).

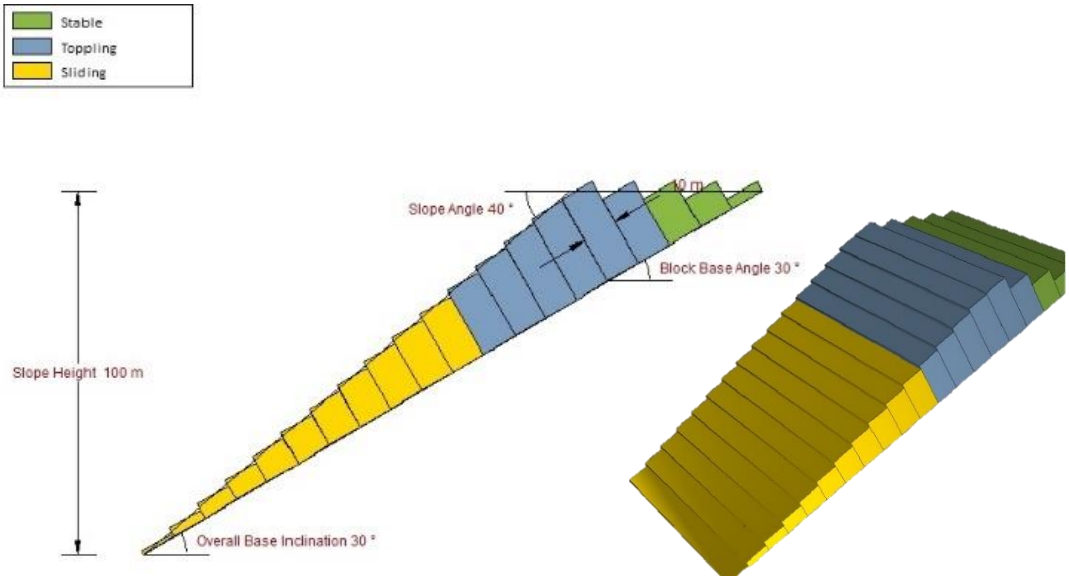

Figure 3.9 A sample block toppling view from limit equilibrium model

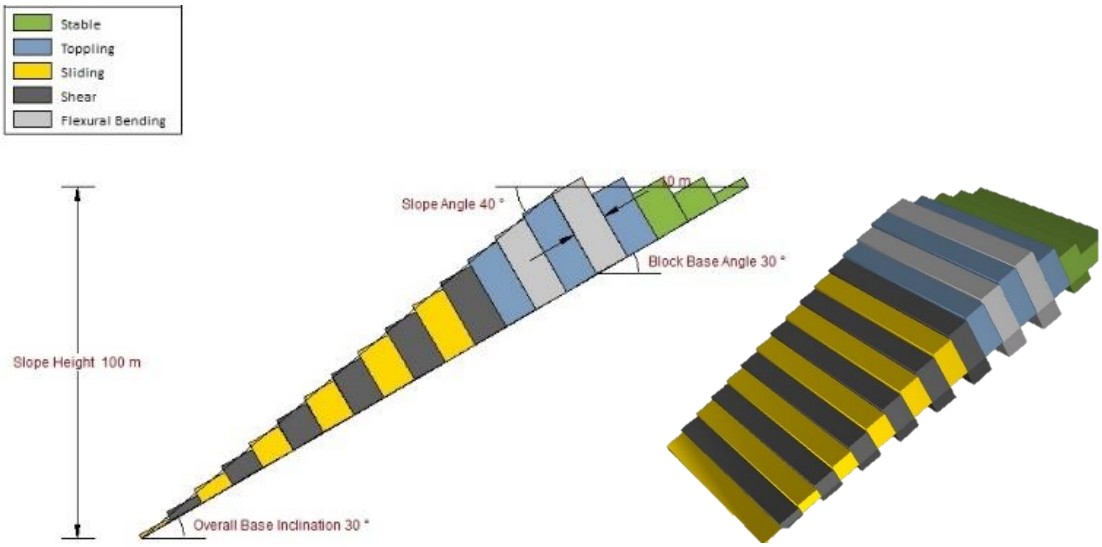

Figure 3.10 A sample block flexure toppling view from limit equilibrium model

Slope safety factor was calculated for different slope geometries and discontinuity conditions in 4262 models. The model parameters were slope height, overall slope angle, joint material property, discontinuity spacing, discontinuity dip, and overall base inclination. The range of input parameters are given in Table 3.6.

Table 3.6 Input parameters for toppling failure models

Model Input Parameters	**Range**							
Slope Height, (m)	50	100	150	200	250	300		
Overall Slope Angle, (°)	10	20	30	40	50	60	70	80
Toppling Joints Spacing, (m)	1	3	5	7	10			
Toppling Joints Dip, (°)	11	20	30	40	50	60	70	80
Overall Base Inclination, (°)	10	20	30	40	50	60	70	79
Joint Material Property	JMP_1	JMP_2	JMP_3					

Regarding the toppling mechanism, the models were subject to certain limitations as listed below:

- Overall base inclination must be less than the overall slope angle. Since maximum OSA was set to 80°, maximum overall base inclination was limited by 79° on the upper extreme.
- Overall base inclination must be greater than the (90° - Toppling Joint Dip). Since maximum overall base inclination was 79°, minimum toppling joints dip were restricted by 11°.

The joint shear strength characteristics were assigned to the base joints, toppling joints, and internal rock joints.

3.3 Interpretation of Numerical Simulations

FEM and LEM models were used to assess the slope performance with different geomechanical, structural and geometrical considerations. While FEM can provide mechanical outputs in terms of stress, strain and displacements, LEM calculates the slope safety factor. In this study, the slope performance indicators were traced and recorded in Excel spreadsheets to create a database, which will serve as a basis for the proposing an alternative slope stability analysis method. The sample layouts of the Excel sheets for each analysis type can be seen between Table 3.7 - Table 3.12.

Table 3.7 Layout of the spreadsheet involving FEM outputs for mass failure

Model Name	Slope Height (m)	Overall Slope Angel (OSA) (°)	Material Property	Upper Face Inclination (°)	Factor of Safety	Max. Total Displacement (m)	Max. Shear Strain

Table 3.8 Layout of the spreadsheet involving LEM outputs for mass failure

Model Name	Slope Height (m)	Overall Slope Angel (OSA) (°)	Material Property	Upper Face Inclination (°)	Factor of Safety	
					Circular	Non-Circular

Table 3.9 Layout of the spreadsheet involving LEM outputs for plane failure

Model Name	Slope Height (m)	Overall Slope Angel (OSA) (°)	Joint Material Property	Failure Plane Angle (°)	Factor of Safety

Table 3.10 Layout of the spreadsheet involving LEM outputs for wedge failure

Model Name	Slope Height (m)	Slope Dip (°)	Joint Material Property Combination	Failure Plane 1		Failure Plane 2		Factor of Safety
				Dip (°)	The Difference Between Slope Dip Direction and First Failure Plane Dip Direction (°)	Dip (°)	The Difference Between Slope Dip Direction and Second Failure Plane Dip Direction (°)	

Table 3.11 Layout of the spreadsheet involving LEM outputs for block toppling failure

Model Name	Slope Height (m)	Overall Slope Angle (°)	Base and Bedding Strength Combination	Toppling Joints		Overall Base Inclination (°)	Factor of Safety
				Spacing (m)	Dip (°)		

Table 3.12 Layout of the spreadsheet involving LEM outputs for block flexure toppling failure

Model Name	Slope Height (m)	Overall Slope Angle (°)	Base and Bedding Strength Combination	Internal Rock Joint Strength	Toppling Joints		Overall Base Inclination (°)	Factor of Safety
					Spacing (m)	Dip (°)		

Similar to the LEM models for mass failure FEM analyses provided the safety factor by SSR method. SSR gradually reduces the shear strength properties by a certain factor until the model becomes unstable. In this study, the SSR factors were searched with an increment of 0.1. Figure 3.11 shows a sample simulation.

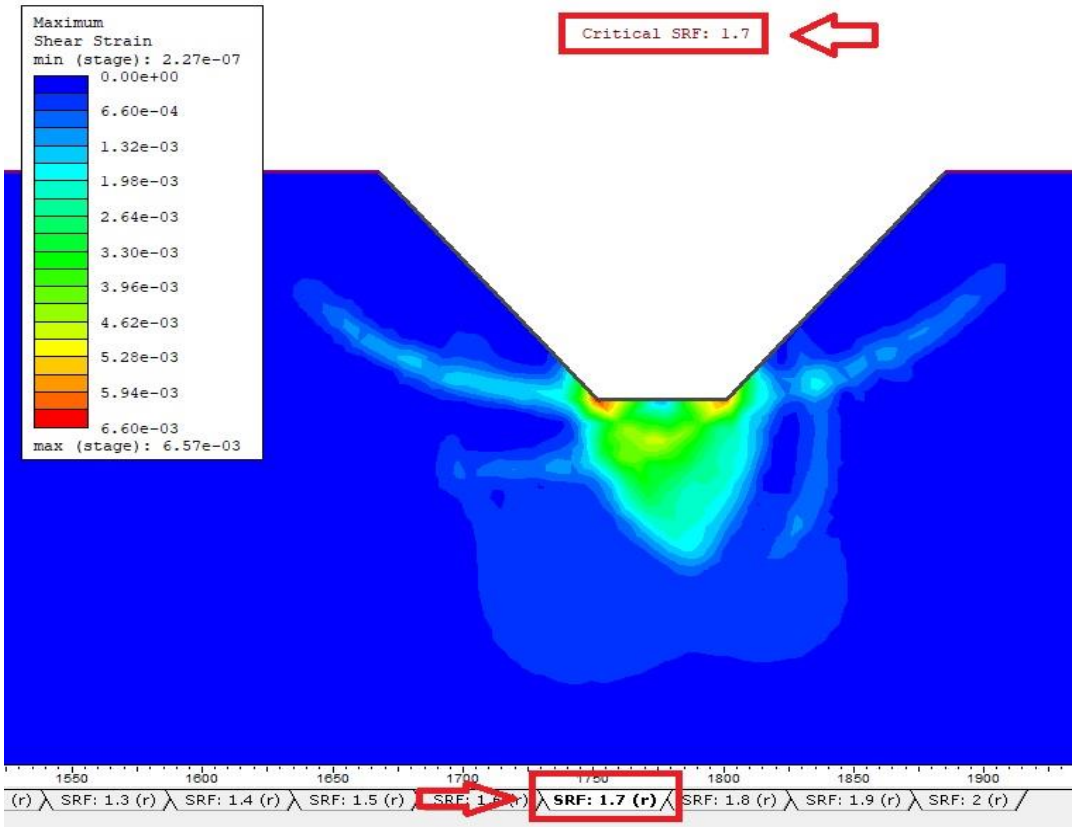

Figure 3.11 A sample FEM model with SSR analysis

To decide on the critical SSR factor, the maximum shear strain localizations were traced as shown in the Figure 3.5.

The maximum total displacement values were extracted from data queries as illustrated in Figure 3.4.

In the LEM models, the safety factor was obtained for each case as shown in the Figure 3.12 and Figure 3.13.

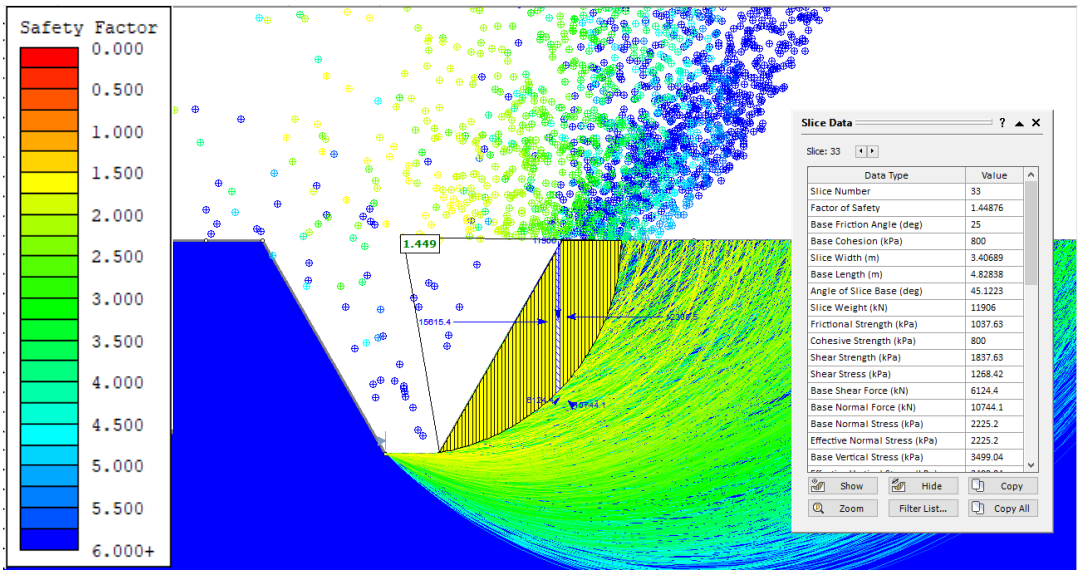

Figure 3.12 A sample view of safety factor values obtained from a mass failure model with LEM

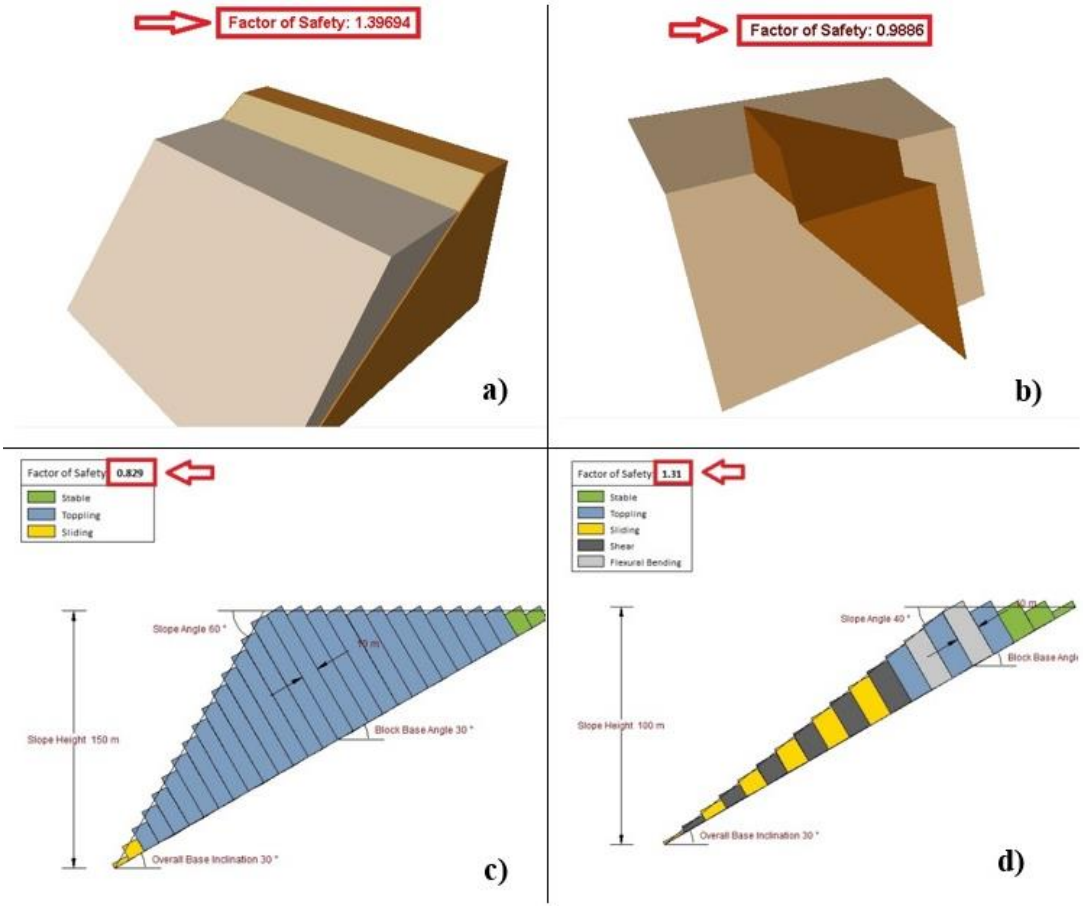

Figure 3.13 Sample views of safety factor values obtained from a plane (a), wedge (b), block toppling (c) and block flexure toppling (d) failure model

CHAPTER 4

MACHINE LEARNING SCHEME FOR THE INTERPRETATION OF NUMERICAL MODELS

This chapter presents the development of a machine learning model for predicting slope performance based on the parametric computational simulations. Structure of the artificial neural network (ANN) model and the training database involving the mechanical indicators of slope performance under various conditions were explained in detail. The trained model was proposed to be used as a preliminary tool in predicting the slope performance. Furthermore, benchmark cases were generated to test the quality of the proposed ANN model. The predictions were compared with the numerical simulation outputs to check the model validity.

4.1 Overview of the Machine Learning Assisted Slope Stability Model

Conventional statistics may perform poorly in correlating multiple variables with nonlinear relationships. Artificial intelligence can discover complex data relationships without suffering the computational efficiency. Considering slope stability is dependent on complex geological, geomechanical and structural variables, novel approaches can be expected to perform better compared to the classical statistics analysis such as multivariable regression. Recently, Artificial Neural Networks (ANN) are commonly used in geomechanics for prediction and forecasting. ANN can identify data patterns and relationships without explicit instructions. Both experiments and expert opinions can be integrated in the prediction model involving weighted neurons in multiple layers. ANN mimics the

structure of a biological brain in terms of processing and analyzing the data to make predictions and decisions (Agatonovic-Kustrin & Beresford, 2000).

This study makes use of feed-forward backpropagation technique to train a machine learning model for slope stability. The technique is popular and efficient due to its capability to improve network predictions over time. The feedback loop helps the network learn from its mistakes and adjusts its internal parameters to achieve better results. Back-propagation neural networks are widely used because they have a simple background and are easy to implement (Shan et al., 2022).

Recent research focuses on the optimization of learning process by generating computationally efficient algorithms. The Levenberg-Marquardt algorithm is one of them that works iteratively to solve nonlinear problems (Kelley, 1999). Computational experiments prove that Levenberg-Marquardt algorithm contributes to faster convergence and also improves the accuracy (Deshpande et al., 2022).

The network is composed of neurons that adjust the correlation regarding the data feed. The hyperbolic tangent sigmoid transfer functions were used in The Levenberg-Marquardt backpropagation training algorithm to obtain an improved predictive capacity (Javed et al., 2015).

Numerical outputs of the parametric slope simulations were used to train the ANN model. In each iteration, the internal parameters were adjusted through backpropagation and the network minimized the difference between the predicted and provided values. This process makes the network more dependable and precise in making future predictions.

After establishing the model, its performance was evaluated through regression analysis. The accuracy of the network's predictions was compared to numerical simulation outputs. Regression plots were used to check the accuracy of the predictive model. R value (the Pearson Product Moment correlation coefficient

(Russo, 2021)) is often considered a measure for the precision of statistical models. A high value of R is accepted to represent success of the ANN model and the quality of its training data. In this study, the regression plots were planned to include the correlation for training, validation, and test stages.

Figure 4.1 shows the network prototype representing the fundamental components with control parameters such as weight (W) and bias (b) for the plane failure case in this study. Other ANN model structures were represented in the Appendix E. These variables are adjusted during the training phase, in order to optimize the network's success.

At the beginning of the training process, random values are assigned to the neuron weights. Iterations of the training stage evolves the weights based on the input/output relationships. Once the output meets the desired requirements, the training stops and the network uses the ideal weights to make decisions (Afram et al., 2017).

The computational cost of model training is directly related to the neuron number. Therefore, the optimal number of hidden neurons was chosen by trial and errors (Jahirul et al., 2021).

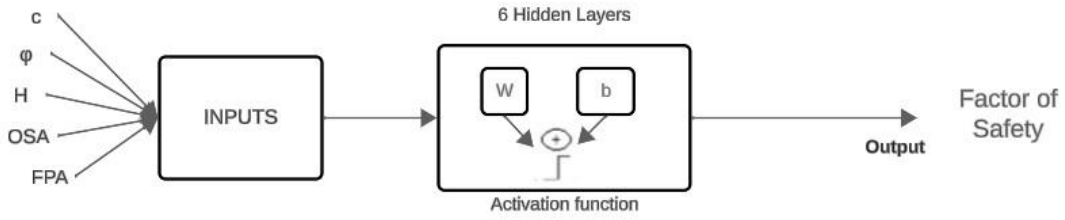

Figure 4.1 ANN model structure for plane failure

In this study, the number of hidden layers determined to maximize the R value for each slope failure mode are represented in Table 4.1. Three different ANN models were trained for mass failure using the FEM model outputs to predict the maximum total displacement, maximum shear strain and safety factor.

Moreover, two models were compiled for mass failure based on LEM models and safety factors for circular and non-circular failure.

Table 4.1 Number of hidden layers for each slope failure type

Failure Type		**Output**	**Number of Hidden Layers**
Mass Failure with FEM		Factor of Safety	6
		Maximum Total Displacement	9
		Maximum Shear Strain	11
Mass Failure with LEM	(circular)	Factor of Safety	6
	(non-circular)	Factor of Safety	7
Plane Failure		Factor of Safety	6
Wedge Failure		Factor of Safety	12
Toppling Failure	Block Toppling	Factor of Safety	6
	Block Flexure Toppling	Factor of Safety	6

A total of 10041 computational models and 90658 outputs (Table 4.2) were used to create a database to train ANN models predicting the slope performance regarding failure modes.

Table 4.2 Number of models, number of inputs and input parameters for ANN models

Failure Type		Number of Models	Number of Inputs	Input Parameters
Mass Failure with FEM		630	8	GSI, E, c, φ, T, H, OSA, UFI
Mass Failure with LEM	(circular)	630	8	GSI, E, c, φ, T, H, OSA, UFI
	(non-circular)	630	8	GSI, E, c, φ, T, H, OSA, UFI
Plane Failure		342	5	c, φ, H, OSA, FPA
Wedge Failure		3547	10	c_1, c_2, φ_1, φ_2, H, OSA, FPD_1, FPD_2, $FPDD_1$, $FPDD_2$
Toppling Failure	Block Toppling	2815	9	c_1, c_2, φ_1, φ_2, H, OSA, TJS, TJD, OBI
	Block Flexure Toppling	1447	9	c_1, c_2, φ_1, φ_2, H, OSA, TJS, TJD, OBI

The ANN models were trained using the neural net fitting tool in MATLAB. The models were divided into three sets: 70% for training, 15% for validation, and the remaining 15% for testing.

Following the training stage, a network function and regression plots were obtained for each slope failure mode. Finally, a total of nine different codes were generated and respective regression plots were obtained.

4.2 Interpretation of the ANN Models

This section presents the interpretation of ANN models. An extensive procedure of training, validating and testing were applied to the ANN model. In model training, testing and validation stages 90658 input entries were processed. the model inputs comprised of geometrical, geomechanical and structural parameters.

ANN model revealed the nonlinear relationship between these inputs and the slope performance indicators like strain, displacement and safety factor.

In order to decide on the optimal hidden layer number, each model was tested on a range of 1-25 layers and the highest R values were determined. A sample view showing the implementation and structure of ANN can be seen in Figure 4.2.

The figure involves the hidden layers, training algorithm, number of data used for each stage (training, validation and testing), R values, mean squared error values and regression plots of the model.

The trained model is stored in terms of a MATLAB function and regression plots were checked to see the quality of the model. A good model was defined to have an R value higher than 90% indicating low error rate in ANN model predictions.

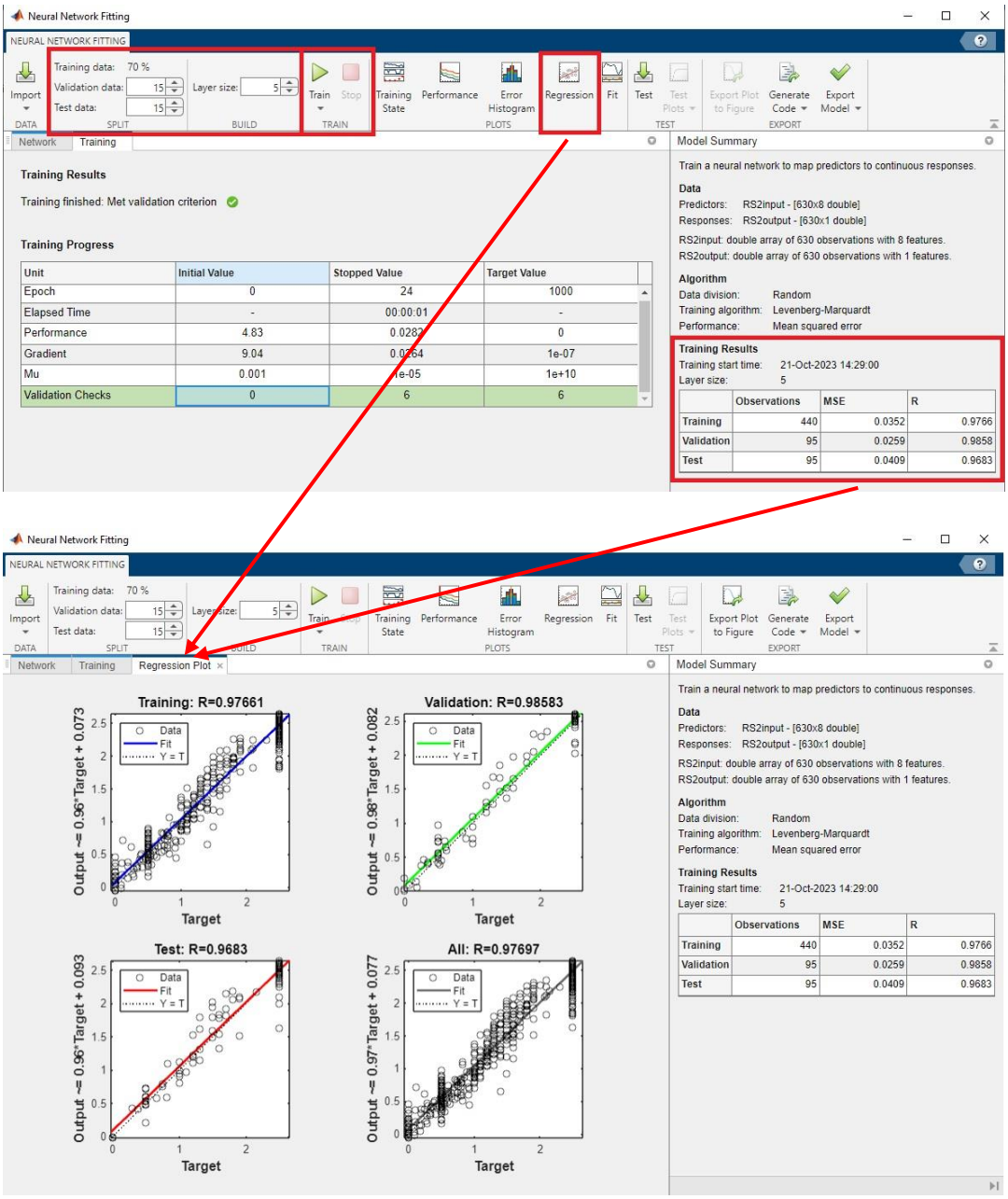

Figure 4.2 Sample ANN model training and validation in MATLAB

The trained model function was used later on to carry out additional quality checks on benchmarking cases. This methodology was aimed to replace the geomechanical simulations explained in the previous sections within the range of training parameter

set and for cases which were not mechanically simulated. Also, the ANN model was aimed to provide a quick prediction with low error instead of precise solutions with long numerical run-time

In this thesis, a total of nine ANN models and trained functions were designed to evaluate the stability of slopes. Out of these nine models, seven of them focused on determining the safety factors for slope failures. Additionally, one of the model functions was dedicated to finding the maximum total displacement values in slope mass failures, while the other one was used to calculate the maximum shear strain in slope mass failures.

CHAPTER 5

RESULTS AND DISCUSSION

This section presents the results of the mechanical simulations and evaluates the performance of the proposed slope design method for different slope failure modes. The parametric FEM and LEM model outcomes were visualized through conventional 2D plots.

5.1 FEM Simulation Outputs of Rock Slope Mass Failure

Firstly, the FEM models of slope mass failure providing the maximum total displacement, the maximum shear strain, and the factor of safety are explained in detail. A total of 630 simulations were run to obtain 1890 data points. The results for MP_3 are displayed in the following Figures 5.1 and 5.2.

The rest of the graphs are represented in the appendices A and B. All models with MP_1 provide a safety factor greater than 2.0. Therefore, the plots for MP_1 were not presented.

The graphs indicate the correlation between the maximum total displacement and the corresponding slope safety factor regarding the geomechanical characteristic of the rock mass. The same approach was followed for the maximum shear strain vs. slope safety factor plots.

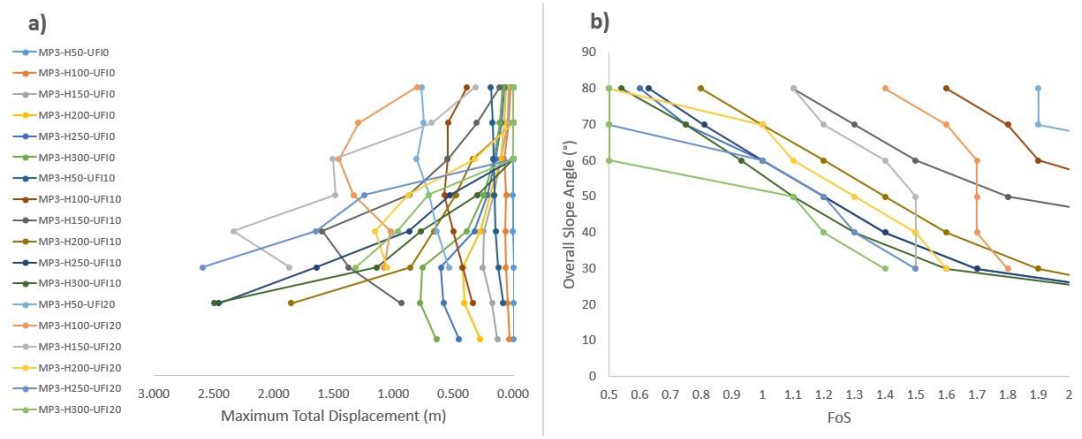

Figure 5.1 a) The maximum total displacement vs. OSA and b) slope safety factor vs. OSA plots for MP_3 rock mass characteristics obtained from FEM simulation of slope mass failure

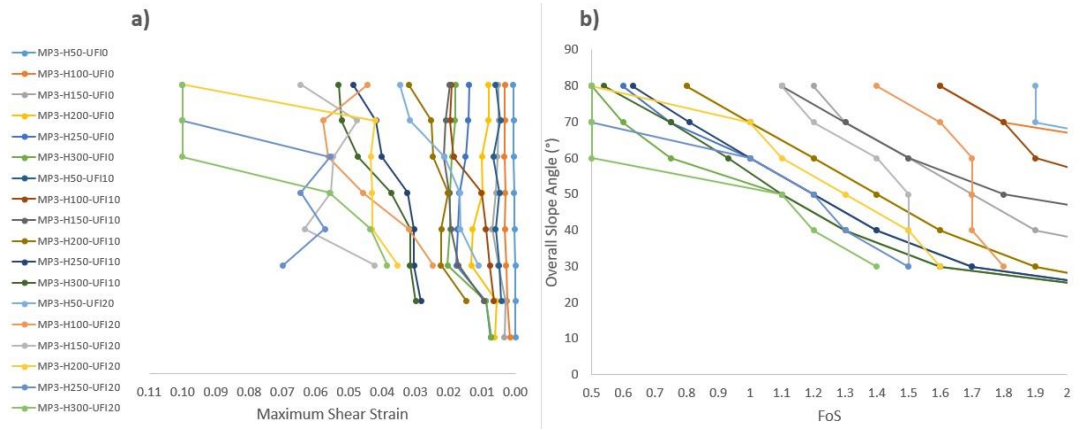

Figure 5.2 a) The maximum shear strain vs. OSA and b) slope safety factor vs. OSA plots for MP_3 rock mass characteristics obtained from FEM simulation of slope mass failure

The data trend presents a clear decrease in slope safety factor with increasing overall slope angle. Additionally, there is a slight decrease in safety factors as the upper face inclination increases. These findings suggest that there may be increased risk in slopes with steeper slope angles and upper face inclination.

Numerical experiments point out that weak rock mass properties in RS2 FEM simulations may lead to convergence problems as the code is not suitable for large deformation simulations. RS2 is capable of simulating the early stages of a failure rather than the covering entire failure involving body motion and progressive plastic deformations. Particularly in rock quality classes like MP_4 and MP_5, which are respectively weaker and tend to lead more displacements, the numerical difficulty in covering the entire failure is clear. However, non-convergence still provides insightful information about the slope stability. Table 5.1 presents the model settings that end up with non-convergence.

Table 5.1 Slope FEM models settings with non-convergence problem

UFI 0°					
H (m)	**MP_1**	**MP_2**	**MP_3**	**MP_4**	**MP_5**
50	none	none	none	none	80°
100	none	none	none	none	40°
150	none	none	none	80°	30°
200	none	none	80°	60°	20°
250	none	none	70°	50°	20°
300	none	none	60°	50°	20°
***UFI 10°**					
50	none	none	none	none	70°
100	none	none	none	none	40°
150	none	none	none	80°	30°
200	none	none	80°	60°	20°
250	none	none	70°	50°	20°
300	none	none	60°	50°	20°
***Note:**	Minimum OSA is 20° since UFI is 10°				
****UFI 20°**					
50	none	none	none	none	30°
100	none	none	none	none	30°
150	none	none	none	70°	30°
200	none	none	80°	60°	30°
250	none	none	70°	50°	30°
300	none	none	60°	50°	30°
****Note:**	Minimum OSA is 30° since UFI is 20°				

5.2 LEM Simulation Outputs of Rock Slope Mass Failure

Similar to the FEM plots, slope safety factor was also plotted for the LEM models. The database involves a total of 1260 simulations with equal numbers of models for circular and non-circular failure. The results for MP_3 were presented in Figure 5.3. For other rock mass material properties' results mentioned in appendices C. Since all the safety factor are higher than 2.0 for MP_1 and MP_2, these graphs were not given.

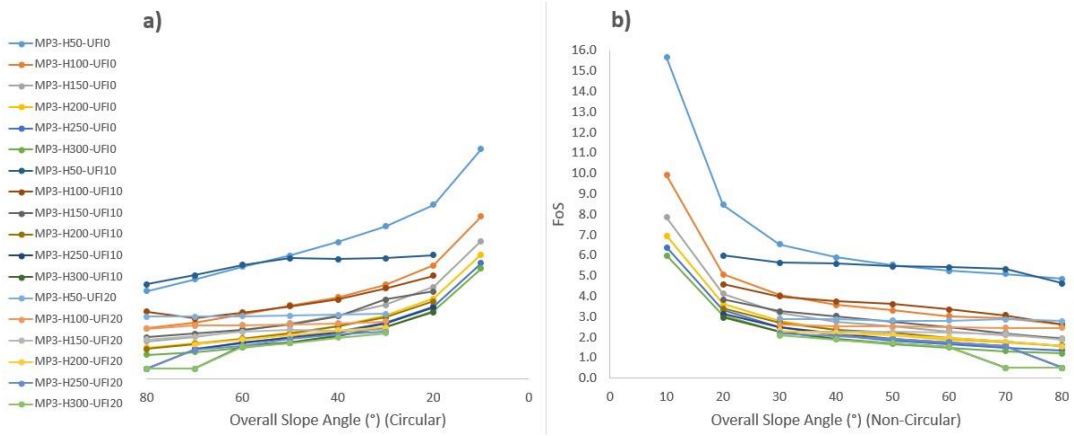

Figure 5.3 Slope safety factor vs. overall slope angle plots a) for circular and b) for non-circular failure surface from LEM simulations for MP_3 rock mass material properties

Based on the graphical representations, it is apparent that the safety factor values in LEM are considerably higher when compared to those in FEM. That is due to the assumptions of these modeling techniques. While LEM assumes rigid slices constituting the slope FEM makes stress and deformation solutions for deformable bodies. Moreover, when comparing circular surfaces to non-circular surfaces under the same conditions, circular surfaces exhibit lower safety factors.

5.3 LEM Simulation Outputs of Discontinuity Driven Rock Slope Failure

This section presents the results of discontinuity-driven rock slope failures. For the plane failure, a total of 342 models were computed and a safety factor was calculated for the major discontinuity dominating the slope stability. The slope safety factors for JMP_1 were given in the Figure 5.4. The other plane orientations were given in the appendices D, which illustrate the relationships between the overall slope angle, the joint material property, and slope height.

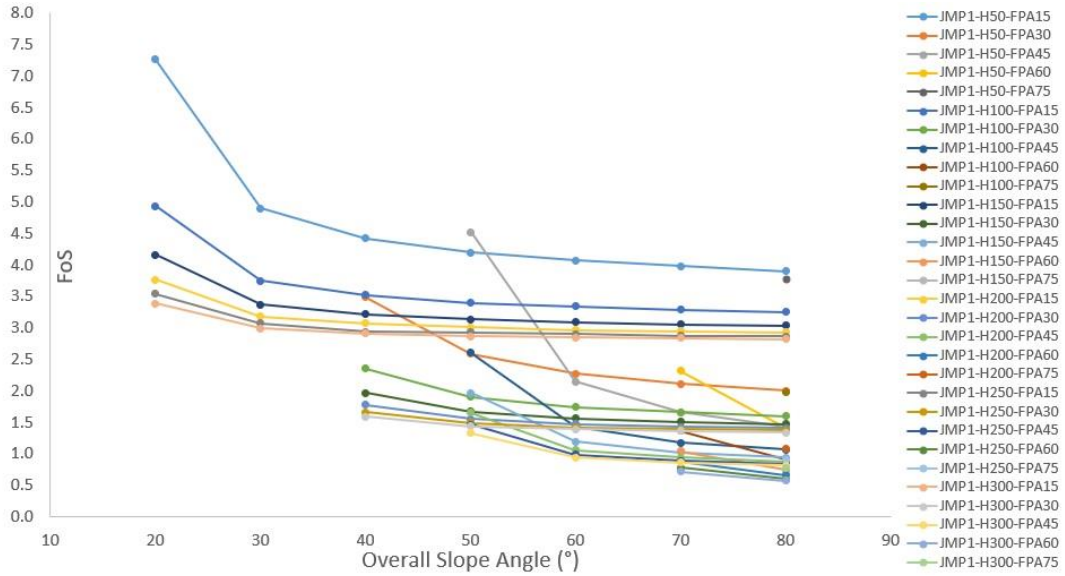

Figure 5.4 JMP_1 safety factor values for planar slope failure

Based on the graphs, it was observed that the factor of safety tends to decrease as the height of the slope and overall slope angle increases for the same plane angle. Moreover, different upper face inclinations were also modelled and computed for planar failures. However, safety factor values did not change with the increase of upper face inclination until 20°. So, the results for those models are not presented.

After planar failure, wedge failure was also investigated in a total of 3547 models. The models were computed to get the safety factors where wedges form on the slope

mass. The simulations outputs were tabulated. However, due to the wide range of inputs and outputs, the wedge failure simulations could not be visualized using traditional 2D or 3D graphical tools. Table 5.2 represents only a subset of the entire dataset.

Table 5.2 A small set of wedge failure data set

Slope Height (m)	Slope Dip (°)	Joint Material Property Combination	Failure Plane 1		Failure Plane 2		Factor of Safety (FoS)
			Dip (°)	The Difference of Slope and First Failure Plane Dip Directions (°)	Dip (°)	The Difference of Slope and Second Failure Plane Dip Direction (°)	
…	…	…	…	…	…	…	…
200	80	JMP1-1	30	270	30	330	1.9
200	80	JMP1-1	30	300	30	330	1.9
200	80	JMP1-1	30	330	30	30	1.8
200	80	JMP1-1	45	30	30	330	1.6
200	80	JMP1-1	45	60	30	330	1.9
200	80	JMP1-1	45	90	30	30	1.6
200	80	JMP1-1	45	120	30	30	1.7
200	80	JMP1-1	45	60	45	330	1.5
200	80	JMP1-1	60	30	30	300	1.8
200	80	JMP1-1	60	30	30	330	1.4
200	80	JMP1-1	60	60	30	330	1.7
200	80	JMP1-1	60	90	30	30	1.9
200	80	JMP1-1	60	120	30	30	1.6
200	80	JMP1-1	75	30	30	300	1.8
200	80	JMP1-1	75	30	30	330	1.5
200	80	JMP1-1	75	60	30	330	1.7
200	80	JMP1-1	75	30	45	270	1.9
200	80	JMP1-1	75	30	45	300	1.3
200	80	JMP1-1	75	30	45	330	0.9
200	80	JMP1-1	75	60	45	300	1.8
200	80	JMP1-1	75	60	45	330	1.2
200	80	JMP1-1	75	90	45	30	1.4
200	80	JMP1-1	75	90	45	330	1.7
200	80	JMP1-1	75	300	60	30	1.0
200	80	JMP1-1	75	300	60	60	1.5
200	80	JMP1-1	75	330	60	30	0.7
200	80	JMP1-1	75	330	60	60	1.1

Table 5.2 (continued)

200	80	JMP1-1	75	330	60	90	1.6
200	80	JMP1-1	75	30	75	270	1.5
200	80	JMP1-1	75	30	75	300	1.3
200	80	JMP1-1	75	30	75	330	1.3
200	80	JMP1-1	75	60	75	300	1.4
200	80	JMP1-1	75	60	75	330	1.3
…	…	…	…	…	…	…	…

As the height of a slope increases and the slope angle becomes steeper, the safety factor of the slope decreases for the same failure plane orientations. In other words, the higher and steeper the slope, the more likely it is to experience a wedge failure.

Additionally, wedge failures were modeled with varying upper face inclinations. However, safety factor values remained constant until 20°, so results for those models were excluded.

Finally, two toppling modes were investigated, which were block toppling and block flexure toppling. A total of 2815 block toppling models and 1447 block flexure toppling models were computed.

However, similar to the wedge failure, the safety factors could not be plotted due to the variety and wide range of inputs. Instead, the entire dataset was presented in a table.

In Table 5.3, a small subset of the entire database, which covers only the slope height of 300 m, overall slope angle of 50° and base and bedding joint material parameters of JMP_1 was shown for block toppling failure.

Table 5.3 A small set of block toppling failure database

Slope Height (m)	Overall Slope Angle (°)	Base and Bedding Strength Combination	Toppling Joints		Overall Base Inclination (°)	Factor of Safety (FoS)
			Spacing (m)	Dip (°)		
…	…	…	…	…	…	…
300	50	JMP 1-1	1	80	10	0.7
300	50	JMP 1-1	3	80	10	0.8
300	50	JMP 1-1	5	80	10	0.8
300	50	JMP 1-1	7	80	10	0.8
300	50	JMP 1-1	10	80	10	0.9
300	50	JMP 1-1	1	70	20	0.8
300	50	JMP 1-1	3	70	20	0.8
300	50	JMP 1-1	5	70	20	0.8
300	50	JMP 1-1	7	70	20	0.9
300	50	JMP 1-1	10	70	20	0.9
300	50	JMP 1-1	1	60	30	1.0
300	50	JMP 1-1	3	60	30	1.0
300	50	JMP 1-1	5	60	30	1.1
300	50	JMP 1-1	7	60	30	1.1
300	50	JMP 1-1	10	60	30	1.1
300	50	JMP 1-1	1	50	40	1.2
300	50	JMP 1-1	3	50	40	1.2
300	50	JMP 1-1	5	50	40	1.2
300	50	JMP 1-1	7	50	40	1.2
300	50	JMP 1-1	10	50	40	1.2
300	50	JMP 1-1	1	41	49	3.6
300	50	JMP 1-1	3	41	49	3.6
300	50	JMP 1-1	5	41	49	3.6
300	50	JMP 1-1	7	41	49	3.6
300	50	JMP 1-1	10	41	49	3.6
…	…	…	…	…	…	…

It can be observed that the factor of safety increases with an increase in the spacing between toppling joints. On the other hand, a decrease in the overall base inclination

and an increase in the dip of toppling joints lead to a decrease in the factor of safety while other variables remain constant. Similarly, a higher slope height and overall slope angle result in a lower factor of safety.

When it comes to block flexure toppling, there is an additional variable to consider known as joint strength. Similar to block toppling failure, safety factors were computed and small subset of the entire database shown in the Table 5.4.

Table 5.4 A small part of the block flexure toppling failure's outputs

Slope Height (m)	Overall Slope Angle (°)	Base and Bedding Strength Combination	Internal Rock Joint Strength	Toppling Joints		Overall Base Inclination (°)	Factor of Safety (FoS)
				Spacing (m)	Dip (°)		
…	…	…	…	…	…	…	…
300	50	JMP 1-1	JMP 1	3	80	10	1.4
300	50	JMP 1-1	JMP 1	5	80	10	1.1
300	50	JMP 1-1	JMP 1	7	80	10	1.1
300	50	JMP 1-1	JMP 1	10	80	10	1.1
300	50	JMP 1-1	JMP 1	3	70	20	1.3
300	50	JMP 1-1	JMP 1	5	70	20	1.1
300	50	JMP 1-1	JMP 1	7	70	20	1.0
300	50	JMP 1-1	JMP 1	10	70	20	1.0
300	50	JMP 1-1	JMP 1	1	60	30	1.4
300	50	JMP 1-1	JMP 1	3	60	30	1.4
300	50	JMP 1-1	JMP 1	5	60	30	1.4
300	50	JMP 1-1	JMP 1	7	60	30	1.3
300	50	JMP 1-1	JMP 1	10	60	30	1.2
300	50	JMP 1-1	JMP 1	3	50	40	1.2
300	50	JMP 1-1	JMP 1	5	50	40	1.2
300	50	JMP 1-1	JMP 1	7	50	40	1.2
300	50	JMP 1-1	JMP 1	10	50	40	1.2
300	50	JMP 1-1	JMP 1	3	41	49	3.6
300	50	JMP 1-1	JMP 1	5	41	49	3.6
300	50	JMP 1-1	JMP 1	7	41	49	3.6
300	50	JMP 1-1	JMP 1	10	41	49	3.6
…	…	…	…	…	…	…	…

For block flexure toppling, the results of the models indicate that when the spacing between toppling joints increase, the safety factor decreases. Conversely, if the overall base inclination decreases and the dip of toppling joints increases, the factor of safety increases, assuming other variables remain constant. Moreover, a higher slope height and overall slope angle result in a lower factor of safety.

5.4 Validation of ANN Model for Rock Slope Stability Prediction

Increasing size and complexity of datasets reveals the weaknesses of conventional 2D graphs for representing relationships between multiple variables. These graphs often too complex to interpret the data trend, and in some cases, they cannot even be drawn. Moreover, in a crowded dataset it difficult to identify the intermediate conditions.

The parametric study in this research generated a rich database comprising of slope performance indicators. Regarding the variety of input and output variables, the conventional methods of data interpretation would be expected to be useless. Therefore, alternative techniques are required for developing this new slope stability analysis method, which is based on reliable computational simulations.

As stated before, ANN is opted for training a statistical predictor for slope stability. Each slope failure mode was trained using MATLAB-ANN toolbox. This way, non-linear equations for accurately predicting the safety factors, maximum total displacement (applicable only for FEM mass failure), and maximum shear strain (applicable only for FEM mass failure) were generated with an acceptable R value denoting the correlation in between the model prediction and simulation outputs.

In order to ensure the accuracy and reliability of the models, an additional stage of testing was established using benchmark cases. This involved generating a series of test cases to check the quality of the prediction. The benchmark cases were designed

to cover a broad range of possible. Once the benchmark cases were executed, the results from the computational models and the ANN predictions were compared. Regression graphs were created to analyze the correlation between the two models, and a determination coefficient was calculated to measure the strength of their relationship.

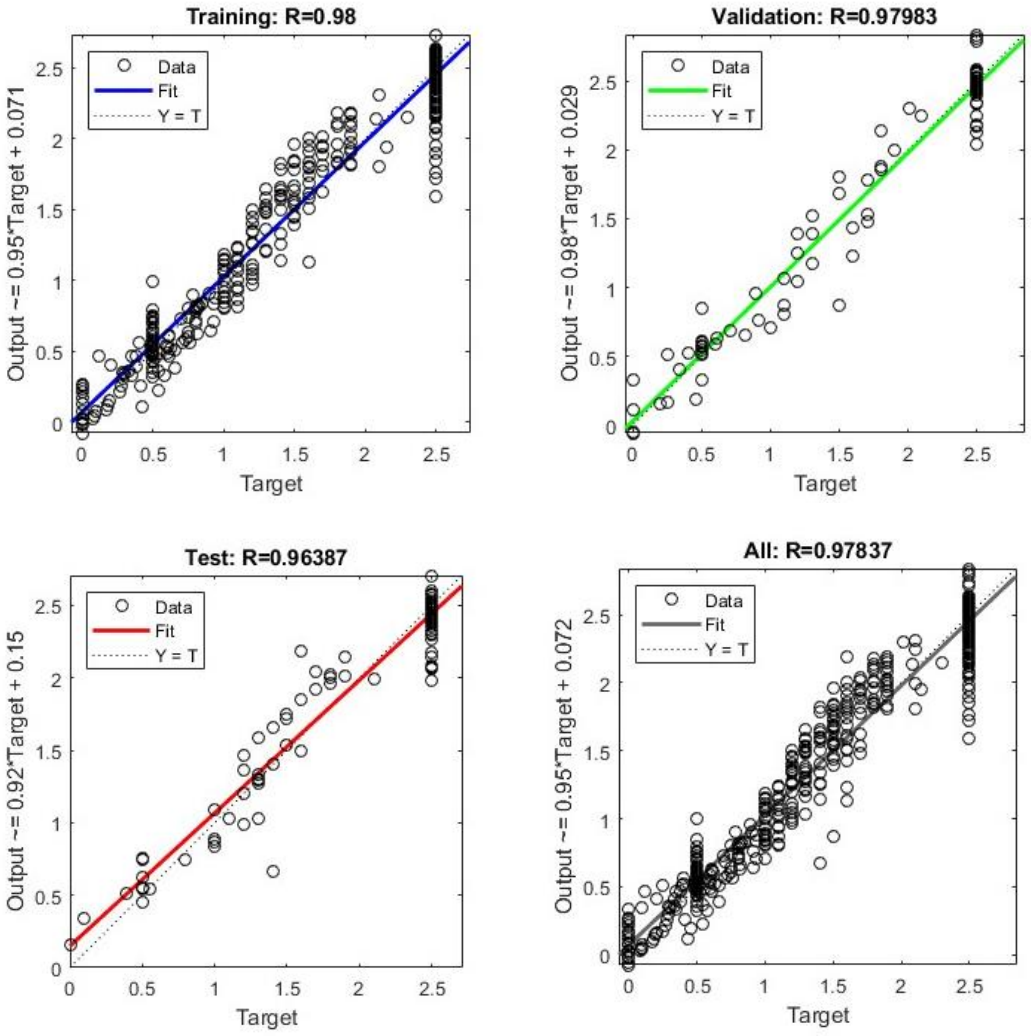

Figure 5.5 Regression plots showing the correlation between ANN predictions and FEM simulations of slope safety factor for mass failure

The Figure 5.5, Figure 5.6 and Figure 5.7 show the regression plots and R values in the training, testing, and validation stages obtained from ANN. These plots indicate that the R values for the factor of safety range from 96% to 98%, while for maximum total displacement they range from 91% to 95% and for maximum shear strain they range from 95% to 98%.

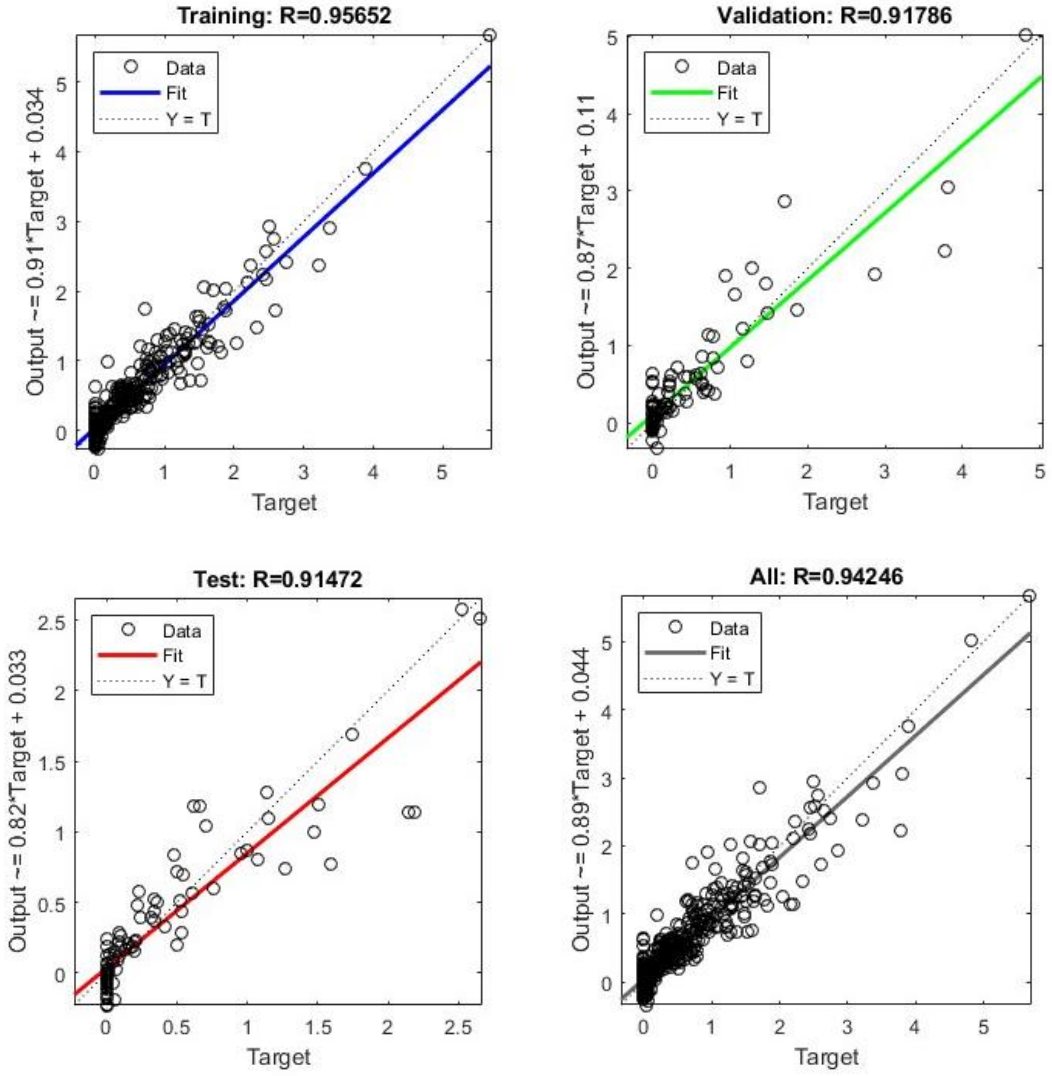

Figure 5.6 Regression plots showing the correlation between ANN predictions and FEM simulations of maximum total displacement for slope mass failure

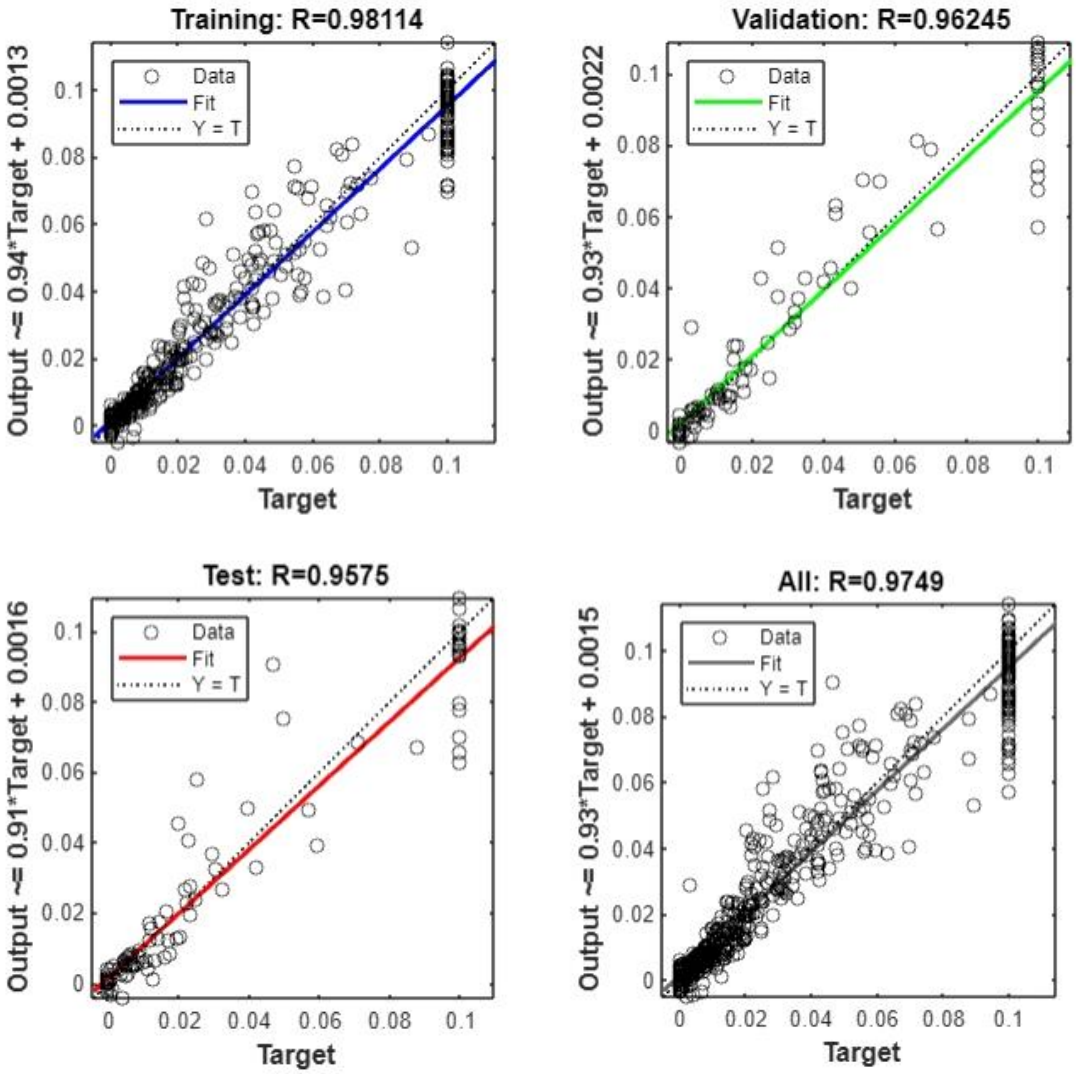

Figure 5.7 Regression plots showing the correlation between ANN predictions and FEM simulations of maximum shear strains for slope mass failure

Following the ANN, a Matlab script was utilized to evaluate the trained machine's prediction capability through 5 different benchmark cases which includes factor of safety, maximum total displacement and maximum shear strain as outputs. The benchmark cases are detailed in Table 5.5. Subsequently, the numerical model outputs were analyzed in conjunction with the ANN predictions through regression

analysis. Comparisons were drawn between these two sets of data, and the results were illustrated in Figure 5.8 for mass failure.

Table 5.5 Benchmark cases for FEM mass failure

Case No	Inputs				Outputs					
	Slope Height (m)	OSA (°)	Material Property	UFI (°)	Factor of Safety		Max. Total Disp. (m)		Max. Shear Strain	
					FEM	ANN	FEM	ANN	FEM	ANN
1	300	50	MP2	10	2.1	2.3	1.37	1.39	0.020	0.029
2	150	50	MP3	10	1.8	1.9	0.87	0.78	0.019	0.017
3	100	60	MP4	0	1.5	1.8	0.08	0.08	0.005	0.004
4	150	50	MP4	0	1.3	1.5	0.14	0.25	0.008	0.009
5	100	30	MP5	0	1.0	1.2	0.31	0.44	0.023	0.028

a)

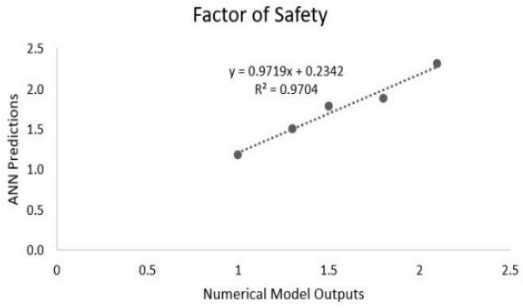

b)

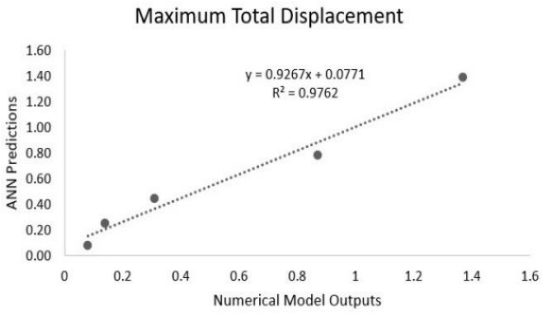

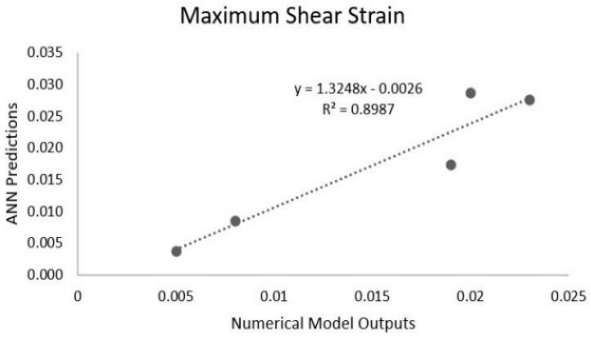

c)

Figure 5.8 FEM mass failure benchmark cases' regression plots for a) factor of safety, b) maximum total displacement and c) maximum shear strain

The correlations were 97% for factor of safety, 97% for maximum total displacement and 89% for maximum shear strain which means strong correlations and ANN results perform well.

For LEM mass failure, the regression plots and R values in training, testing and validation stages that were from ANN were presented in the Figure 5.9 and Figure 5.10 and the plots show that R values are around 99% for circular failure and around 96% for non-circular failure.

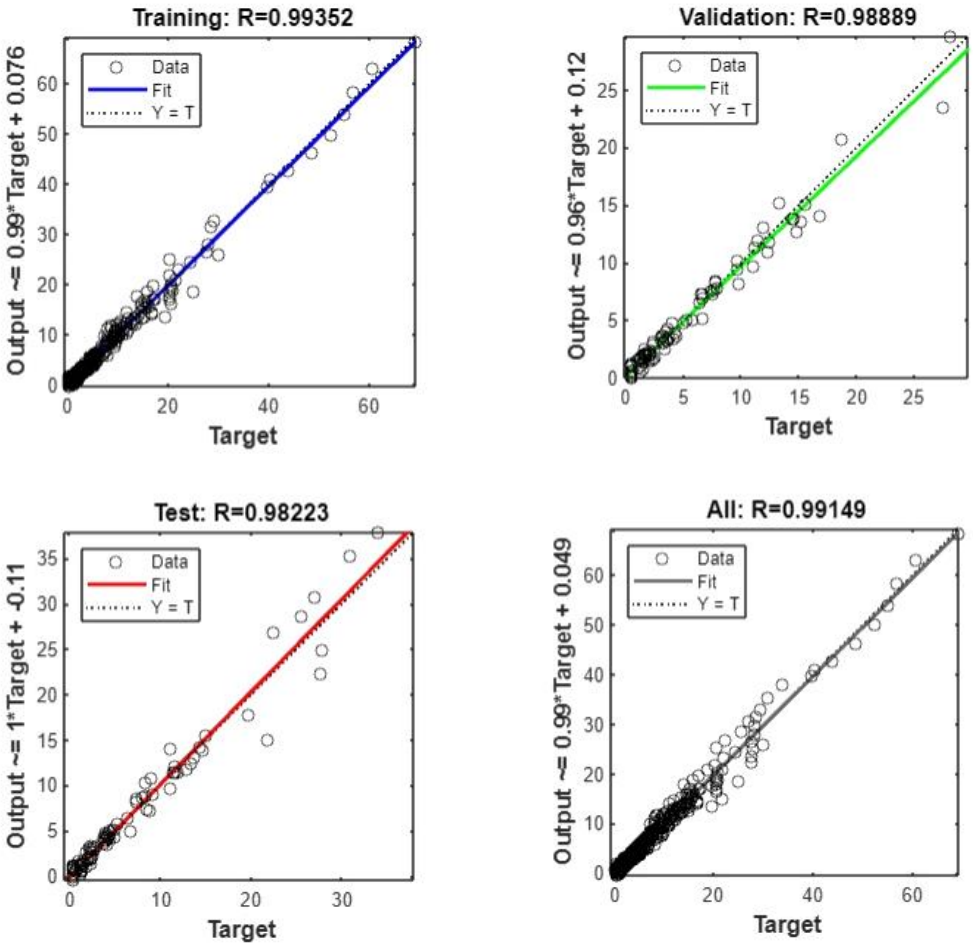

Figure 5.9 Regression plots showing the correlation between ANN predictions and LEM simulations of slope safety factor for circular failure

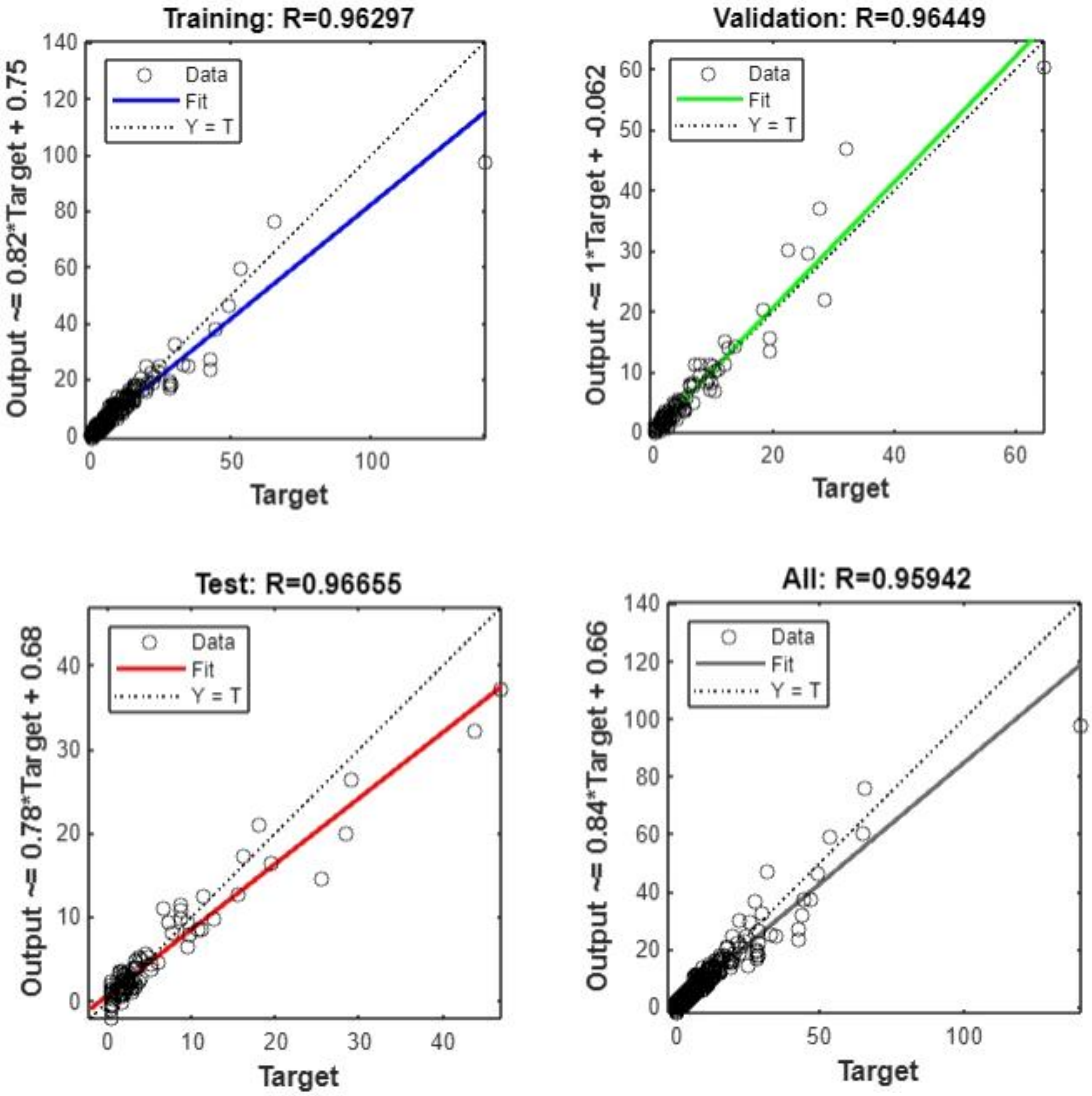

Figure 5.10 Regression plots showing the correlation between ANN predictions and LEM simulations of slope safety factor for non-circular failure

Another 5 different benchmark cases were determined for LEM mass failure. The benchmark cases are detailed in Table 5.6 and regression analysis were shown in Figure 5.11 for mass failure.

Table 5.6 Benchmark cases for LEM mass failure

Case No	Inputs				Outputs			
	Slope Height (m)	OSA (°)	Material Property	UFI (°)	Factor of Safety (Circular)		Factor of Safety (Non-circular)	
					LEM	ANN	LEM	ANN
1	300	50	MP1	20	7.5	7.3	7.0	8.0
2	250	60	MP2	10	3.3	3.8	3.3	2.2
3	250	70	MP3	0	1.5	1.8	1.5	1.5
4	200	40	MP4	10	2.0	2.2	1.8	1.8
5	100	40	MP5	0	1.3	1.3	1.2	1.3

a) b)

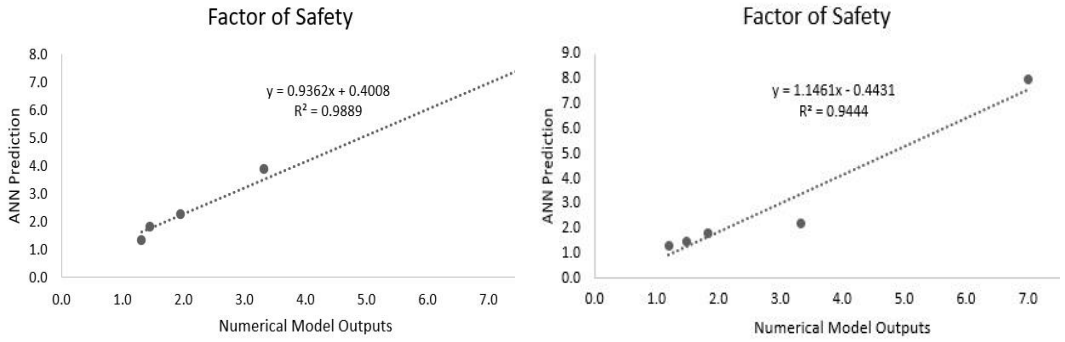

Figure 5.11 LEM mass failure benchmark cases' regression plots for a) circular failure, b) non-circular failure

The correlations between numerical model outputs and ANN predictions were 98% for circular failure and 94% for non-circular failure.

For plane failure, the regression plots and R values in training, testing and validation stages that were from ANN were presented in the Figure 5.12 and the plots show that R values are around 99%.

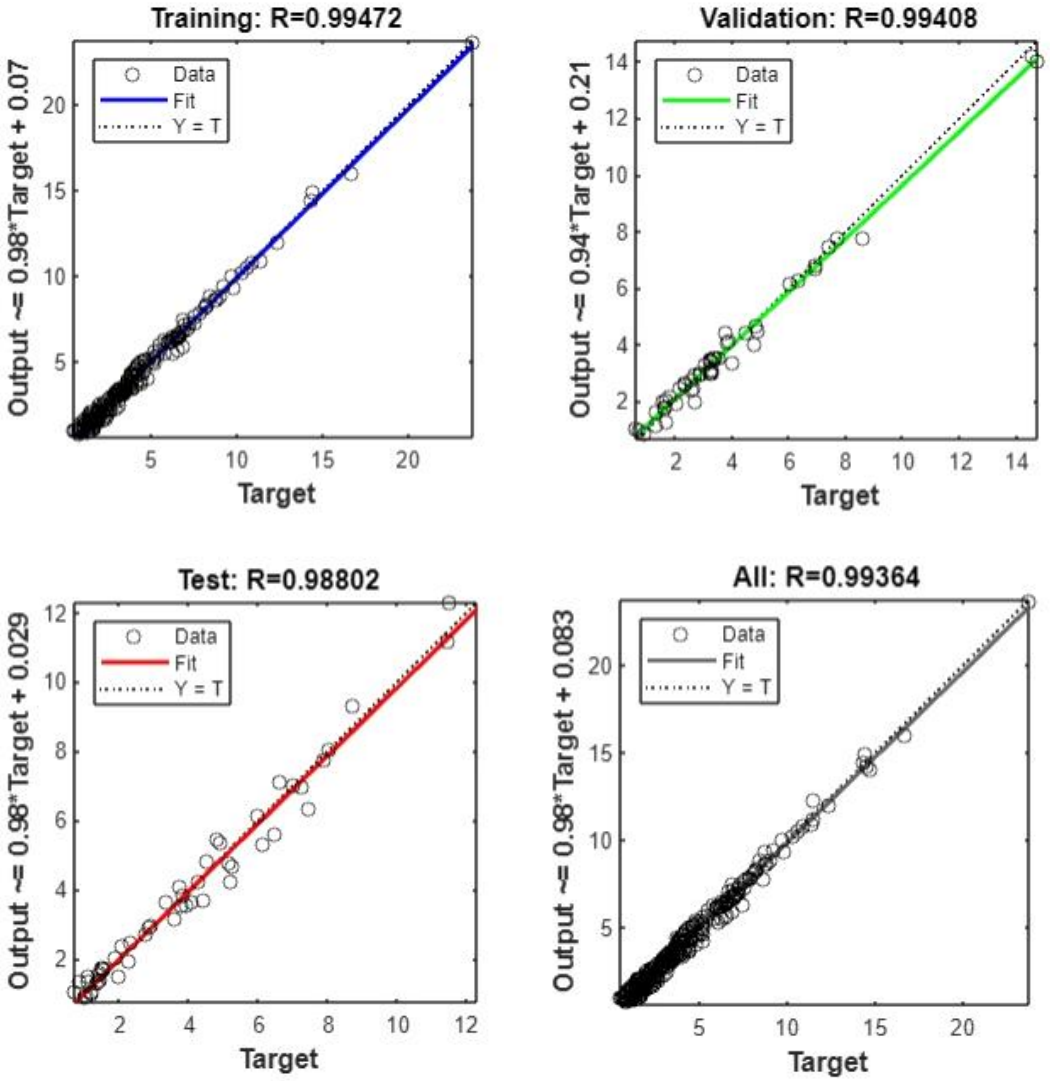

Figure 5.12 Regression plots showing the correlation between ANN predictions and LEM simulations of slope safety factor for planar failure

Another 5 different benchmark cases were determined for plane failure. The benchmark cases are detailed in Table 5.7 and regression analysis were shown in Figure 5.13.

Table 5.7 Benchmark cases for plane failure

Case No	Inputs				Outputs	
					Factor of Safety	
	Slope Height (m)	OSA (°)	Joint Material Property	Failure Plane Angle (°)	LEM	ANN
1	250	60	JMP3	45	2.5	2.5
2	300	50	JMP2	30	1.9	1.6
3	250	50	JMP1	30	1.5	1.5
4	200	60	JMP1	45	1.1	1.0
5	100	70	JMP1	45	1.2	1.0

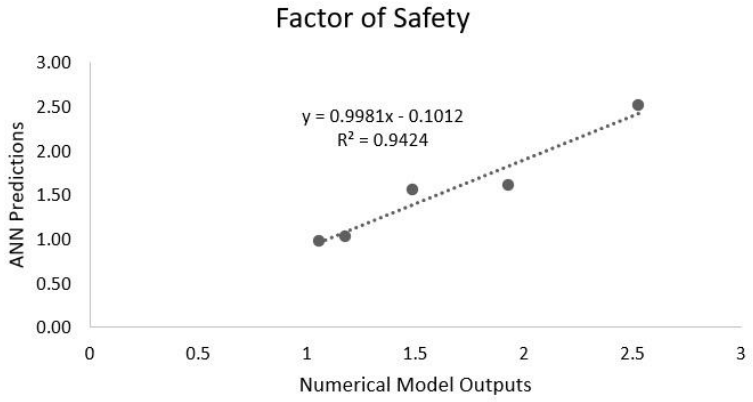

Figure 5.13 Plane failure benchmark cases' regression plot

The correlation was 94% which means strong correlation between numerical model outputs and ANN predictions for plane failure.

For wedge failure, the regression plots and R values in training, testing and validation stages that were from ANN were presented in the Figure 5.14 and the plots show that R values are between 42-61%.

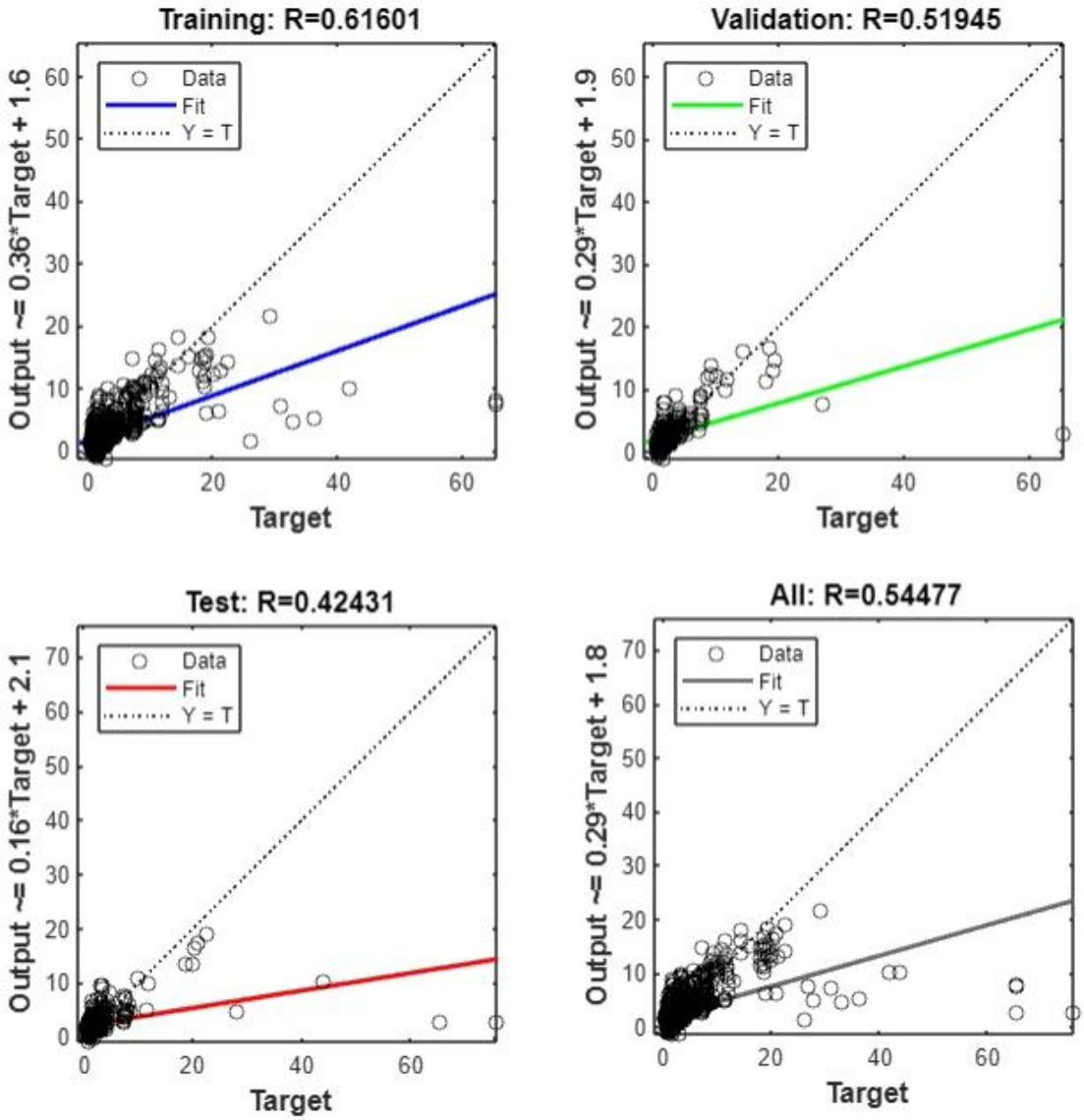

Figure 5.14 Regression plots showing the correlation between ANN predictions and LEM simulations of slope safety factor for wedge failure

In addition, 5 different benchmark cases were determined for wedge failure. The benchmark cases are detailed in Table 5.8 and regression analysis were shown in Figure 5.15.

Table 5.8 Benchmark cases for wedge failure

Inputs								Outputs	
				Failure Plane 1		Failure Plane 2		Factor of Safety	
Case No	Slope Height (m)	Slope Dip (°)	Joint Material Property Combination	Dip (°)	The Difference Between Slope Dip Direction and First Failure Plane Dip Direction (°)	Dip (°)	The Difference Between Slope Dip Direction and Second Failure Plane Dip Direction (°)	LEM	ANN
1	300	50	JMP 1-2	45	30	45	300	2.0	2.5
2	200	60	JMP 1-2	45	30	45	330	1.8	1.9
3	200	60	JMP 1-1	45	330	45	30	1.3	0.8
4	150	70	JMP 1-1	60	30	45	330	1.3	1.5
5	100	80	JMP 1-1	60	30	75	330	1.0	1.5

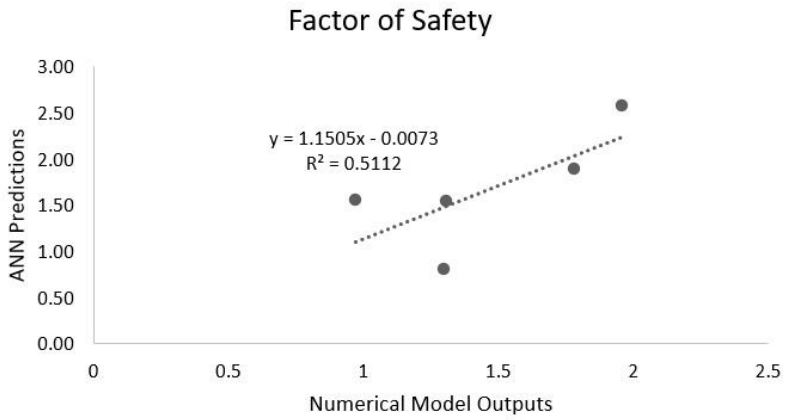

Figure 5.15 Plane failure benchmark cases' regression plot

The correlation was 51% which is the lowest correlation among the slope failures in this study.

For block toppling failure, the regression plots and R values in training, testing and validation stages that were from ANN were presented in the Figure 5.16 and the plots show that R values are 99%.

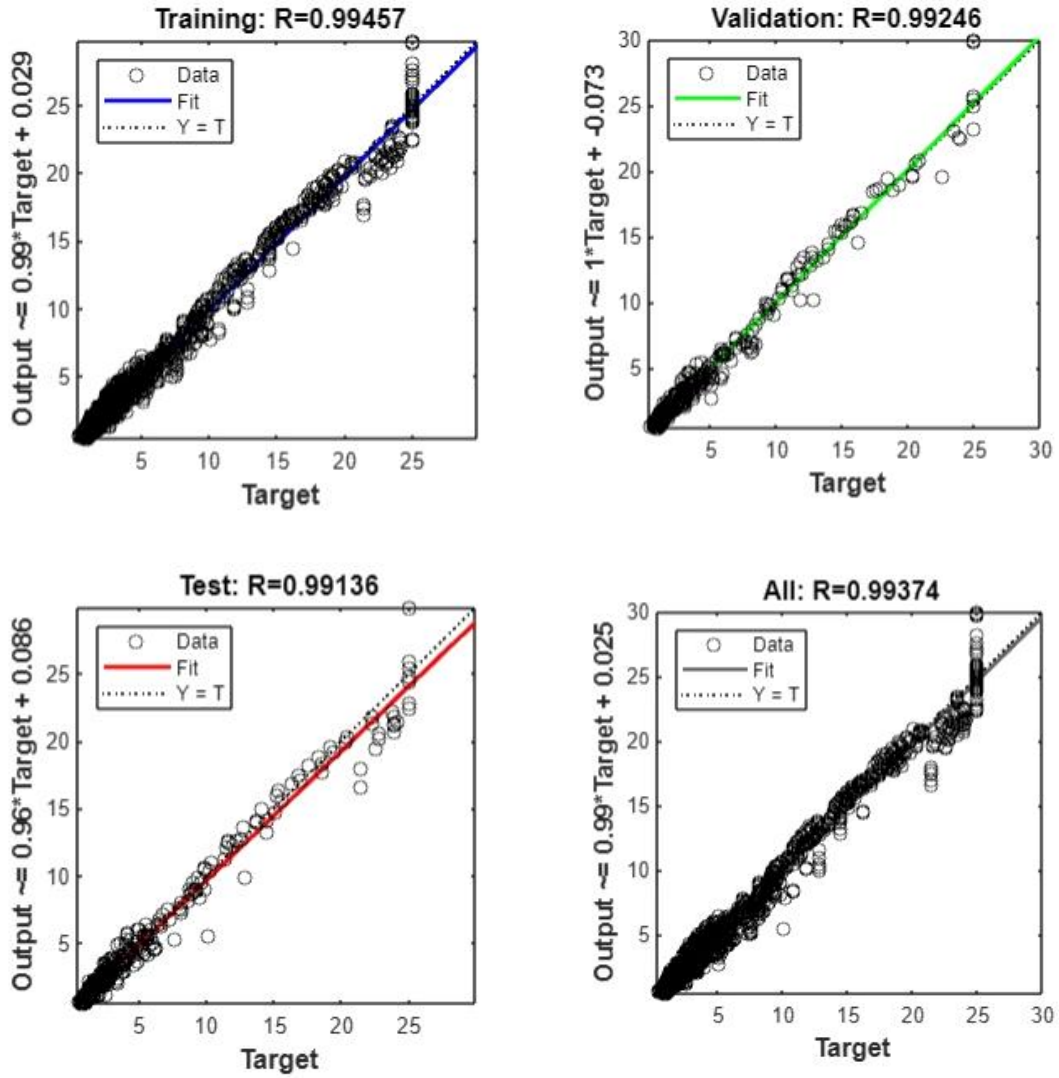

Figure 5.16 Regression plots showing the correlation between ANN predictions and LEM simulations of slope safety factor for block toppling failure

Same as other failures, 5 different benchmark cases were determined for block toppling failure. The benchmark cases are detailed in Table 5.9 and regression analysis were shown in Figure 5.17.

Table 5.9 Benchmark cases for block toppling failure

Inputs							Outputs	
Case No	Height (m)	OSA (°)	Base and Bedding Strength Combination	Toppling Joints		Overall Base Inclination (°)	Factor of Safety	
				Spacing (m)	Dip (°)		LEM	ANN
1	300	40	JMP 3-3	1	80	10	2.5	2.9
2	250	70	JMP 2-2	3	60	30	0.9	1.0
3	200	50	JMP 2-2	5	70	20	1.7	1.8
4	150	50	JMP 1-1	1	80	10	1.1	1.3
5	100	80	JMP 1-1	10	30	60	0.9	0.9

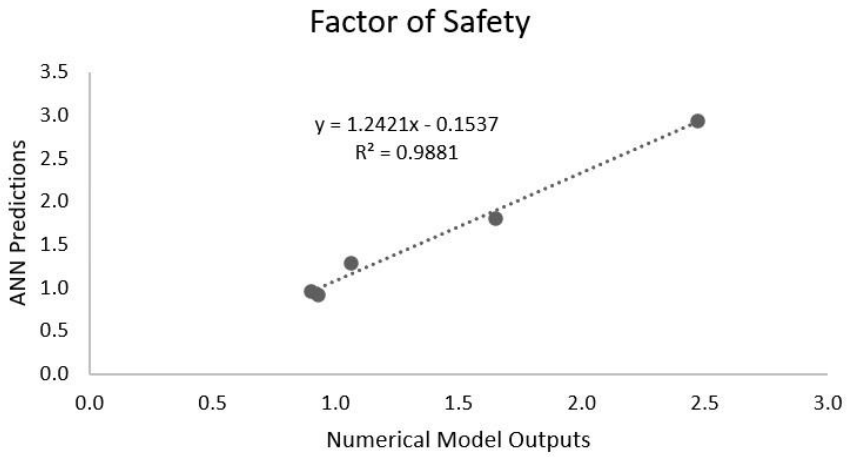

Figure 5.17 Block toppling failure benchmark cases' regression plot

The correlation between numerical model outputs and ANN outputs was 98% for block toppling failure.

For block flexure toppling failure, the regression plots and R values in training, testing and validation stages that were from ANN were presented in the Figure 5.18 and the plots show that R values are 98%.

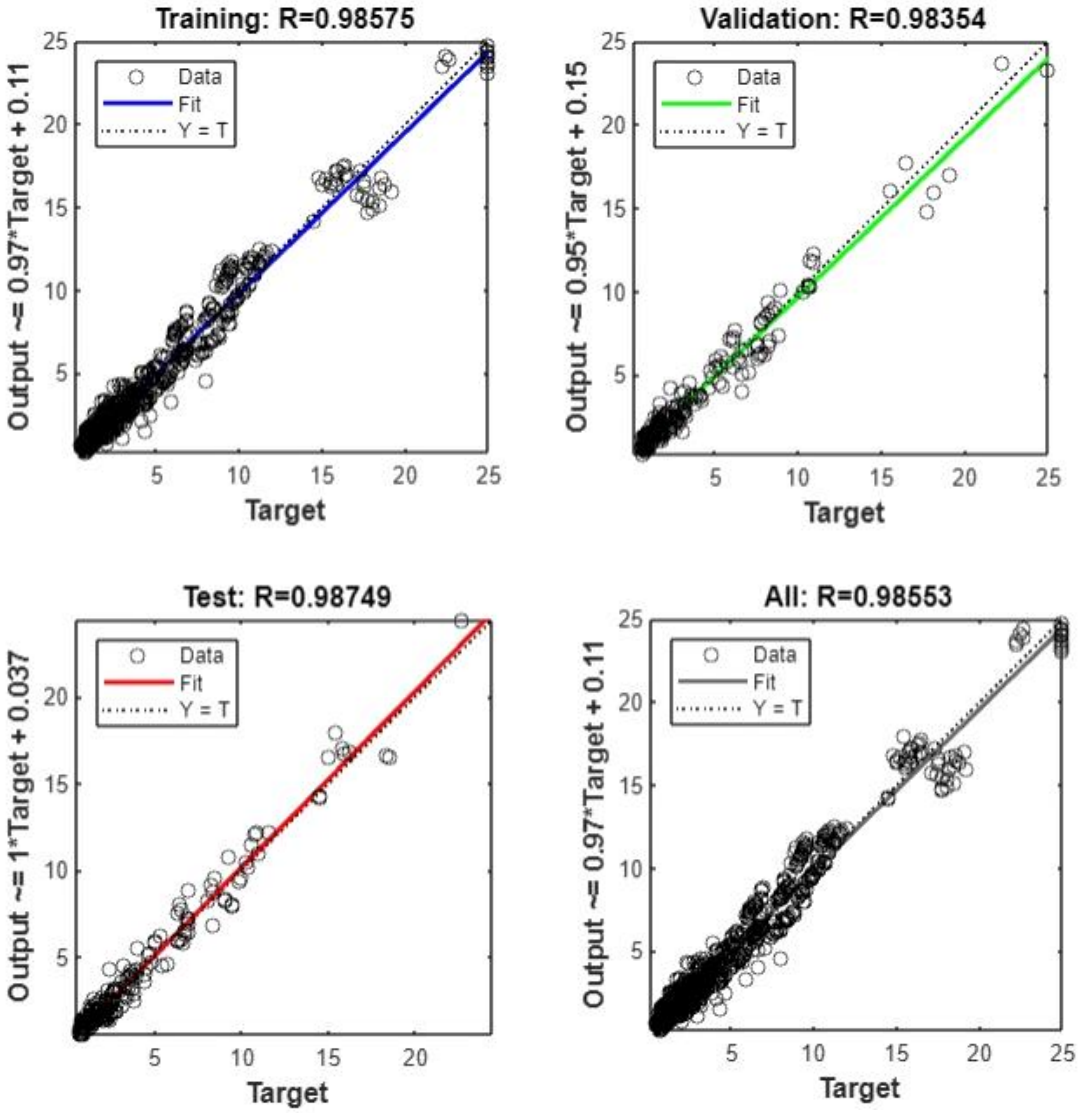

Figure 5.18 Regression plots showing the correlation between ANN predictions and LEM simulations of slope safety factor for block flexure toppling failure

For the last slope failure, 5 different benchmark cases were determined for block flexure toppling failure. The benchmark cases are detailed in Table 5.10 and regression analysis were shown in Figure 5.19.

Table 5.10 Benchmark cases for block flexure toppling failure

Inputs								Outputs	
Case No	Height (m)	Overall Slope Angle (°)	Base and Bedding Strength Combination	Internal Rock Joint Strength	Toppling Joints		Overall Base Inclination (°)	Factor of Safety	
					Spacing (m)	Dip (°)		LEM	ANN
1	300	40	JMP 2-2	JMP 1	5	60	30	2.0	2.5
2	250	50	JMP 2-2	JMP 1	5	70	20	1.9	2.2
3	200	60	JMP 1-1	JMP 1	7	60	30	1.0	1.3
4	150	70	JMP 1-1	JMP 1	10	70	20	0.9	0.8
5	100	60	JMP 1-1	JMP 1	3	60	30	1.4	1.5

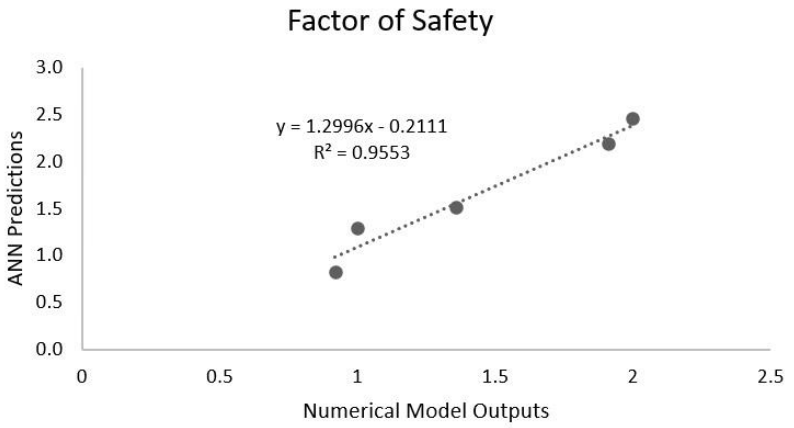

Figure 5.19 Block flexure toppling failure benchmark cases' regression plot

The correlation between numerical model outputs and ANN outputs was 95%.

The ANN models demonstrated strong correlation with the numerical simulations, as evidenced by the values of R ranged from 0.91 to 0.99. However, the models did not perform as well in predicting cases of wedge failure. With benchmarking in total, 45 different scenarios were analyzed using 9 different ANN models, each with 5 different scenarios. The results of the analysis indicated that there was a strong correlation between the predicted outcomes and the numerical simulation outcomes.

Specifically, the correlation was found to be between 89-98% (except wedge failure which was same for ANN), which demonstrates a high level of accuracy in predicting the outcomes. Despite using 3547 models for wedge failure, the prediction of all cases proved to be a challenging task due to the criterion required to form a wedge. The wedge formation criterion only applies to certain inputs of dip and dip direction, which meant that the available input data was limited. Additionally, the program attempted to make predictions even in cases where the wedge did not occur, which added to the complexity of the analysis.

In short, slope analysis is a complex process that requires consideration of various factors and failure modes. ANN provides a basis for quick assessment of slope instability risks based on lab, field and computational experiments.

CHAPTER 6

CONCLUSIONS AND RECOMMENDATIONS

Continuum and discontinuum behaviors generate completely different rock slope failure mechanisms and require unique analysis techniques to investigate the slope safety factor. The dominant failure mode is related to various factors concerning geology, geomechanics and structural characteristics of the field. Once the active failure mode can be identified in the early stages of a slope design, the numerical solutions conforming to the mechanism can be used. Regarding the far-field loadings, manipulation of the stress field and external loads, conventional or advanced mechanical simulation techniques may be opted such as 2D or 3D models with limit equilibrium methods and numerical solutions. Not only the slope performance can be tested under different circumstances but also proactive measures can be taken to improve the slope stability.

Computational efficiency concerns require to define the model inputs at least roughly. Therefore, practical tools for the preliminary slope stability analysis are always considered useful. The current methods are either locally valid empirical tools or lacks of mechanical assessment. This researched delved into employing computational methods like LEM and FEM to test rock slope performance under various conditions and create a reliable database for robust and efficient predictive models operated with ANN that no more require exhaustive mechanical simulations.

FEM provided insightful information about the changes in stress and deformation fields driving through slope mass failure. Slope safety factor could be calculated and interpreted together with the maximum total displacement and maximum shear

strain. On the other hand, LEM provided only the safety factors for circular and non-circular failure surfaces.

ANN was incorporated into the research due to its capacity in capturing non-linear relationships between multiple input parameters. The outputs of FEM and LEM were used to train the ANN models for estimating the slope safety factor, maximum total displacement and maximum shear strain. To create a comprehensive training data set, 10041 computational mechanical models were run and 90658 entries were obtained. The range of variables were designed to be representative for a wide range of cases, which saves the proposed methodology from being locally valid. However, the proposed model is more suitable to be used form preliminary analysis and requires to be validated and improved by more comprehensive techniques. The ANN models were proven to have a high correlation with an R value ranging from 0.91 to 0.99. This indicates that the ANN models were in agreement with the computational models in terms of predicting the slope stability. Some of the research highlights and recommendations are as follows:

- Rock mass geomechanical characteristics have a significant influence on the slope stability
- Slope safety factors obtained from LEM models are higher than FEM solutions. This is mainly due to rigid body assumption in LEM analysis.
- For planar and wedge failure, upper face inclination does not have a significant influence on the safety factor up to 20°.
- 2D plots are not sufficient and user-friendly to investigate multi-parameter relationships in slope stability analysis. ANN proposes an efficient, quick and reliable alternative.
- The proposed method is only valid for isotropic and homogeneous geology settings.

- Groundwater conditions were not included in the computational modeling study. Therefore, the proposed method can be used only for dry slope mass.

The proposed machine learning model can be further developed with an extensive numerical simulation database. It has potential to serve as a useful tool in preliminary analysis of slope stability.

REFERENCES

Afram, A., Janabi-Sharifi, F., Fung, A. S., & Raahemifar, K. (2017). Artificial neural network (ANN) based model predictive control (MPC) and optimization of HVAC systems: A state of the art review and case study of a residential HVAC system. *Energy and Buildings*, *141*, 96–113. https://doi.org/10.1016/j.enbuild.2017.02.012

Agatonovic-Kustrin, S., & Beresford, R. (2000). Basic concepts of artificial neural network (ANN) modeling and its application in pharmaceutical research. In *Journal of Pharmaceutical and Biomedical Analysis* (Vol. 22). www.elsevier.com/locate/jpba

Agharazi, A., Tannant, D. D., & Derek Martin, C. (2012). Characterizing rock mass deformation mechanisms during plate load tests at the Bakhtiary dam project. *International Journal of Rock Mechanics and Mining Sciences*, *49*, 1–11. https://doi.org/10.1016/j.ijrmms.2011.10.002

Alamri, A. H. (2022). Application of machine learning to stress corrosion cracking risk assessment. *Egyptian Journal of Petroleum*, *31*(4), 11–21. https://doi.org/10.1016/J.EJPE.2022.09.001

Alejano, L. R., Ferrero, A. M., Ramírez-Oyanguren, P., & Álvarez Fernández, M. I. (2011). Comparison of limit-equilibrium, numerical and physical models of wall slope stability. *International Journal of Rock Mechanics and Mining Sciences*, *48*(1), 16–26. https://doi.org/10.1016/j.ijrmms.2010.06.013

Amirkiyaei, V., & Ghasemi, E. (2022). Stability assessment of slopes subjected to circular-type failure using tree-based models. *International Journal of Geotechnical Engineering*, *16*(3), 301–311. https://doi.org/10.1080/19386362.2020.1862538

Ardestani, A., Amini, M., & Esmaeili, K. (2021). A two-dimensional limit equilibrium computer code for analysis of complex toppling slope failures. *Journal of Rock Mechanics and Geotechnical Engineering*, *13*(1), 114–130. https://doi.org/10.1016/j.jrmge.2020.04.006

Arya Babu, P., & Chandrakaran, S. (2022). Numerical Methods in the Stability Analysis of Slopes. *Lecture Notes in Civil Engineering*, *171*, 997–1004. https://doi.org/10.1007/978-3-030-80312-4_86

Ashby, J. (1971). *Sliding and toppling modes of failure in models and jointed rock slopes*. Imperial College.

Azarafza, M., Akgün, H., Ghazifard, A., Asghari-Kaljahi, E., Rahnamarad, J., & Derakhshani, R. (2021). Discontinuous rock slope stability analysis by limit equilibrium approaches–a review. In *International Journal of Digital Earth* (Vol. 14, Issue 12, pp. 1918–1941). Taylor and Francis Ltd. https://doi.org/10.1080/17538947.2021.1988163

Azarafza, M., Hajialilue Bonab, M., & Derakhshani, R. (2022). A novel empirical classification method for weak rock slope stability analysis. *Scientific Reports*, *12*(1). https://doi.org/10.1038/s41598-022-19246-w

Azarafza, M., Koçkar, M. K., & Zhu, H. H. (2022). Correlations of SMR-Qslope Data in Stability Classification of Discontinuous Rock Slope: A Modified Relationship Considering the Iranian Data. *Geotechnical and Geological Engineering*, *40*(4), 1751–1764. https://doi.org/10.1007/s10706-021-01991-w

Azarafza, M., Nanehkaran, Y. A., Rajabion, L., Akgün, H., Rahnamarad, J., Derakhshani, R., & Raoof, A. (2020). Application of the modified Q-slope classification system for sedimentary rock slope stability assessment in Iran. *Engineering Geology*, *264*. https://doi.org/10.1016/j.enggeo.2019.105349

Baker, R. (2006). A relation between safety factors with respect to strength and height of slopes. *Computers and Geotechnics*, *33*(4–5). https://doi.org/10.1016/j.compgeo.2006.07.001

Bar, N., & Barton, N. (2017). The Q-Slope Method for Rock Slope Engineering. *Rock Mechanics and Rock Engineering*, *50*(12), 3307–3322. https://doi.org/10.1007/s00603-017-1305-0

Barton, N., & Choubey, V. (1977). The shear strength of rock joints in theory and practice. *Rock Mechanics Felsmechanik Mécanique Des Roches*, *10*(1–2). https://doi.org/10.1007/BF01261801

Barton, N., & Grimstad, E. (2014). *Q-System An Illustrated Guide Following Forty Years In Tunnelling*. https://www.researchgate.net/publication/321875931

Barton, N., Lien, R., & Lunde, J. (1974). Engineering classification of rock masses for the design of tunnel support. *Rock Mechanics Felsmechanik Mécanique Des Roches*, *6*(4). https://doi.org/10.1007/BF01239496

Bieniawski, Z. T. (1989). *Engineering Rock Mass Classifications A Complete Manual for Engineers and Geologists in Mining, Civil, and Petroleum Engineering*. John Wiley & Sons, Inc.

Bishop, A. W., & Morgenstern, N. (1960). Stability coefficients for earth slopes. *Geotechnique*, *10*(4). https://doi.org/10.1680/geot.1960.10.4.129

Bobet, A., Fakhimi, A., Johnson, S., Morris, J., Tonon, F., & Yeung, M. R. (2009). Numerical Models in Discontinuous Media: Review of Advances for Rock Mechanics Applications. *Journal of Geotechnical and Geoenvironmental Engineering*, *135*(11). https://doi.org/10.1061/(asce)gt.1943-5606.0000133

Bowa, V. M. (2020). Wedge Sliding Analysis of the Rock Slope Subjected to Uplift Forces and Surcharge Loads Conditions. *Geotechnical and Geological Engineering*, *38*(1), 367–374. https://doi.org/10.1007/s10706-019-01027-4

Cala, M., Flisiak, J., & Tajdus, A. (2004). Slope stability analysis with modified shear strength reduction technique. In *Landslides: Evaluation and Stabilization/Glissement de Terrain: Evaluation et Stabilisation, Set of 2 Volumes*. https://doi.org/10.1201/b16816-160

Cecil, O. S. (1975). Correlations Of Rock Bolt-Shotcrete Support and Rock Quality Parameters In Scandinavian Tunnels. *Correl of Rock Bolt-Shotcrete Support and Rock Qual Parameters in Scan Tunnels*. https://doi.org/10.1016/0148-9062(76)90886-x

Chen, Z. (1995). Recent developments in slope stability analysis. *8th ISRM Congress*.

Cheng, Y. M. (2003). Location of critical failure surface and some further studies on slope stability analysis. *Computers and Geotechnics*, *30*(3). https://doi.org/10.1016/S0266-352X(03)00012-0

Cheng, Y. M., & Lau, C. K. (2014). *Slope stability analysis and stabilization: new methods and insight*.

Corkum, B., Hoek, E., Carranza-Torres, C., Hoek, E., Carranza-Torres, C., & Corkum, B. (2002). *Hoek-Brown failure criterion-2002 Edition Discrete Element Modeling of Particulate Material Behavior View project 2D and 3D LEM and FEM analysis of Geotechnical structures View project Hoek-Brown failure criterion-2002 Edition HOEK-BROWN FAILURE CRITERION-2002 EDITION* (Vol. 1). www.d.umn.edu/~carranza

Cundall, P. A., & Strack, O. D. L. (1979). A discrete numerical model for granular assemblies. *Geotechnique*, *29*(1). https://doi.org/10.1680/geot.1979.29.1.47

Daftaribesheli, A., Ataei, M., & Sereshki, F. (2011). Assessment of rock slope stability using the fuzzy slope mass rating (FSMR) system. *Applied Soft Computing Journal*, *11*(8). https://doi.org/10.1016/j.asoc.2011.08.032

Das, S. K., Biswal, R. K., Sivakugan, N., & Das, B. (2011). Classification of slopes and prediction of factor of safety using differential evolution neural networks. *Environmental Earth Sciences*, *64*(1), 201–210. https://doi.org/10.1007/s12665-010-0839-1

Deere, D., U., & Deere, D., W. (1988). The Rock Quality Designation (RQD) in Practice. *Rock Classification Systems for Engineering Purposes*.

Deshpande, V., Modi, P., & Sant, A. V. (2022). Analysis of Levenberg Marquardt - ANN based reference current generation for control of shunt active power filter. *Materials Today: Proceedings*, *62*(P13), 7104–7108. https://doi.org/10.1016/j.matpr.2022.02.030

Donati, D., Stead, D., & Borgatti, L. (2023). The Importance of Rock Mass Damage in the Kinematics of Landslides. In *Geosciences (Switzerland)* (Vol. 13, Issue 2). MDPI. https://doi.org/10.3390/geosciences13020052

Duncan, J. M. (1996). *State of the Art: Limit Equilibrium and Finite-Element Analysis of Slopes*.

Feng, X., Li, S., Yuan, C., Zeng, P., & Sun, Y. (2018). Prediction of Slope Stability using Naive Bayes Classifier. *KSCE Journal of Civil Engineering*, *22*(3), 941–950. https://doi.org/10.1007/s12205-018-1337-3

Gao, W., Raftari, M., Rashid, A. S. A., Mu'azu, M. A., & Jusoh, W. A. W. (2020). A predictive model based on an optimized ANN combined with ICA for

predicting the stability of slopes. *Engineering with Computers*, *36*(1). https://doi.org/10.1007/s00366-019-00702-7

Griffiths, D. V, Asce, F., Fenton, G. A., & Asce, M. (2004). Probabilistic Slope Stability Analysis by Finite Elements. *Journal of Geotechnical and Geoenvironmental Engineering*. https://doi.org/10.1061/ASCE1090-02412004130:5507

Hack, R. (2002). An Evaluation of Slope Stability Classification. In *Av. do Brasil* (Vol. 101).

Hack, R., Price, D., & Rengers, N. (2003). A new approach to rock slope stability - A probability classification (SSPC). *Bulletin of Engineering Geology and the Environment*, *62*(2), 167–184. https://doi.org/10.1007/s10064-002-0155-4

Hammah, R. E., Curran, J. H., & Yacoub, T. (2004). *Stability Analysis of Rock Slopes Using the Finite Element Method*.

Harris, C., Smith, J. S., Davies, M. C. R., & Rea, B. (2008). An investigation of periglacial slope stability in relation to soil properties based on physical modelling in the geotechnical centrifuge. *Geomorphology*, *93*(3–4), 437–459. https://doi.org/10.1016/j.geomorph.2007.03.009

Havaej, M., Stead, D., Eberhardt, E., & Fisher, B. R. (2014). Characterization of bi-planar and ploughing failure mechanisms in footwall slopes using numerical modelling. *Engineering Geology*, *178*, 109–120. https://doi.org/10.1016/J.ENGGEO.2014.06.003

Hoek, E., & Bray, J. (1981). *Rock Slope Engineering* (3rd ed.). The Institution of Mining and Metallurgy.

Hoek, E., & Brown, E. T. (1997). Practical estimates of rock mass strength. *International Journal of Rock Mechanics and Mining Sciences*, *34*(8). https://doi.org/10.1016/S1365-1609(97)80069-X

Hoek, E., & Brown, E. T. (2019). The Hoek–Brown failure criterion and GSI – 2018 edition. *Journal of Rock Mechanics and Geotechnical Engineering*, *11*(3), 445–463. https://doi.org/10.1016/j.jrmge.2018.08.001

Hoek, E., & Diederichs, M. S. (2006). Empirical estimation of rock mass modulus. *International Journal of Rock Mechanics and Mining Sciences*, *43*(2). https://doi.org/10.1016/j.ijrmms.2005.06.005

Huang, X. wen, Yao, Z. shu, Wang, W., Zhou, A. zhao, & Jiang, P. (2021). Stability analysis of soil-rock slope (SRS) with an improved stochastic method and physical models. *Environmental Earth Sciences*, *80*(18). https://doi.org/10.1007/s12665-021-09939-2

Idris, M. A. (2022). Probabilistic slope stability assessment of laterite borrow pit using artificial neural network. *International Journal of Geotechnical Engineering*, *16*(9), 1152–1164. https://doi.org/10.1080/19386362.2022.2090697

İşleyen, E. (2017). *Laboratory Investigation of Shear Behavior of Rock Discontinuities Based on Shear Rate, Size and Roughness Characteristics*. Middle East Technical University.

Jahirul, M. I., Rasul, M. G., Brown, R. J., Senadeera, W., Hosen, M. A., Haque, R., Saha, S. C., & Mahlia, T. M. I. (2021). Investigation of correlation between chemical composition and properties of biodiesel using principal component analysis (PCA) and artificial neural network (ANN). *Renewable Energy*, *168*, 632–646. https://doi.org/10.1016/j.renene.2020.12.078

Jaiswal, A., Verma, A. K., & Singh, T. N. (2023). Evaluation of slope stability through rock mass classification and kinematic analysis of some major slopes along NH-1A from Ramban to Banihal, North Western Himalayas. *Journal of Rock Mechanics and Geotechnical Engineering*. https://doi.org/10.1016/j.jrmge.2023.02.021

Janbu, N. (1973). Slope Stability Computations. *Embankment-Dam Eng*. https://doi.org/10.1016/0148-9062(75)90139-4

Javed, S., Satyanarayana Murthy, Y. V. V., Baig, R. U., & Prasada Rao, D. (2015). Development of ANN model for prediction of performance and emission characteristics of hydrogen dual fueled diesel engine with Jatropha Methyl Ester biodiesel blends. *Journal of Natural Gas Science and Engineering*, *26*, 549–557. https://doi.org/10.1016/j.jngse.2015.06.041

Kelley, C. T. (1999). *Iterative methods for optimization*. Society for Industrial and Applied Mathematics.

Kheok, S. C., & Leung, C. F. (1986). Automated kinematic analysis of rock slope stability. *Advances in Engineering Software (1978)*, *8*(4). https://doi.org/10.1016/0141-1195(86)90061-6

Khorasani, E., Amini, M., Hossaini, M. F., & Medley, E. (2019). Statistical analysis of bimslope stability using physical and numerical models. *Engineering Geology*, *254*, 13–24. https://doi.org/10.1016/j.enggeo.2019.03.023

Kusumayudha, S. B., Thamrin, A., & Purwanto, H. S. (2023). Rock slope kinematics analysis by Markland method of the Bener District, Purworejo Regency, Central Java, Indonesia. *International Journal of Advances in Applied Sciences*, *12*(2), 111–120. https://doi.org/10.11591/ijaas.v12.i2.pp111-120

Lauffer, H. (1958). Gebirgsklassi fizierung für den stollenbau. *Geologie Und Bauwesen*.

Lee, C. Y., & Wang, I. T. (2011). Analysis of highway slope failure by an application of the stereographic projection. *World Academy of Science, Engineering and Technology*, *75*.

Lin, Y., Wang, X., Ma, J., & Huang, L. (2022). A finite-discrete element based appoach for modelling the hydraulic fracturing of rocks with irregular inclusions. *Engineering Fracture Mechanics*, *261*. https://doi.org/10.1016/j.engfracmech.2021.108209

Liu, S. Y., Shao, L. T., & Li, H. J. (2015). Slope stability analysis using the limit equilibrium method and two finite element methods. *Computers and Geotechnics*, *63*. https://doi.org/10.1016/j.compgeo.2014.10.008

Lu, P., & Rosenbaum, M. S. (2003). Artificial Neural Networks and Grey Systems for the Prediction of Slope Stability. In *Natural Hazards* (Vol. 30).

Mafi, R., Javankhoshdel, S., Cami, B., Jamshidi Chenari, R., & Gandomi, A. H. (2021). Surface altering optimisation in slope stability analysis with non-circular failure for random limit equilibrium method. *Georisk*, *15*(4), 260–286. https://doi.org/10.1080/17499518.2020.1771739

Mantrala, S., Kumar, H., Verma, A. K., & Sitharam, T. G. (2022). Wedge Failure Analysis of Slopes in Highly Jointed Rock Masses in the Zones of High Seismicity. *Indian Geotechnical Journal*, *52*(3), 626–649. https://doi.org/10.1007/s40098-022-00600-8

Mantrala, S., Verma, A. K., & Sitharam, T. G. (2021). A systematic approach for the analyses and design of jointed rock mass slopes against wedge and toppling failures: a case study of the stability of the abutments of the bridge

across the Chenab River. *International Journal of Geotechnical Engineering*, *15*(1). https://doi.org/10.1080/19386362.2018.1480151

Marinos, V., Marinos, P., & Hoek, E. (2005). The geological strength index: Applications and limitations. *Bulletin of Engineering Geology and the Environment*, *64*(1), 55–65. https://doi.org/10.1007/s10064-004-0270-5

Marrapu, B. M., Kukunuri, A., & Jakka, R. S. (2021). Improvement in Prediction of Slope Stability & Relative Importance Factors Using ANN. *Geotechnical and Geological Engineering*, *39*(8). https://doi.org/10.1007/s10706-021-01872-2

Miščević, P., & Vlastelica, G. (2014). Impact of weathering on slope stability in soft rock mass. *Journal of Rock Mechanics and Geotechnical Engineering*, *6*(3), 240–250. https://doi.org/10.1016/j.jrmge.2014.03.006

Morgenstern, N. R., & Tchalenko, J. S. (1967). Microscopic structures in kaolin subjected to direct shear. *Geotechnique*, *17*(4). https://doi.org/10.1680/geot.1967.17.4.309

Neves, M., Cavaleiro, V., & Pinto, A. (2016). Slope Stability Assessment and Evaluation of Remedial Measures Using Limit Equilibrium and Finite Element Approaches. *Procedia Engineering*, *143*. https://doi.org/10.1016/j.proeng.2016.06.109

Nickmann, M., Spaun, G., & Thuro, K. (2006). Engineering geological classification of weak rocks. *International Association for Engineering Geology and the Environment*, *492*(492).

Öge, İ. F. (2008). *Slope Stability Analysis and Design in Elbistan-Çöllolar Open Cast Mine*. Middle East Technical University.

Pereira, T. D. S., Robaina, A. D., Peiter, M. X., Braga, F. D. V. A., & Rosso, R. B. (2016). Performance of analysis methods of slope stability for different geotechnical classes soil on earth dams. *Engenharia Agricola*, *36*(6), 1027–1036. https://doi.org/10.1590/1809-4430-Eng.Agric.v36n6p1027-1036/2016

Qi, C., & Tang, X. (2018). Slope stability prediction using integrated metaheuristic and machine learning approaches: A comparative study. *Computers and Industrial Engineering*, *118*, 112–122. https://doi.org/10.1016/j.cie.2018.02.028

Raghuvanshi, T. K. (2019a). Governing factors influence on rock slope stability – Statistical analysis for plane mode of failure. *Journal of King Saud University - Science*, *31*(4), 1254–1263. https://doi.org/10.1016/j.jksus.2019.01.002

Raghuvanshi, T. K. (2019b). Plane failure in rock slopes – A review on stability analysis techniques. In *Journal of King Saud University - Science* (Vol. 31, Issue 1, pp. 101–109). Elsevier B.V. https://doi.org/10.1016/j.jksus.2017.06.004

Raghuvanshi, T. K., Ibrahim, J., & Ayalew, D. (2014). Slope stability susceptibility evaluation parameter (SSEP) rating scheme - An approach for landslide hazard zonation. *Journal of African Earth Sciences*, *99*(PA2). https://doi.org/10.1016/j.jafrearsci.2014.05.004

Raghuvanshi, T. K., Negassa, L., & Kala, P. M. (2015). GIS based Grid overlay method versus modeling approach – A comparative study for landslide hazard zonation (LHZ) in Meta Robi District of West Showa Zone in Ethiopia. *The Egyptian Journal of Remote Sensing and Space Science*, *18*(2), 235–250. https://doi.org/10.1016/J.EJRS.2015.08.001

Read, J., & Stacey, P. (2019). Guidelines for Open Pit Slope Design. In *Guidelines for Open Pit Slope Design*. https://doi.org/10.1071/9780643101104

Ritter, W. (1879). Die Statik der Tunnelgewolbe. *Springer*.

Robertson, A. M. G. (1988). Estimating Weak Rock Strength. *Preprint - Society of Mining Engineers of AIME*.

Romana, M., Serón, J. B., & Montalar, E. (2003). SMR geomechanics classification: Application, experience and validation. *10th ISRM Congress*.

Rukhaiyar, S., Alam, M. N., & Samadhiya, N. K. (2018). A PSO-ANN hybrid model for predicting factor of safety of slope. *International Journal of Geotechnical Engineering*, *12*(6), 556–566. https://doi.org/10.1080/19386362.2017.1305652

Russo, R. (2021). The Pearson product-moment correlation coefficient r. In *Statistics for the Behavioural Sciences*. https://doi.org/10.4324/9780203641576-23

Sah, N. K., Sheorey, P. R., & Upadhyaya, L. N. (1994). Maximum likelihood estimation of slope stability. *International Journal of Rock Mechanics and Mining Sciences And*, *31*(1). https://doi.org/10.1016/0148-9062(94)92314-0

Sakellariou, M. G., & Ferentinou, M. D. (2005). A study of slope stability prediction using neural networks. *Geotechnical and Geological Engineering*, *23*(4), 419–445. https://doi.org/10.1007/s10706-004-8680-5

Sánchez, L. K., Emery, X., & Séguret, S. A. (2021). Geostatistical modeling of Rock Quality Designation (RQD) and geotechnical zoning accounting for directional dependence and scale effect. *Engineering Geology*, *293*, 106338. https://doi.org/10.1016/J.ENGGEO.2021.106338

Selby, M. J. (1980). A rock mass strength classification for geomorphic purposes: with tests from Antarctica and New Zealand. *Zeitschrift Fur Geomorphologie*, *24*(1). https://doi.org/10.1127/zfg/24/1984/31

Shan, P., Sun, H., Lai, X., Dai, J., Gao, J., Yang, P., Li, W., Li, C., & Yan, C. (2022). Numerical Method for Predicting and Evaluating the Stability of Section Coal Pillars in Underground Longwall Mining. *Frontiers in Earth Science*, *10*. https://doi.org/10.3389/feart.2022.894118

Sharma, S., Raghuvanshi, T. K., & Anbalagan, R. (1995). Plane failure analysis of rock slopes. In *Geotechnical and Geological Engineering* (Vol. 13).

Sheorey, P. R. (1997). Empirical rock failure criteria. In *Empirical rock failure criteria*.

Singh, B., & Goel, R. K. (1999). Rock Mass Classification. A Practical Approach in Civil Engineering. In *Rock mass classification. A practical approach in civil engineering.*

Singh, B., & Goel, R. K. (2011). Engineering rock mass classification: Tunnelling, foundations and landslides. In *Engineering Rock Mass Classification: Tunnelling, Foundations and Landslides*. https://doi.org/10.1016/C2010-0-64994-7

Sjöberg, J. (1996). *Large Scale Slope Stability in Open Pit Mining - A Review*.

Sonmez, H., & Ulusay, R. (1999). Modifications to the geological strength index (GSI) and their applicability to stability of slopes. *International Journal of Rock Mechanics and Mining Sciences*, *36*(6). https://doi.org/10.1016/S0148-9062(99)00043-1

Sonmez, H., Ulusay, R., & Gokceoglu, C. (1998). A practical procedure for the back analysis of slope failures in closely jointed rock masses. *International Journal of Rock Mechanics and Mining Sciences*, *35*(2). https://doi.org/10.1016/S0148-9062(97)00335-5

Stead, D., Eberhardt, E., & Coggan, J. S. (2006). Developments in the characterization of complex rock slope deformation and failure using numerical modelling techniques. *Engineering Geology*, *83*(1–3). https://doi.org/10.1016/j.enggeo.2005.06.033

Sullivan, T. (2013). *Global slope performance index*. https://doi.org/10.36487/acg_rep/1308_0.4_sullivan

Taheri, A. (2013). *Design of Rock Slopes using SSR Classification System*. https://doi.org/10.3850/978-981-07-3560-9_07-0701

Tang, H., Yong, R., & Ez Eldin, M. A. M. (2017). Stability analysis of stratified rock slopes with spatially variable strength parameters: the case of Qianjiangping landslide. *Bulletin of Engineering Geology and the Environment*, *76*(3), 839–853. https://doi.org/10.1007/s10064-016-0876-4

Tao, Z., Geng, Q., Zhu, C., He, M., Cai, H., Pang, S., & Meng, X. (2019). The mechanical mechanisms of large-scale toppling failure for counter-inclined rock slopes. *Journal of Geophysics and Engineering*, *16*(3), 541–558. https://doi.org/10.1093/jge/gxz020

Tehrani, F. S., Calvello, M., Liu, Z., Zhang, L., & Lacasse, S. (2022). Machine learning and landslide studies: recent advances and applications. *Natural Hazards*, *114*(2), 1197–1245. https://doi.org/10.1007/s11069-022-05423-7

Terzaghi, K. (1946). Rock defects and loads on Tunnel Supports. In *Rock Tunneling with Steel Supports*.

Tomás, R., Cuenca, A., Cano, M., & García-Barba, J. (2012). A graphical approach for slope mass rating (SMR). *Engineering Geology*, *124*(1). https://doi.org/10.1016/j.enggeo.2011.10.004

Tomás, R., Delgado, J., & Serón, J. B. (2007). Modification of slope mass rating (SMR) by continuous functions. *International Journal of Rock Mechanics and Mining Sciences*, *44*(7). https://doi.org/10.1016/j.ijrmms.2007.02.004

Turrini, M. C., & Visintainer, P. (1998). Proposal of a method to define areas of landslide hazard and application to an area of the Dolomites, Italy. *Engineering Geology*, *50*(3–4). https://doi.org/10.1016/S0013-7952(98)00022-2

Wojtecki, Ł., Iwaszenko, S., Apel, D. B., Bukowska, M., & Makówka, J. (2022). Use of machine learning algorithms to assess the state of rockburst hazard in underground coal mine openings. *Journal of Rock Mechanics and Geotechnical Engineering*, *14*(3), 703–713. https://doi.org/10.1016/J.JRMGE.2021.10.011

Wyllie, D., & Mah, C. (2004). *Rock Slope Engineering: Civil and Mining, 4th Edition*.

APPENDICES

A. The Maximum Total Displacement vs. OSA and Slope Safety Factor vs. OSA Plots of Circular Failure from FEM Results

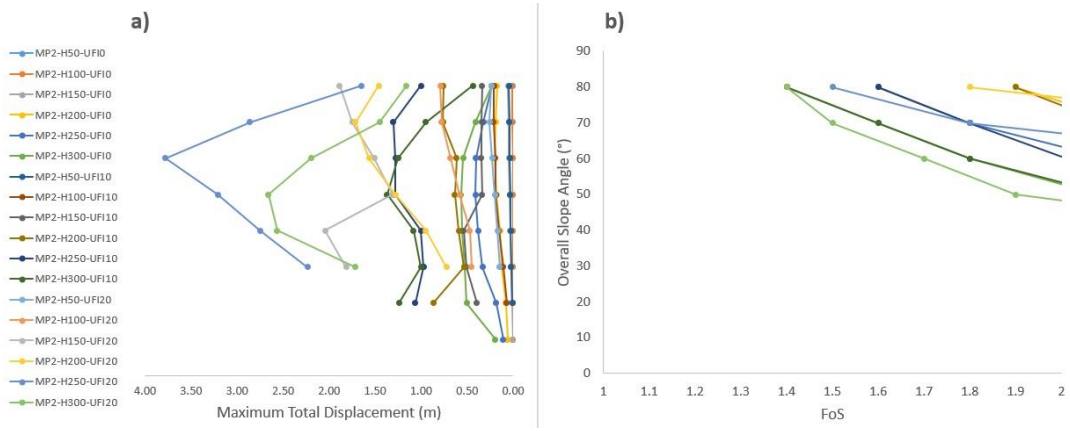

Figure A. 1 a) The maximum total displacement vs. OSA and b) slope safety factor vs. OSA plots for MP_2 rock mass characteristics obtained from FEM simulation of circular failure

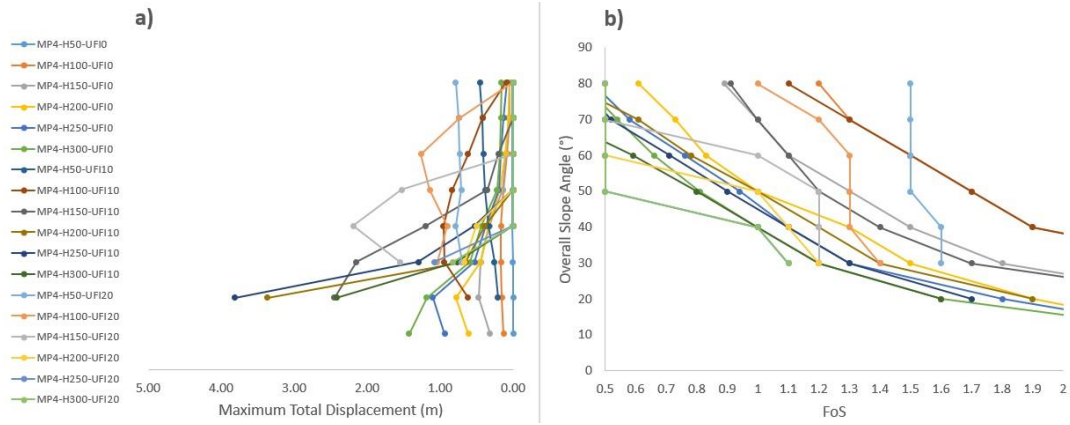

Figure A. 2 a) The maximum total displacement vs. OSA and b) slope safety factor vs. OSA plots for MP_4 rock mass characteristics obtained from FEM simulation of circular failure

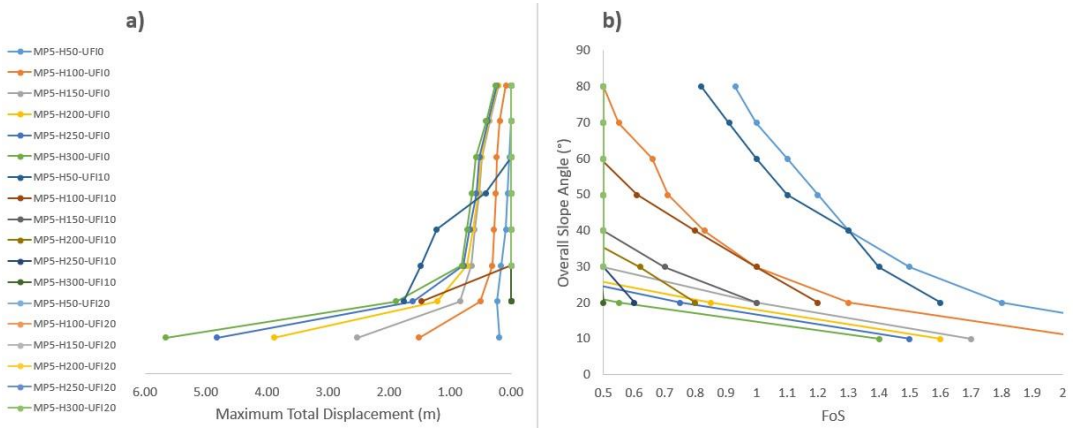

Figure A. 3 a) The maximum total displacement vs. OSA and b) slope safety factor vs. OSA plots for MP_5 rock mass characteristics obtained from FEM simulation of circular failure

B. The Maximum Shear Strain vs. OSA and Slope Safety Factor vs. OSA Plots of Circular Failure from FEM Results

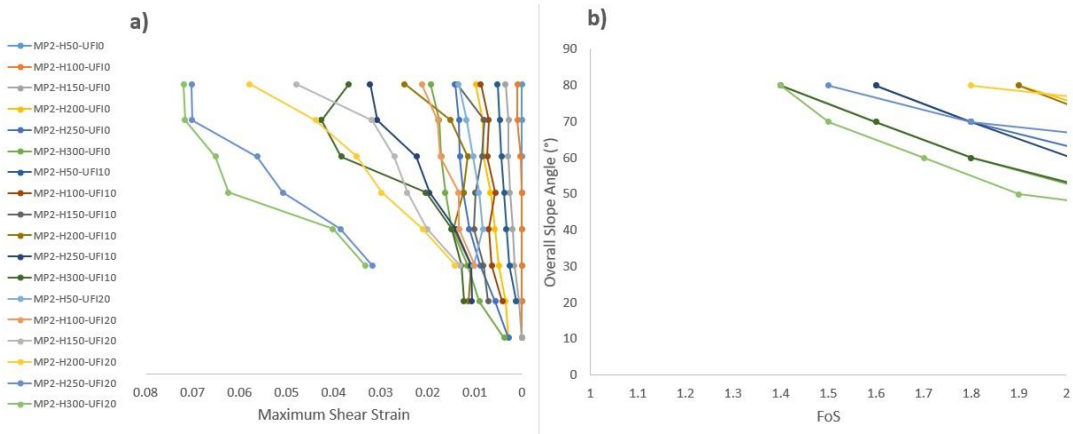

Figure B. 1 a) The maximum shear strain vs. OSA and b) slope safety factor vs. OSA plots for MP_2 rock mass characteristics obtained from FEM simulation of circular failure

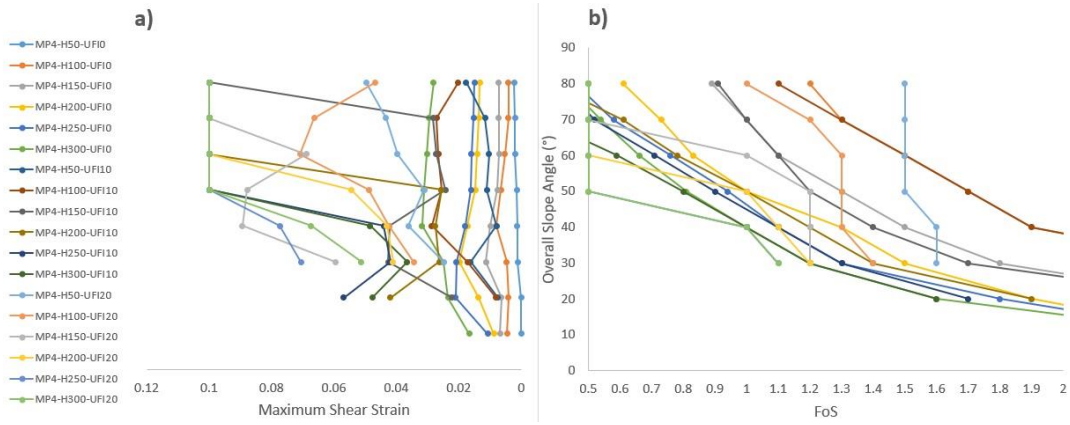

Figure B. 2 a) The maximum shear strain vs. OSA and b) slope safety factor vs. OSA plots for MP_4 rock mass characteristics obtained from FEM simulation of circular failure

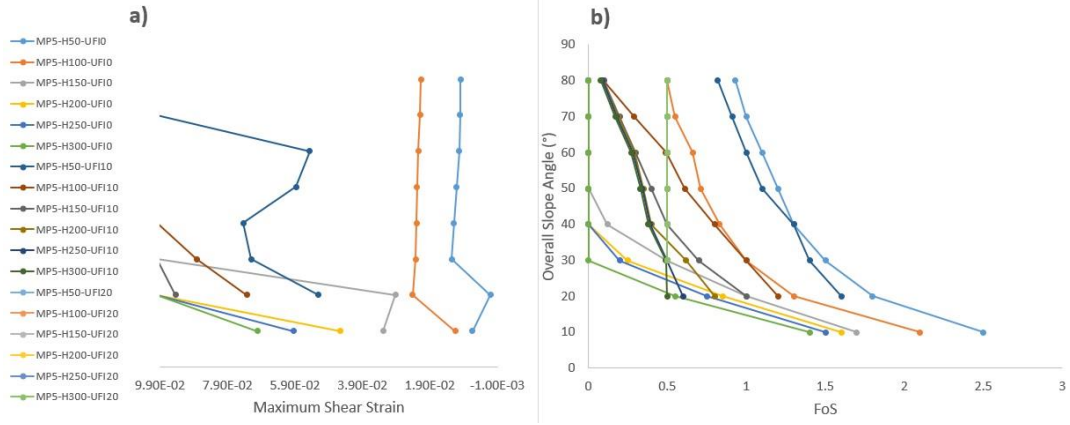

Figure B. 3 a) The maximum shear strain vs. OSA and b) slope safety factor vs. OSA plots for MP_5 rock mass characteristics obtained from FEM simulation of circular failure

C. Slope Safety Factor vs. Overall Slope Angle Plots from LEM Simulations

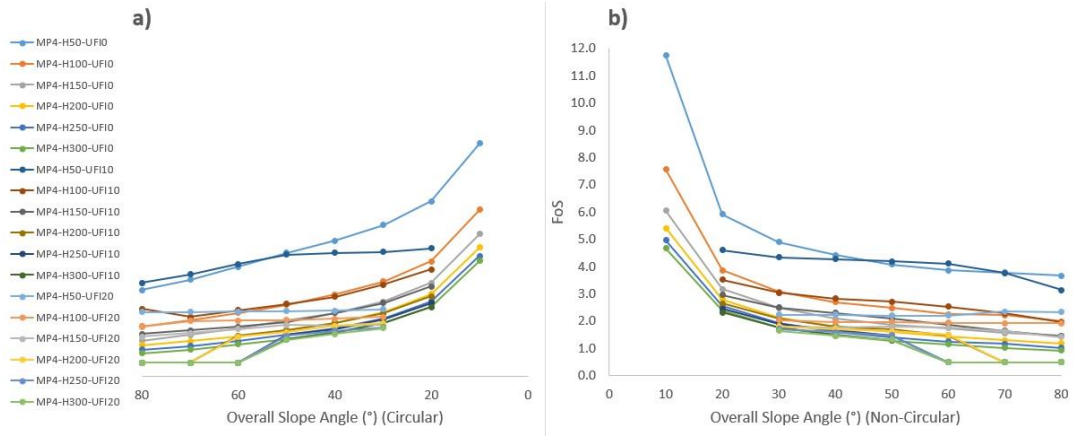

Figure C. 1 Slope safety factor vs. overall slope angle plots a) for circular and b) for non-circular failure surface from LEM simulations for MP_4 rock mass material properties

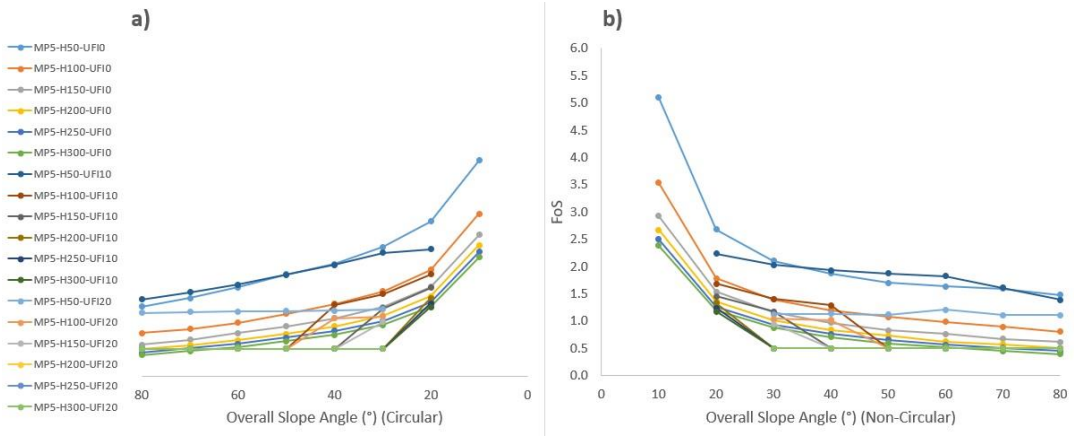

Figure C. 2 Slope safety factor vs. overall slope angle plots a) for circular and b) for non-circular failure surface from LEM simulations for MP_5 rock mass material properties

D. Safety Factor Values for Planar Slope Failure

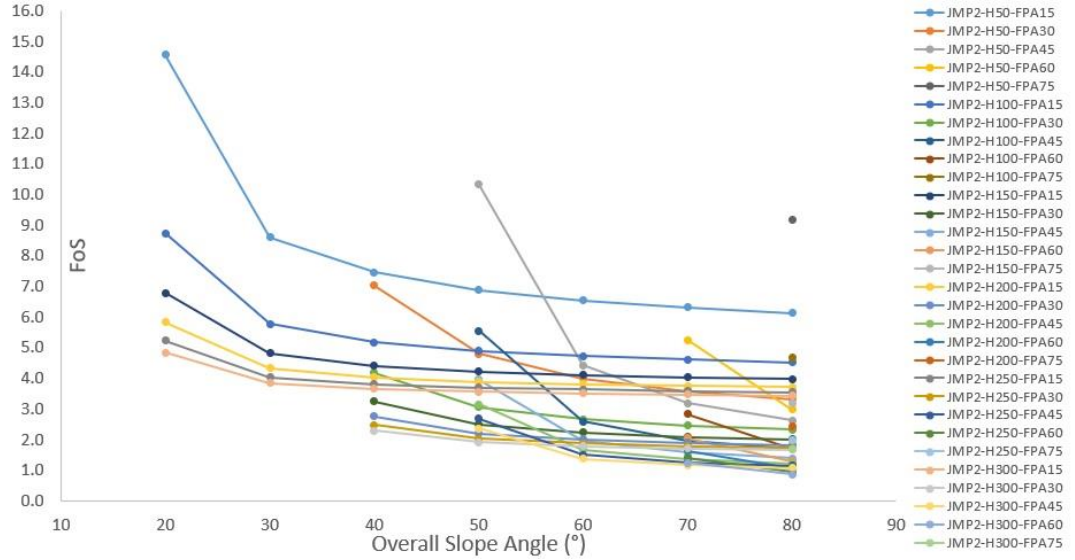

Figure D. 1 JMP_2 safety factor values for planar slope failure

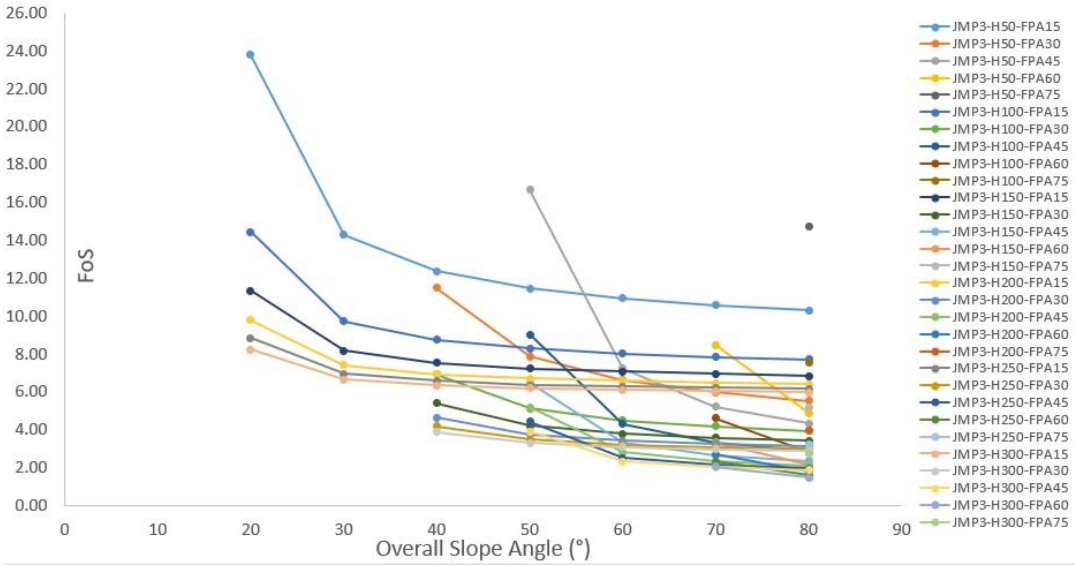

Figure D. 2 JMP_3 safety factor values for planar slope failure

E. ANN Model Structure for Each Slope Failure Type

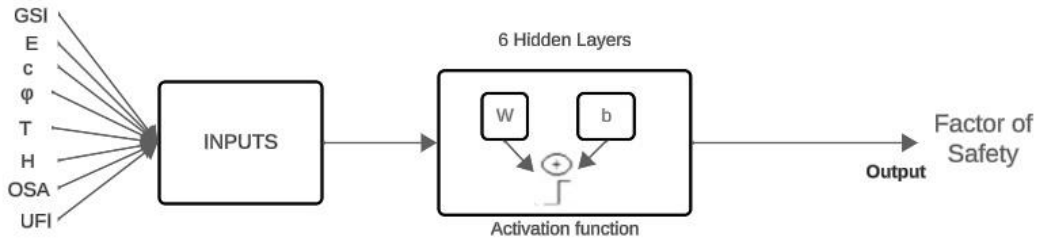

Figure E. 1 FEM mass failure ANN model structure for factor of safety

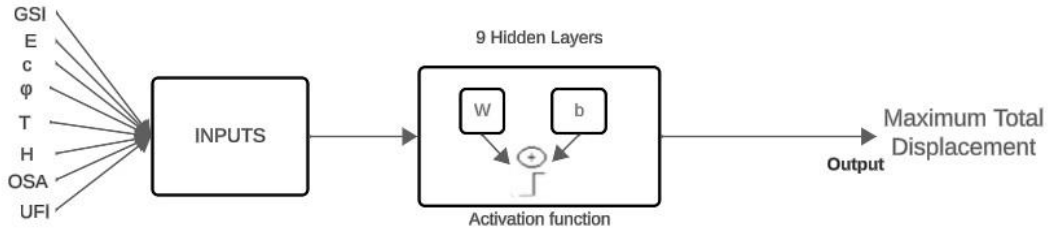

Figure E. 2 FEM mass failure ANN model structure for maximum total displacement

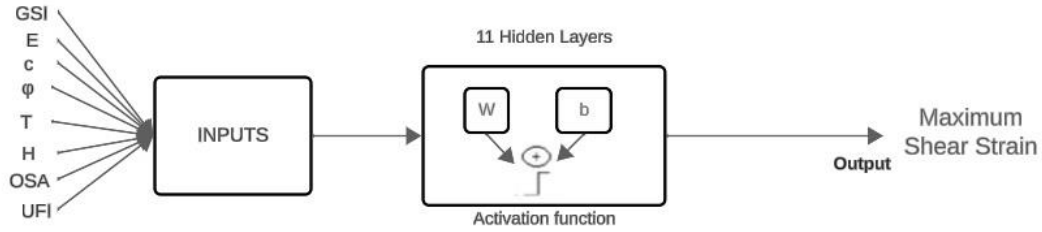

Figure E. 3 FEM mass failure ANN model structure for maximum shear strain

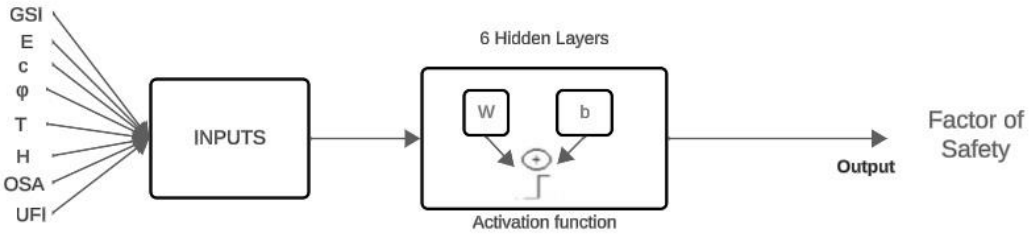

Figure E. 4 LEM mass failure (circular) ANN model structure for factor of safety

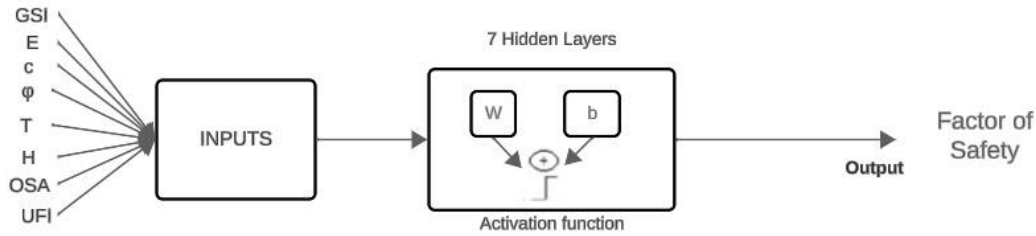

Figure E. 5 LEM mass failure (non-circular) ANN model structure for factor of safety

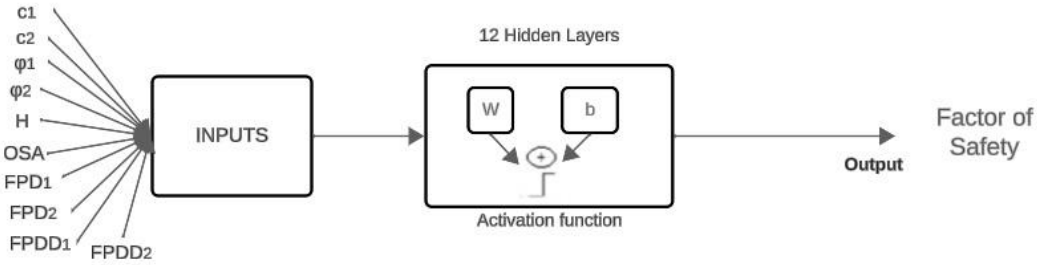

Figure E. 6 Wedge failure ANN model structure for factor of safety

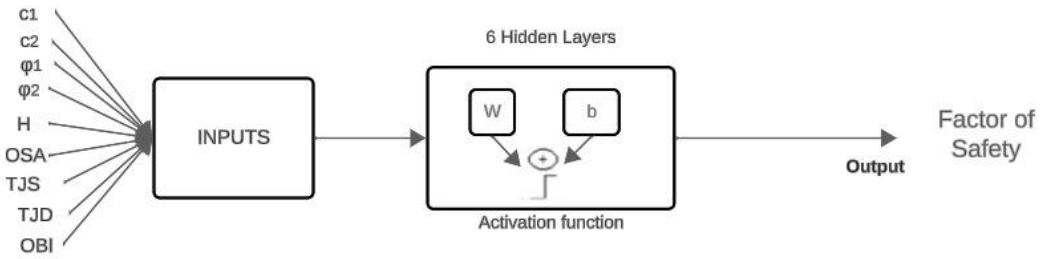

Figure E. 7 Block toppling failure ANN model structure for factor of safety

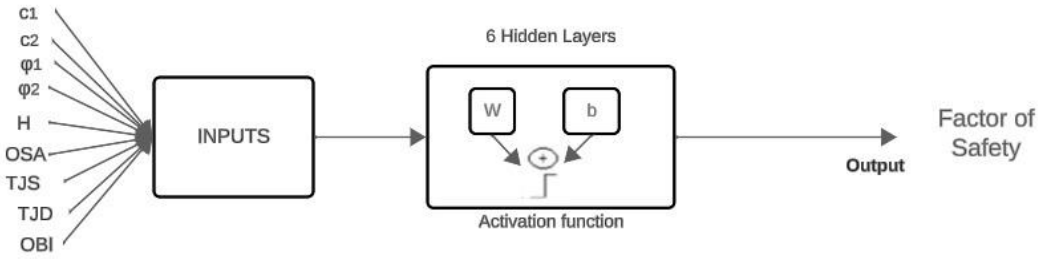

Figure E. 8 Block flexure toppling failure ANN model structure for factor of safety